REMOVAL OF PHOSPHATE AND AMMONIUM ION FROM DOMESTIC WASTEWATER USING CLAY FELDSPAR IN WUPA SEWAGE TREATMENT PLANT ABUJA

BY

SHIRU, Adama Grace
MEng/SEET/2016/6412

DEPARTMENT OF CHEMICAL ENGINEERING
FEDERAL UNIVERSITY OF TECHNOLOGY
MINNA.

OCTOBER, 2021

ABSTRACT

The aim of this study is centered on the sustainability of feldspar as an adsorbent as opposed to other clay minerals such as plastic clay, red clay and barite. BET analysis of the clay minerals considered in this study revealed that raw feldspar had the highest surface area and pore volume of 332.8 m^2/g and 0.218 cc/g respectively. Similarly, the clay minerals were used in adsorption study with feldspar producing the best removal efficiency of 90.00 % and 73.96 % for ammonium and phosphate ions respectively. The BET results and the adsorption test showed that feldspar was a better adsorbent than the other adsorbents. Thermal activation of feldspar was carried out at temperatures of 500-700℃ using muffle furnace. The BET results of the thermal activation revealed that feldspar activated at 600℃ has the highest surface area and pore volume of 533.9 m^2/g and 0.272 cc/g respectively. The FT-IR results indicated that several functional groups were involved in the adsorption process of the phosphate and ammonium ions some of which were O-H, N-H and C-O groups. The SEM results showed that irregular-layered structures of the raw feldspar became smooth and regular after thermal activation. The effects of pH, adsorbent dosage, temperature, contact time and initial PO_4^{3-} and NH_4^+ concentrations on the adsorption of phosphate ions and ammonium ions were investigated using atomic adsorption spectrocopy (ASS). The adsorption studies of phosphate ion and ammonium ion onto feldspar increased with contact time, adsorbent dosage and temperatures until optimum values were reached. The maximum adsorption efficiency of the activated feldspar for 4 mg/L phosphate ion and 15 mg/L ammonium ion solution amounted to 80.25 % and 90.89 % respectively with pH of 6.2, temperature of 30 ℃, adsorbent dose of 0.5 g and contact time of 30 min. Isotherm studies indicated that the Temkin model can well describe the adsorption process due to the high correlation coefficient (R^2) values of 0.836, 0.6931 and 0.8685 at 30, 40 and 50 ℃ for phosphate ion removal and similarly 0.9221, 0.8483 and 0.9222 for ammonium ion removal. Kinetic studies revealed that the adsorption process was best fitted to the pseudo-second order kinetics with high R^2 values ranging from 0.9958-0.99875 and 0.985-0.9997 for phosphate ion and ammonium ion removal respectively. The thermodynamic studies showed that the reactions were spontaneous and exothermic in nature due to the increasing negative values of the free energy (ΔG^o), the positive values of the entropy (ΔS^o) and the negative values of the enthalpy (ΔH^o).

CHAPTER ONE

1.0 INTRODUCTION

1.1 Background of the Study

Safe disposal of wastewater remains a serious problem in Nigeria where it has the potential of causing contamination and creates environmental pollution. This result in corresponding increase in polluted water generating in urban areas, raising concerns resulting from the quality of wastewater disposed to sensitive environments (Adewumi and Oguntuase, 2016).

Water is a universal resource and due to its free occurrence in nature, it has over time been taken for granted and abused, especially in third world nations where information is neither readily accessible nor disseminated to society. However, as abundant as it may seem, water, in its clean state, is one of the rarest resources in the world. Like all scarce resources which have global regulations guiding their exploitation, ownership, preservation, and sustenance, water in Nigeria is protected by a body of laws, policies, and regulations in order to prevent abuse (Saminu *et al*., 2017).

The importance of water in human life is growing and the supply of fresh water is becoming increasingly difficult, because of population growth and urbanization which have led to production of much sewage in homes that are harmful and has effect on human health if not removed. However, human, industrial, urban and agricultural activities have largely contributed to the reduction of pollution due to the sewages (Allam *et al*., 2018).

The sewage if it is not treated before being discharged into waterways, serious pollution is the result. Rapid industrialization and urbanization have led to the continuous and

excessive release into the environment, thereby causing significant impacts on human and wild life (Bhutiani *et al*., 2016).

Wastewater comprises of liquid wastes discharged by domestic residences, commercial, industrial and/or agricultural activities. It can encompass a wide range of potential contaminants and concentrations. Domestic wastewater contains substances such as human waste, food scraps, oil, soaps, chemical, and countless numbers of living organisms (Saminu *et al*., 2017). To deal with this major threat to the environment, much work has been done to address water pollution. To this effect a wide variety of physical, chemical, and biological techniques has been developed; these methods include flocculation, precipitation, ion exchange, membrane filtration, irradiation and ozonation (Allam *et al*., 2018). However, adsorption method still remains the best, it also happens to be inexpensive, readily available and easy to operate (Dias *et al*., 2015).

Adsorption is a transfer process of a substance (adsorbate) that is in solution in a liquid or gas phase to the surface of a solid phase (adsorbent). The adsorption process can occur by means of physical forces, in which the Van Der Walls forces are involved. It can also occur by means of chemisorptions, which involves chemical interaction between the adsorbate molecules and the surface of the adsorbent (Dias *et al*., 2015).

Adsorbents are solid particles that present porous structure and pore volume up to 50% of the total volume of particles, which justify their use in adsorption processes. Adsorbents can be modified by various means, and the objective is to increase their adsorption capacity. This increase can be obtained by intensifying the linkage strength between the adsorbent and the adsorbate, substituting cation with higher affinity to the adsorbate, increasing the porosity of the adsorbent, increasing the specific surface area

and activating the adsorbent. Acidic, basic, pillaring and hydrothermal treatments are ways to modify adsorbents (Dias *et al*., 2015).

There are different types of adsorbents such as activated carbon, silica gel, chitosan and zeolite (Yu and Han, 2015). However, clays and clay minerals such as plastic clay, red clay, Barite and feldspar are of significant interest because of their interesting characteristics that make them suitable for industrial applications. They have been accepted as one of the most appropriate low-cost adsorbents and common component in different industrial applications. Among the various types of clays, their physicochemical and adsorption properties depend on the montmorillonite content, the crystalline structure of the clay minerals that constitute them and the nature of the inter-layer cations. In order to eliminate impurities and different exchangeable cations from clay minerals and to prepare a well-defined material for use as catalyst and adsorbent, various activations methods have been used, most often with acids. Indeed, the treatment with minerals acids significantly changed their textural characteristics and effects on the mineralogical, composition of the raw material and related properties. This process causes increase in surface area, surface acidity and introduces permanent mesoporosity which removes metal ions from the crystal interlayer, which partially delaminated the clay (Amari *et al.,* 2018). Clay can be modified to enhance its efficiency for the removal of pollutant from water and wastewater (Dias *et al.,* 2015).

By 2050, the global population is expected to reach up to 9.3 billion and the world may be under great fresh water scarcity. Therefore, the removal of toxic organic pollutants from water is essential in the present scenario (Adeyemo *et al,* 2017).

1.2 Statement of the Research Problem

The deleterious effects of sewage on human health cannot be overemphasised as more evidence on the negative consequences on human health and ecosystems has begun to emerge. In light of the increased recognition of the health and environmental impacts of insufficient wastewater treatment, several measures need to be put in place to mitigate these impacts. A watercourse sited a few meters from the facility currently receives the treated effluent from WUPA sewage treatment plant and under certain conditions (especially during the dry season), the sewage treatment plants becomes the only source of flow into the watercourse.

The quality of effluent is a concern to consumers (WUPA dwellers) and public health regulators like the Abuja Environmental Protection Board. The mindboggling question is the conformity of the effluent discharged into the river with World Health Organization (WHO) standards. The quality of domestic wastewater effluent is a major cause of degradation of receiving water bodies such as rivers, lakes and streams.

1.3 Aim and Objectives of the Study

The aim of this research work is the application of thermally activated feldspar as an adsorbent to remove phosphate and ammonium ion in domestic wastewater.

This aim will be achieved by carrying out the following objectives:

i. Preliminary investigation of plastic clay, red clay, barite and feldspar as adsorbent.
ii. Thermal treatment of the selected adsorbent, feldspar.
iii. Characterisation of the raw and thermally activated feldspar by FT-IR, XRF, BET, SEM and XRD
iv. Batch adsorption of phosphate and ammonium ion using the activated feldspar

1.4 Justification of the Study

Adsorbents are solid particles that present porous structure and volume which justify their use in adsorption processes. Clay mineral can remove approximately 70 % of the waste and the remaining 30 % can be removed using activated carbon. However, activated carbon is costly and cannot be used at large scale. This situation compelled scientists toward the development of low-cost adsorbents that is readily available and eco-friendly. The source of clay has received little or no investigative study on its pollutants.

1.5 Scope of the Study

This research work is limited to:

Selection of adsorbent, thermal treatment of the selected adsorbent (feldspar), characterisation of the feldspar and adsorption studies of feldspar in the removal of phosphate and ammonium ions from domestic wastewater.

The characterization of feldspar will be evaluated by means of Brauner-Emmert-Teller (BET), screening electronic microscopy (SEM), Fourier's transformed infrared, FTIR and X-ray fluorescence spectrophotometer (XRF).

CHAPTER TWO

2.0 LITERATURE REVIEW

2.1 The Preamble

The start of the 20th century saw the introduction of septic tanks for use in treating domestic sewage from households in sub-urban and rural areas. The recognition by a few cities and industries has health implications on direct discharge of sewage into streams ushered in the development of sewage treatment facilities in the form of wastewater treatment plants. Wastewater Treatment plants (WWTPs) are complex systems which include a large number of biological, physiochemical, and biochemical processes (Chukwu and Oranu, 2018).

The WUPA sewage Water Treatment plant is an oxidation ditch type designed to treat waste generated from the City. It has three operating units one of which is under operation with the other two on standby in the event of failure (Akpen *et al.*, 2016). The flow chart of WUPA sewage water treatment plant is as shown in Figure 2.1.

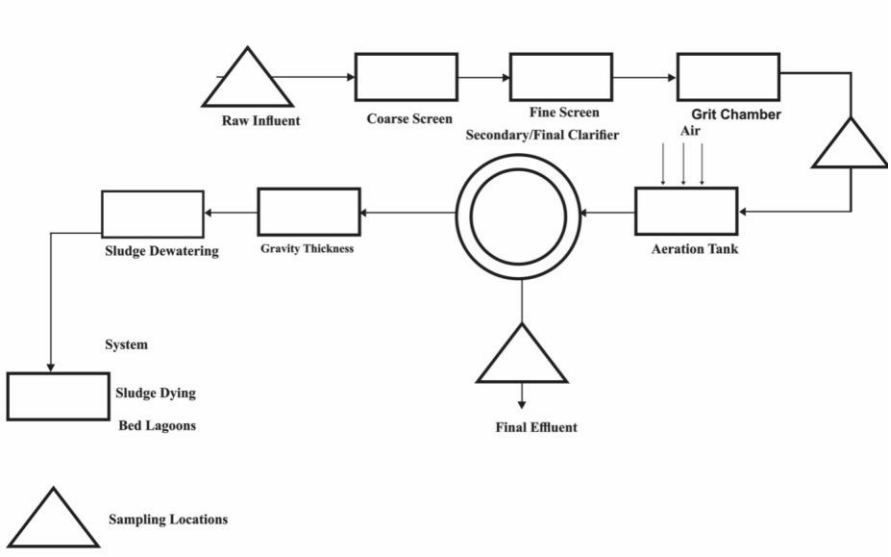

Figure 2.1: Flow chat of WUPA sewage Water Treatment plant

Water is an important component of the ecosystem and safe water is essential for life on earth. Water and energy are interdependent and policy formulation on them needs to be harmonised. Rapid urbanization with the attendant population explosion has led to increased pressure on scarce water resources in many regions of the world. Though it is a generally accepted notion that global water supply can be constantly increased to meet new demands, freshwater supply can only be increased slightly (Ali and Khan, 2012).

The total volume of water in the world stays constant but the quality and availability are subject to change. Water covers about 75% of the earth but over 95% of it is salt water and a large proportion of the freshwater is bound up in the ice caps of the poles and the glaciers. The result of this is that freshwater accounts for only 0.01% of the world's water volume. The utilization of large amounts of freshwater annually to support agriculture, urbanization, industry and mining has put pressure on the global supply of freshwater with the ensuing consequence of compromised water quality (Idris-Nda *et al.*, 2013). The actual supply of freshwater available for human use is minute compared to the potential volume of freshwater because of imbalance in rainfall distribution around the globe and the fact that people do not always settle in locations with maximal water availability. Another factor contributing to the scarcity of freshwater is the astronomical increase in volume of water consumed worldwide. The contaminants from agricultural, industrial and residential activities also portend negative outcomes for water quality (Odlare, 2013).

Wastewater is a mixture of organic and inorganic materials. It can be divided into domestic wastewater (sewage), industrial wastewater, and municipal wastewater (Odlare, 2013). Black water refers to wastewater from human waste and includes water from lavatories, septic tanks (soak away), and washing water, while grey water is wastewater that comes from urban rainfall runoff from roads, roofs, and sidewalks (Idris-Nda *et al.*, 2013).

2.2 Environmental and Health Impacts of Domestic Wastewater Discharge

The major source of the natural water pollution burden is effluent generated from domestic activities (wastewater). This is a massive challenge for wastewater management as the resultant point source pollution problem could introduce a host of pollutants and microbial contaminants into water sources. This poses environmental and health risk to human life as the major breeding sites for mosquitoes, houseflies, rodents and other vectors of communicable diseases like dysentery, diarrhea, kidney damage and blindness is formed by wastewater released into the environment (Idris-Nda *et al.,* 2013).

In developing countries such as Nigeria, the wastewater management system is very poor and ineffective. Water bodies like lakes, rivers, and streams are at the receiving end of wastewater effluent. The quality of such receiving water bodies is affected by the pollutants contained in wastewater effluent and this has grave implications for the health of individuals and communities. The potential health danger constituted by contamination of water bodies depends on the type of discharge, number of suspended solids or hazardous pollutants like heavy metals or organic matter. The risk is increased in situations where humans are exposed to the contaminated water through recreational activities such as swimming. Contamination of water bodies also has negative effects on ecosystems including release of toxic substances, decreased levels of dissolved oxygen, increased nutrient load and bioaccumulation in aquatic life. Inadequate finance for optimal water treatment in the face of increased release of domestic wastewater may be associated with an increased incidence of waterborne diseases and environmental degradation (Idris-Nda *et al., 2013*).

2.3 Characteristics of Wastewater

The characteristics of wastewater are vital in ensuring the effective design of wastewater treatment and disposal system, and enabling the development and application of water conservation and waste load reduction strategies (Idris-Nda *et al.*, 2013). Table 2.1 shows some wastewater characteristics.

Table 2.1: Physical characteristics of wastewater

Temperature	• Slightly higher than in the drinking water • Variations according to the seasons of the years (more stable than the air temperature) • Influences microbial activity • Influences solubility of gases • Influences viscosity of the liquid
Colour	• fresh sewage: slight grey • Septic sewage: dark grey or black
Odour	• fresh sewage: oily odour, relatively unpleasant ▪ Septic sewage: foul odour (unpleasant) ▪ Gas and other decomposition by products ▪ Industrial waste water: characteristic odour
Turbidity	• caused by a great variety of suspended solids ▪ Fresher or more contracted sewage: generally greater turbidity

Source: (Dias *et al.*, 2014)

2.4 Wastewater Management in Nigeria

Most African countries do not have a proper wastewater treatment system. Untreated wastewater constitutes the major source of pollution around urban rivers and in groundwater sources in many West African countries (Omosa *et al.,* 2012).

An important commercial city, Abia, in the Southeastern region of Nigeria lacks a central wastewater system management. There are also no septic tanks for domestic wastewater. The outcome of this is that sewers for industrial water generated from the large industries and open drains from the smaller industries are channeled to empty their content into the Aba River. Wastewater produced by the industries does not undergo any form of treatment and this situation is likely to continue in the future (Giwa, 2014).

In Minna, Niger State, domestic wastewater management consists of the use of septic tanks and open drainage. About 35% of domestic wastewater generated are channeled into the septic tank while the remaining 65% flows freely on ground surface sometimes forming stagnant pools. As a result of this, the residents in some areas are forced to turn to unlined channels to convey wastewater away from their homes. This leads to the creation of an artificial pool of stagnant water at the terminal end and production of obnoxious odors. (Idris-Nda *et al.,* 2013*).*

In Kano, one of Nigeria's most densely populated cities; there is absence of wastewater treatment facilities in most industries leading to discharge of untreated effluents into the adjoining water bodies. Unfortunately, the polluted water bodies are extensively used for water supply, irrigation, fishing, and recreational activities while the only treatment plant in the city remains nonfunctional (Kura *et al*., 2013).

Adesogan (2013) noted that Kaduna State, the capital of the defunct Northern Region, is the only state in Northern Nigeria with a functional industrial wastewater treatment

facility (Nigerian Brewery, Kaduna). In the Middle Belt region, only the Federal Capital Territory has a functional wastewater treatment system as the facilities in Benue, Niger, Kogi, Kwara and Plateau states are non-functional. There are more treatment facilities in Southern Nigeria but states like Bayelsa, Cross River, Akwa Ibom, Ebonyi, Imo, Abia, and Ondo completely lack wastewater treatment facilities.

It is appalling to note that in most parts of the country, domestic and industrial wastewater still get dumped directly into surface waters without any form of treatment and this has continued unabated as stakeholders in the environmental sector are yet to come up with a plan to check this unpleasant trend. The indiscriminate release of wastewater into the environment has adversely affected sanitation and led to loss of lives through diseases like cholera, hepatitis B, and typhoid fever (Giwa, 2014). Certain substances in untreated wastewater have the capacity to alter the endocrine system in human beings leading to infertility, malignancies, and teratogenic effects. Groundwater contamination is common in densely populated areas such as Lagos State where septic tanks have been left in dilapidated conditions. As Nigeria's economic hub, the state produces about 1.4trillion cubic centimeters of wastewater on a daily basis.

2.5 Wastewater Reuse Application

Treated wastewater has been used to supplement or replace natural water resources in several ways. The intended reuse application is the major factor that influences the degree of treatment needed to ensure public health safety. It also determines the degree of reliability needed for treatment processing operation. The major non-portable reuse activities include irrigation, industrial use, toilet flushing, general cleaning, replenishment of surface water, and groundwater recharge. A change of attitude toward wastewater management is imperative for sustainable management of water resources, Governments at all levels need to ensure implementation of wastewater treatment and

reuse programs and policies (Giwa, 2014). Agricultural irrigation has been the major beneficiary of wastewater reuse as large volume of water is used in irrigation with a relatively lower quality requirement in comparison to other use (Adewumi and Oguntuase, 2016).

2.6 Water Pollutants

A pollutant is a substance that alters the natural quality of the environment by physical, chemical or biological means. Pollution may be in air, water or land (Gupta *et al*., 2009).

The major source of water pollution is wastewater containing industrial, domestic and environmental pollutants. Water pollution also occurs when rainwater runoff from urban and industrial areas arising from agriculture and mining activities which flows back to the receiving water bodies and groundwater (Bhutiani *et al*., 2016).

Domestic, agricultural and industrial activities consume large volumes of freshwater discharged as wastewater containing various pollutants depending on the type of activity. The pollutants could be chemical (inorganic or organic), biological, thermal (heat), or radiological in nature (Bhutiani *et al*., 2016).

2.7 Sources of Water Pollution

2.7.1 Biologic agents

Domestic effluent and sewage may contain biologically active agents like *Vibrio cholera, Salmonella typhi, Yersinia enterocolitica, Escherichia coli,* and *Shigella* which need to be removed to prevent disease causation. Waterborne diseases caused by biological agents include cholera caused by *Vibrio cholerae,* Typhoid fever caused by *Salmonella typhi,* dysentery caused by *Escherichia coli,*Gastroenteritis caused by *Shigella* (Gupta *et al*., 2009).

2.7.2 Heat sources

Many industries use water as a cooling medium because of its high heat capacity leading to discharge of water carrying waste heat away. The discharged water leads to high temperature wastewater that harms aquatic organisms and causes formation of Trihalomethane (THM) and increased corrosive activity (Omosa *et al*., 2021).

2.7.3 Dissolved and non-dissolved chemicals

Gupta *et al*, (2009) stated that various chemicals generated from domestic, industrial and agricultural processes are mix with freshwater and are then expelled as wastewater in dissolved or non-dissolved forms. The non-dissolved chemicals are usually present as suspended solids in dispersed form which increases water turbidity. The suspended solids slowly settle down to form silt. Apart from their toxic effects on aquatic life, they lead to clogging up of waterways and filling of dams.

The dissolved chemicals in wastewater with potential for pollution include heavy metals, pesticides, detergents, phenols, dyes, polychlorinated biphenyls (PCBs), and a host of other inorganic and organic substances.

2.8 Importance of Wastewater Treatment

Untreated wastewater is associated with major consequences that are unsuitable for environment and human health. Wastewater treatment is essential to decrease the rate of transmission of excreta-related diseases, reduce water pollution and the attendant damage to aquatic life (Mara, 2013). Table 2.2 gives some wastewater contaminants and their health hazards.

Table 2.2: Contaminant in wastewater and their health hazards

Contaminant	Health hazards/impact
Nitrate	Cyanosis and asphyxia (blue baby syndrome) in infant under 3 months.
Iron	May cause conjunctivitis, choroiditis and retinitis if it contacts and remains in the tissues.
Cadmium	Carcinogenic, causes lungs fibrosis and weight loss.
Zinc	Causes short-term illness called metal fume fever and restlessness.
Phosphate	Eutrophication and kidney damage
Ammonium	Immediate burning of the eyes which can lead to blindness. Causes cough and throat irritation.
Copper	Headache, stomachache, dizziness and diarrhea

Source: (Dias *et al*., 2014).

2.9 The Parameters in Domestic Wastewater

2.9.1 Temperature of wastewater

Temperature of wastewater is usually high because of addition of warm water from industrial activities; the temperature has adverse effect on chemical reactions, reaction rate, aquatic life and the suitability of water for beneficial uses. Increased temperature can cause unusual changes in the species of fish existing in the receiving body (Akpor and Munchie, 2011).

2.9.2 pH of the wastewater

pH is the degree of intensity of acidity and alkalinity and measures the concentration of hydrogen ion in water. The pH determination is crucial to the treatment of water and variation in pH, values in effluent can affect the rate of biological reactions and survival of various microorganisms. High or low pH values in water have been reported to affect aquatic life and alter toxicity of their pollutant in one form or the other (Sankpal and Naikwade, 2012).

2.9.3 Conductivity of the wastewater

The electric conductivity of water is a measure of the ability of a solution to conduct electricity. The conductivity of water is an important indicator of the overall salt content of the wastewater,

It is a useful parameter used to determine the suitability of water for irrigation (Akpor and Munchie, 2011).

2.9.4 Total solids (TS) of the wastewater

Wastewater has variety of solid materials. Total solid is determined as residue left after evaporation of unfiltered samples. The value ranges from 8400 to 15600 mg/L. (Kolhe and Pawar 2011) found total solid of 1310 mg/L in effluent in dairy industry.

2.9.5 Total dissolved solids (TDS)

The solid in the filtrate that passes through a filter with a normal pore size of 2 µm or less are categorised as dissolved solids. Wastewater contains high fraction of dissolved solids. The size of colloidal particles in wastewater is typically in the range from 0.01 to 1.0 µm (Sankpal and Naikwade, 2012).

2.9.6 Total suspended solids (TSS)

Total suspended solids play an important role in wastewater treatment. TSS test results are done routinely to evaluate the operation of conventional treatment processes and are useful for effluent filtration in reuse application. TSS is the samples under suspension and remains in water sample (Kolhe and Pawar 2011).

2.9.7 Chemical oxygen demand (COD)

It is the measure of oxygen required by organic matter for its oxidation by strong COD substance in water. The COD is a test, which is used to estimate pollution of domestic and industrial waste. The waste is measured in terms of equality of oxygen required for oxidation of organic matter to produce CO_2 and water (Akpor and Munchie, 2011).

2.9.8 Biological oxygen demand (BOD)

BOD is used to estimate the amount of oxygen needed by bacteria to break down simpler substances to the decomposable organic matter present in any water, wastewater or treated effluent. It is also seen as a measure of the concentration of organic matter present in any water. The greater the decomposable matter present, the greater the oxygen demand and the greater the BOD values. Low value of BOD may be due to lesser quantity of total solids, suspended solids in water as well as to the quantitative number of microbial population (Akpor and Munchie, 2011).

2.10 Contaminants in Wastewater

2.10.1 Phosphate ion in wastewater

Phosphate (P) is a non-metal in the 15^{th} group of the periodic table and is one of the most indispensable materials for everyday life, affecting each and every organism on earth. The elemental form of phosphate can be mainly found in two different physical forms;

white (or yellow) phosphate and red phosphate. These two allotropes have miscellaneous physical and Chemical characteristics. White phosphate, which is widely in the form P_4, has considerably high reactivity, due to its tetrahedral structure causing ring strain. This is due to the fact that this compound can be oxidised very easily in air. While it is believed that phosphate may have an important role in the biogeochemical phosphorus cycle, there is still a need for more extended studies on its origins and impacts on such cycle (Daneshgar *et al.*, 2018).

Phosphorus as an essential nutrient that is needed for plant growth and is required for many metabolic roles. However, if excessive amount of phosphorus enters the water it can potentially lead to eutrophication. Once a water body is eutrophicated due to excessive amounts of nutrients it can create a green layer on the water surface, it will lose its primary functions and subsequently influence sustainable for development of economy and society. Oxygen depletion may occur in contaminated water when many plants die and decompose; The decaying organic matter produce some pleasant odours and makes the water cloudy which increase turbidity. Adsorption is one of the potential separation techniques and can be proposed to remove PO_4^{3-} from water. Many types of adsorbent materials such as carbons, silica gels and alumina exist, of which the most industrially used are to remove inorganic and organic matters from waters (Ler and Stanforth, 2003).

2.10.2 Nitrates in wastewater

A high concentration of nitrate is often encountered in treated wastewater because of ammonium nitrogen. High nitrate levels in wastewater could also contribute to eutrophication effects, particularly in freshwater. Many workers have been reported to have potential health risk from nitrate in drinking water above threshold of 45 mg/L, which may give rise to a condition known as methaemoglobinemia in infants and pregnant women (Akpor and Munchie, 2011).

2.10.3 Ammonium ion in wastewater

Ammonium ions in wastewater pollution have become one of the most serious environmental problems today. The treatment of ammonium ions is a special concern due to their recalcitrance and persistence in the environment. In recent years, various methods for ammonium ion removal from wastewater have been extensively studied. Ammonium ions are the primary form of wide spread nitrogen pollution in the hydrosphere and causes remarkable increase of oxygen demand and biological eutrophication in aquatic sources and results proved that increased in concentration of this beyond the permissible cause damage to aquatic life (For example, ammonia is toxic to fish and other forms of aquatic life in very low concentration, about 0.2 mg/L) (Gupta *et al*., 2015).

Ammonium has a hazardous and toxic effect on human health and biotic resources, only if the intake becomes higher than the capacity to detoxify and predefined permissible limits. If ammonia is administered in the form of its ammonium salts, the effects of the anion must also be taken into account with ammonium chloride, the acidotic effects of the chloride ion seem to be of greater importance than those of the ammonium ion (Gupta *et al*., 2015).

2.11 Wastewater Treatment Methods

The purpose of wastewater treatment is removal of water from contaminants for the treated water to meet acceptable quality standards. The quality standard is determined by the intended purpose or destination of the water; reuse or discharge into a receiving water body. The stages of sewage treatment can be broadly divided into physical, chemical and biological. Wastewater treatment is a complex process involving many steps all geared toward ensuring water safety. The first step is mechanical treatment which involves removal of heavy materials and large objects by the use of a screening chamber (coarse

and fine screening) and a degritor. Biological treatment is then done to remove soluble organic matter and nitrogen. Disinfection then follows with the use of a chlorine contact tank (Bhutiani *et al*., 2016). Table 2.3 shows the wastewater treatment unit operations and their processes.

Table 2.3: Wastewater treatment unit operations and processes

Physical unit operations	Screening
	Comminution
	Flow equalization
	Sedimentation
	Flotation
	Granular-medium filtration
Chemical unit operations	Chemical precipitation
	Adsorption
	Disinfection
	DE chlorination
	Other chemical applications
Biological unit operations	Activated sludge process
	Aerated lagoon
	Trickling filters
	Rotating biological contactors
	Pond stabilization
	Anaerobic digestion
	Biological nutrient removal

Source: (Bhutiani *et al*., 2016).

2.11.1 Physical unit operations

2.11.1.1 *Screening operation*

Screening is done to remove large pollutants from the waste stream. This prevents damage to equipment and allows for smooth plant operations. Large floating or suspended materials are blocked by screening devices such as parallel bars, rods or wires, wire mesh, grating and perforated plates. The material retained from the cleaning of bar racks and screens is either disposed of by incineration or burning or returned into the waste flow after grinding (Bhutiani *et al*., 2016). The major types of screening devices are listed in Table 2.4.

Table 2.4: Screening devices and their application

Screen category	Size of Openings (mm)	Application	Types of screens
Coarse screens	≥ 6	Remove large solids, rags and debris.	• Manually and Mechanically cleaned bar screens/trash racks • Chain or cable driven with front or back cleaning • Reciprocating rake Screens • Continuous self-cleaning Screens
Fine screens	1.5-6	Reduce suspended solids to primary treatment Levels	• Rotary-drum screens • Rotary-drum screens with outward or inward Flow • Inclined revolving disc screens • Traveling water screens • Endless band • Vibrating screens
Very fine screens	0.2-1.5	Reduce suspended solids to primary treatment levels	
Micro screens	0.001-0.3	Upgrade secondary effluent to tertiary standards	

Source: (Bhutiani *et al*., 2016).

2.11.1.2 *Comminution operation*

Large floating materials in the waste flow are crushed into small pieces by Comminutors. Comminutors are installed between the grit chamber and the primary settling tanks. A comminutor may possess rotating or oscillating cutters. Rotating-cutter comminutors could have a separate stationary screen alongside the cutters, or a combined screen and cutter rotating together. Barminutors are special types of comminutors that involve a combination of a bar screen and rotating cutters (Bhutiani *et al*., 2016).

2.11.1.3 *Floatation operation*

This is a separation process with different types of collectors (nonionic or Ionic). Effective for removal of small particles and low-density particles, which would require long settling periods. It is used for primary clarification, low retention time and also used as an efficient tertiary treatment in the pulp and paper industry mechanisms: true flotation, entrainment and aggregation. Some of the disadvantages are energy costs, high initial capital cost maintenance and operation costs, no negligible chemicals required (to control the relative hydrophobicities between the particles and to maintain proper froth characteristics) Selectivity is pH dependent. (Crini and Lichtfouse, 2019).

2.11.1.4 *Granular medium filtration*

Filtration involves removal of suspended solids from wastewater effluents of biological and chemical treatment processes. The complete process consists of filtration and cleaning or backwashing. It involves passing the wastewater through a filter bed made up of granular material (sand, anthracite and/or garnet). A complex process involving mechanisms like straining, interception, impaction, sedimentation, flocculation and adsorption eliminates the suspended solids in the wastewater (Bhutiani *et al*., 2016).

2.11.2 Chemical unit processes

The chemical processes work by means of chemical reactions and are always used together with physical and biological processes. Unlike the physical processes, the chemical processes usually cause a net increase in the dissolved constituents of wastewater. This is a disadvantage especially if the wastewater is intended for reuse.

2.11.2.1 *Chemical precipitation*

In this process, the interaction between chemicals and heavy metals in wastewater leads to the formation of insoluble precipitates. This aids removal of the heavy metals. Mechanisms of achieving precipitation include raising the temperature, adding solvents, salts or polymers, and altering the pH of the solution. A major drawback of this precipitation process is that a large amount of toxic sludge is formed. The precipitates are removed by sedimentation and the clean water is obtained by decantation (Djedidi *et al*., 2009; Fu and Wang, 2011).

2.11.2.2 *Dechlorination process*

This is the removal of chlorine residue from chlorinated wastewater effluent prior to discharge to receiving waters or reuse. Chlorine compounds have long term toxic effects on aquatic life. Activated carbon and sulfur dioxide are used to achieve dechlorination (Bhutiani *et al*., 2016).

2.11.2.3 *Adsorption process*

Adsorption may be defined as a mass transfer process involving the transfer of a substance from the liquid or gaseous phase to a solid surface and its subsequent binding with the solid by physical and/or chemical interactions. High adsorption capacity and surface reactivity result from large surface area (Rashed, 2013). Adsorption is a major industrial separation technique for the purification of effluent media. It is a mass transfer

operation through which a solid material can selectively remove dissolved components from an aqueous solution by attracting the dissolved solute to its surface (Adeyemo *et al*, 2017). It ultimately, leads to accumulation of substances at the interface of two phases, such as, liquid–liquid, gas–liquid, gas–solid or liquid–solid interface (De Gisi *et al*., 2016).

In the adsorption process, the isotherm represents the equilibrium relationship between the concentration in the liquid phase and the concentration on the adsorbent at a given temperature. The isotherm provides information to evaluate the affinity and the adsorption capacity of an adsorbent by an adsorbate. In order to produce the best evaluation, the models most frequently used are those of Langmuir and Freundlich. The Langmuir isotherm model considers that the adsorption is restricted to a monolayer, and it is assumed that the surface of the pores of the adsorbent is homogeneous. The characteristics of the Freundlich isotherm are expressed in terms of intensity of the adsorption process. When there are more than one adsorbent to choose, the adsorption isotherms represent a tool to identify the one that is most adequate for one particular condition (Dias *et al*., 2015).

2.12 Types of Adsorption

2.12.1 Physical adsorption (Physiosorption)

Dawood and Sen (2014) define this type of adsorption as the effect of intermolecular attraction between the adsorbent and the adsorbate. Whereby the adsorbate bond itself to the adsorbent surface through intermolecular interactions such as; hydrogen bonding, hydrophobicity polarity, static interactions, dipole-dipole interactions and Van der Waals forces which are all considered weak bonds. Physical adsorption is an easily reversible

process and Chen (2012) stated that this reversibility is for the recovery of substances, or some fractions of the substance for recycle.

2.12.2 Chemical adsorption (Chemisorption)

Artioli (2008) defines this type of adsorption as a contact between the adsorbate and the adsorbent in which the adsorbate molecules bond to the adsorbent surface through the formation of a chemical type of bond, which involves the exchange of electrons. The amount of heat released and adhesive forces here are greater than in the physical. Unlike the other type, chemisorption is not mostly reversible, and substances under high temperature undergo chemisorptions more than low temperature substances, but in some cases low temperature substances too under this kind of adsorption. In catalysis, chemisorption is of specific significance in catalysis.

2.12.3 Adsorption phenomenon

Adsorption is a surface phenomenon with the same mechanism for removal of both organic and inorganic pollutants. Contact between a solution containing absorbable solute and a solid with a porous surface structure, liquid-solid intermolecular forces of attraction cause deposition of solute particles from the solution on the solid surface. The retained solute is referred to as the adsorbate, while the solid on which it is retained is called an adsorbent. Adsorption is therefore, the surface accumulation of the adsorbate on the adsorbent. Separation by adsorption technology is based on the creation of an adsorbed phase with a different composition to that of the bulk fluid phase (Gupta, *et al* 2009).

2.13 Adsorbent and Adsorbate

Adsorbate is any substance that concentrates at the surface. The possession of a porous structure is the most important quality of a good adsorbent as this guarantees a large surface area for adsorption. The time to attain adsorption equilibrium should be as short

as possible. This enables quick removal of contaminants. Adsorbents with high surface area and porosity, and showing fast adsorption kinetics are thus preferred (Gupta, *et al* 2009).

Adsorption efficiency is directly proportional to adsorption usage; the more adsorbent used, the greater the number of active sites available thus leading to higher adsorption efficiency. Adosrbent dosage of 0.5g/L was seen to result in 85% removal of heavy metals. 92% removal of heavy metals was achieved by increasing the dose to 0.8g/L (Bellir *et al.,* 2013).

2.13.1 Natural source adsorbents

Clay's adsorption potential is a result of the net negative charge possessed by silicate minerals. Clay attracts and binds to cations such as heavy metals because they neutralize its negative charge. Clay has a large surface area of up to 800 m^2; this also enhances its adsorption capacity (Zwain *et al.,* 2014).

2.13.2 Types of adsorbents

Adsorbents can be categorised based on origin into natural adsorbents and synthetic adsorbents.

Examples include ores, minerals, clay, charcoal, and zeolites. Natural adsorbents are cheap, readily available and have large potential for modification to enhance their adsorption capacities. The synthetic adsorbents are produced from agricultural, household, and industrial wastes. They are also sourced from sludge and polymeric adsorbents. A wide variety of waste materials are used including coconut shells, fertilizer wastes, fly ash, chitosan and seafood processing wastes, seaweed and algae, peat moss, clays, red mud, scrap tyres, bark and other tannin-rich materials, petroleum waste, rice husk, ore minerals (Rashed, 2013). Below are some of the adsorbents.

2.13.2.1 *Activated carbon*

This is the oldest known and most commonly used adsorbent. Its large surface area of up to 500-2000 m^2 makes it a good adsorbent material that is capable of adsorbing heavy metals in water. Physical and chemical methods are used to prepare activated coal from materials like coal, coconut shell, timber, and lignite. The physical method utilizes heat while the chemical method involves adding chemicals to the carbonised material (Rashed, 2013).

Powder activated carbon (PAC) and Granular activated carbon (GAC) are the two major forms of activated carbon for water treatment. Activated carbon is simple to use, but its high price limits its utilization on a large scale (Yu and Han, 2015).

2.13.2.2 *Silica gel*

This is the product of the coagulation of colloidal silicic acid, which leads to the production of porous and non-crystalline granules of different sizes. It shows a higher surface area of 70 m^2/g as compared to alumina. It is used in many industries to dry gases and liquids and in the purification of hydrocarbons (Yu and Han, 2015).

2.13.2.3 *Chitosan adsorbent*

As reported by Yu and Han (2015), Chitosan has a high adsorption capacity for heavy metals. It has a similar molecular structure with chitin, which is one of the largest biological polymers, surpassed only by cellulose. Chitosan has however been more widely used than chitin because of its good adsorption potential. Chitosan is produced by chemical modification of chitin. The earliest use of chitosan as an adsorbent was in 1988 when it was used to remove cadmium.

2.13.2.4 *Zeolite*

Zeolite is a common mineral adsorbent. Zeolite can undertake ion exchange with other metal ions because it has a lot of space in its structure. This ability to undertake ion exchange accounts for the adsorbent power of zeolite. The adsorbent power of zeolite has been in existence the 1980s. Clinoptilolite is a form of zeolite that was discovered to attract heavy metals like strontium and cesium. Clinoptilolite has a strong adsorption capacity for heavy metals like Lead, Cadmium, Zinc and Copper ions. The adsorption capacities of Clinoptilolite for Lead and Cadmium were 1.4 mg/g and 1.2 mg/g respectively. Studies have demonstrated increased adsorption capacity of clinoptilolite as an outcome of increasing its temperature. Zeolite has the potential to function as a substitute for activated carbon. (Yu and Han, 2015).

2.13.2.5 *Clay*

Clay takes up cations and anions either through ion exchange, adsorption or both. The surface of clay contains anions and cations like Ca^{2+}, Mg^{2+}, H^{+}, NH_4^{+}, Na^{+}, $SO4^{2-}$, Cl^{-} and NO^{3-} that can be exchanged with other ions without affecting the mineral structure of clay due to clay's large specific surface area, chemical and mechanical stability, layered structure, high cation exchange capacity (CEC) and so on. Clays exhibit first class adsorbent properties. Bronsted and Lewis type of acidity in clays have also improved to great extent the adsorption capacity of clay minerals (Dias et al., 2015). The Bronsted acidity arises by dissociation of water molecules of hydrated exchangeable metal cations on the surface, thereby forming H^{+} ions on the surface. If there is net negative charge on the surface, Bronsted acidity may arise due to the substitution of Si by Al^{3+} in some of the tetrahedral positions and H_3O^{+} cations that balanced the resultant charge. The exposure of trivalent cations mostly Al^{3+} at the edges, or Al^{3+} arising from rupture of Si–O–Al bonds, or through dihydroxylation of some Bronsted acid sites absorb anions,

cations and nonionic and polar contaminants from natural water. The contaminants that saturate the clay surface cannot easily be removed through the processes of ion exchange, coordination or ion–dipole interactions because pollutants can be held through H-bonding, Van der Waals interactions orhydrophobic bonding arising from either strong or weak interactions. The strength of the interactions is determined by various structural and other features of the clay mineral. Till date, several adsorbents such as porous carbon, biological, agricultural and industrial waste materials have been used to remove pollutants from wastewater but have one deficiency over each other (Nwosu *et al.*, 2018). Factors that contribute to clay's adsorbent ability are its large specific surface area, chemical and mechanical stability, layered structure, and high cation exchange capacity (CEC).

2.14 Clay Minerals

Clay minerals are a various group of hydrous layer aluminosilicates that constitute the greater part of the phyllosilicate family of minerals. They are generally described by geologists as hydrous layer aluminosilicates with a particle size <2 mm, while engineers and soil scientists define clay as any mineral particle < 4 mm. However, clay minerals are commonly >2 mm, or even 4 mm in at least 1 dimension. Their small size and large ratio of surface area to volume gives clay minerals a set of unique properties, including catalytic properties high cation exchange capacities, and plastic behavior when moist.

Clay minerals are the major constituent of fine-grained sediments and rocks (mudrocks, shales, clayey siltstones, clayey oozes, and argillites). They are an important component of estuarine, delta, soils, lake and the ocean sediments that cover most of the Earth's surface. They are also present in almost all sedimentary rocks, the outcrops of which cover approximately 75% of the Earth's land surface. Clays who form in soils or through weathering principally reflect climate, drainage, and rock type. It is now recognised that

re-deposition as mud-rock only seldom preserves these assemblages and clay accumulation in ocean sediments (Nwosu *et al*., 2018). This should not be interpreted in terms of climate alone, as has been done in the past. Most clay in sediments and sedimentary rocks is in fact reworked from older clay-bearing sediments and many are not stable at the Earth's surface. This does not preclude the use of clays in stratigraphic correlation; indeed, it can be a used in provenance studies. A few clays, notable the iron-rich clays form at the Earth's surface either by transformation of pre-existing clays or from solution. These clays are useful environmental indicators, so long as they are not reworked (Huggett *et al*., 2013).

2.14.1 Types of clay and clay minerals

2.14.1.1 *Bentonite clay*

Bentonite is an adsorbent aluminum phyllosilicate consisting mostly of montmorillonite. The various types of bentonite are named after the dominant element contained in them. They include sodium (Na), potassium (K), aluminum (Al), and Calcium (Ca). Bentonite is formed from weathering of volcanic ash in the presence of water. It has good adsorbent and rheological properties. Bentonite clay has an overall neutral charge with an excess negative charge on its lattice. The negatively charged lattice may have an affinity for cationic dye (Adeyemo *et al.,* 2017). Bentonite is readily available making it a promising economic option for the removal of dyes (Karima, 2010).

2.14.1.2 *Kaolinite clay*

Kaolin is a soft, white plastic made up of the mineral kaolinite, a hydrated aluminum silicate $Al_2Si_20_5(OH)_4$. Silica sheets (Si_2O_5) bonded to Aluminum oxide/ hydroxide layers ($Al_2(OH)_4$ form the basic structure of the kaolinite group. Kaolinite is a non-swelling clay

(Adeyemo *et al*, 2017). Rocks that are rich in kaolinite are known as kaolin or china clay (Anderson, 2013).

Kaolinite is the least reactive clay but its high pH dependency improves or inhibits the adsorption of metals depending on environmental pH (Adeyemo *et al*, 2017).

2.14.1.3 *Montmorillonite/smectites*

Montmorillonite is a soft phyllosilicate material that usually forms in microscopic crystals. It belongs to a group of non-metallic clays known as the smectite family. The smectites are chemically hydrated sodium calcium aluminum magnesium silicate hydroxide $(Na, Ca)_x (Al, Mg)_2(Si_4 O_{10}) (OH)_{2\ n}H_2O$. The basic structural unit is a layer of tetrahedral sheets with a central alumina octahedral sheet. The bonds between the layers are weak and have excellent cleavage which allows entry water and other molecules leading to expansion. The uptake mechanism of metal ions by smectites is determined by ionic strength, pH, and the type of ion being absorbed (Adeyemo *et al.,* 2017).

2.14.1.4 *Sepiolite/palygorskite*

These are natural clay minerals containing magnesium hydrosilicate. They are both magnesium silicates, but palygorskite has more structural diversity, more aluminum and less magnesium than sepiolite. They have a high adsorption capacity because their structures have tetrahedral and octahedral layers with canal cavities. The crystals are inert and non-swelling in water; they form a random lattice which traps liquids and provides good thickening, suspending and gelling properties. Methylene blue has been absorbed using Sepiolite (Adeyemo *et al.,* 2017).

2.14.1.5 *Feldspars*

Feldspars are among the most significant minerals in the Earth's crust. They show a broad range of compositional and structural characteristics that present ample information that can be tied to their genesis, but at the same time makes the analysis difficult. In particular, due to extensive solid solutions at temperatures higher than about 700 °C and large immiscibility gaps at lower temperatures, the majority of feldspars begin their history as homogeneous crystals, which subsequently evolve into unmixable components on cooling (Balić-Zunic *et al*, 2013).

They are aluminum silicates of sodium, potassium, calcium and barium. The sodium, potassium, and calcium aluminum silicates are known as soda feldspar, potash feldspar and lime feldspar respectively. Feldspars are important in production of ceramics because they enhance their strength and durability. They are also used in glass production, serving as a source of alkalis and alumina. Feldspars are therefore important economic raw materials for manufacture of glass, porcelain, and ornamental stones (Jaya, 2018). Figure 2.2 shows an idealised projection of feldspar structure onto (001). All points where lines join are the centers of Si-O or Al-O tetrahedral (T sites).

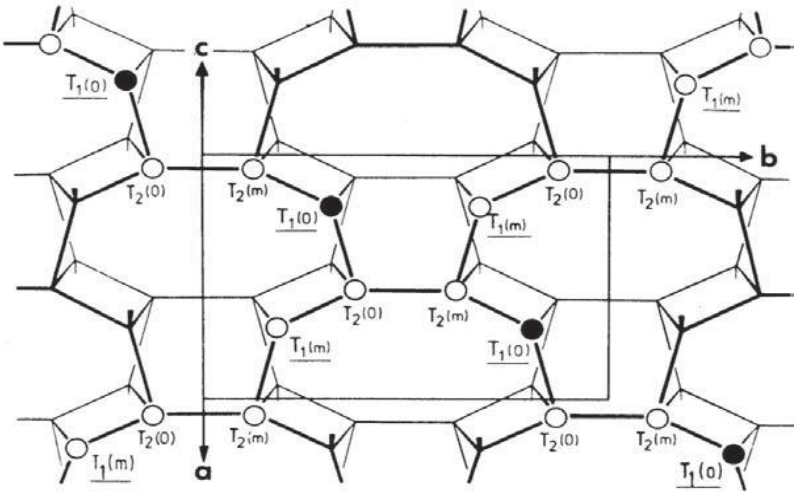

Figure 2.2: Idealised projection of feldspar structure (Parsons and Lee, 2005)

2.14.1.6 *Barite clay*

A typical barite sample is expected to have 65.70% and 34.30% of the element Barium and SO_4^{2-} respectively. Barite has a specific gravity (SG) of 4.5 in pure state and is often referred to as 'heavy spar'. A high density, chemical inertness and widespread occurrence are the properties that are valued for barites application as a weighting agent in drilling fluids. Colour and chemical purity are important properties when considering the suitability of barite for non-drilling applications. Barite has various uses. For instance, high purity grades of barite with fine and well-sorted particles are used as fillers in marine and industrial paints, in brake lining/friction materials and in plastics (Ekwueme *et al.*, 2015). A specialised use of barite based on its high density and ability to take in radiation is as an aggregate in dense concrete for shielding applications in the nuclear industry and hospital radiation departments. For barite to be used in the non-petroleum industries, it needs to pass through processing through beneficiation methods such as tabling, floatation washing, jigging, heavy metal separation and magnetic separation. Most crude barite requires to be upgraded to some minimum priority of density. The texture and size distribution of various species of gangue minerals affect the beneficiation of barite. Petrographic examination of barite specimens is very vital in this beneficiation process. There has been hypothesis that barites occur in many parts of Cross River State of Nigeria. There have also been attempts to mine barites in some parts of the state using "trial and error" method. This study was undertaken to geologically map out the host rocks and the barite deposits, and determine their relationship with other rocks in the area. It is also the goal of this study to carry out a detailed petrography and geochemical analysis of these barites to determine their suitability for industrial use (Ekwueme *et al.*, 2015). Figure 2.3 shows the structure of barite at ambient conditions projected onto ac-plane.

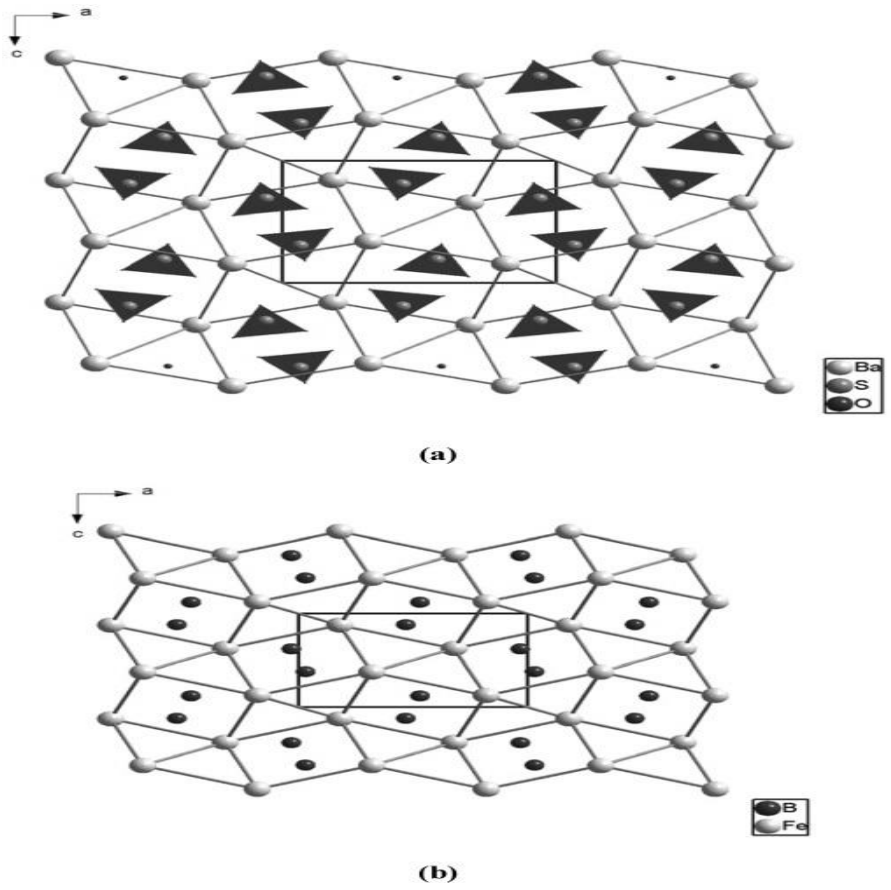

Figure 2.3: (a) Structure of barite at ambient conditions where the Light, medium and dark grey circles represent Ba, S and O atoms respectively. (b) Barite structure where the light and dark grey circles represent Fe and B atoms respectively. (Santamaria-Perez *et al.*, 2015).

2.14.2 Methods of modification of clay minerals

The term activation refers to chemical and physical treatments applied to enhance the adsorption capacity of the clays. There are diverse methods of modification of clay minerals, such as acid activation, thermal activation, microwave treatment and base treatment (Toor, 2011).

2.14.2.1 *Thermal activation of clay minerals*

The thermal activation of clay is a physical treatment, which involves calcinations of clays at high temperature. Clay calcinations lead to changed physical and chemical

properties. The initial change in temperature causes to liberation of inter-layer water. The process of dehydration began afterwards and is accelerated at later. Process of dehydration is reached when an atomic structure is destroyed (Bijeljić, *et al.,* 2017). Activation of Kaolin might be thermal or mechanochemical. Thermal activation is based on kaolin clays heating to the point of kaolin dehydroxylation. Thermal activation to the temperature that is less than it is needed for dehydroxylation leads to insufficiently reactive kaolinite material that containing residues. To the other way, heating up to the temperature higher that it's needed for observed material, effects of sintering and formation of non-active mullite are always expected (Bijeljić, *et al.*,2017).

2.14.2.2 *Base treatment*

Base treatment produces positive surface charge which in turn is helpful to adsorb negatively charged species in higher amounts. The easiest way of producing porous carbons with base surface properties is to treat it at high temperature in inert, hydrogen or ammonia atmosphere. The presence of functional groups affects the adsorption capacity of the produces samples (Bhatnagar *et al.*, 2013).

2.14.2.3 *Microwave treatment*

According to Bhatnagar *et al.* (2013), modification by microwave radiation is gaining wide attention due to its capacity in heating at molecular level leading to homogenous and quick thermal reactions. Compared with conventional heating microwave heating offers many advantages such as heating the material from inside out, therefore there is no need for heats convention through a fluid. Microwave energy provide rapid heating and there is no direct contact between the microwave heating source and the heated materials. It also eases the heating process control, high temperature capacity, energy saving and time and increase the chemical reactivity.

2.14.2.4 *Acid treatment*

Acid activation consists of the reaction of clay minerals with a mineral acid solution, usually Hydrogen chloride (HCl) or Tetraoxosulphate (VI) acid (H_2SO_4). The objective of this is to obtain a partly dissolved material with increased SSA, porosity and surface acidity. The materials thus manufactured are generally available, relatively inexpensive solid sources of protons, and effective in a number of industrially significant reactions and processes (Komadel, 2016). Clay minerals are low-cost adsorbents for the removal of industrial contaminants (Zhao *et al.*, 2015).

The resulting dehydroxylation is connected with the successive release of the central atoms from the octahedral as well as with the removal of Aluminum from the tetrahedral sheets. At the same time, a gradual transformation of the tetrahedral sheets into a three-dimensional framework proceeds. Depending on the extent of acid activation, the resulting solid product contains unaltered layers and amorphous silica, while the ambient acid solution contains cations according to the chemical composition of the clay mineral and the acid used (Komadel, 2016).

Acid treatment improves the structural and adsorption qualities of clay. Acid treatment involves leaching of cations from octahedral sheets, dissolution of impurities like dolcite and calcite, and replacement of exchangeable cations by hydrogen ions. These result in an increase in the specific surface area of clay. (Alver and Sakizci, 2012). The activation force and number of acidic sites are increased by increasing the concentration of acid (Bieseki, 2013).

2.14.1.5 *Factors affecting acid activation*

Acid treatment strips octahedral ions (Fe, Al, Mg) and removes tetrahedral ions from the clay minerals through isomorphous substitution in the crystal lattices. The factors affecting acid activation include:

i. The nature of acid
ii. The mass percentage of acid
iii. The temperature of the activation reaction
iv. Contact time of solid-to-liquid
v. The stirring rate of the mixture
vi. The size of the solid particle and the liquid-to-solid mass ratio.

Of the factors listed above, the factors with the biggest impact on the structural properties and hence the acid activation process are temperature, contact time, solid-to-liquid ration and mass percentage of acid. (Amari *et al*., 2018).

2.15 Characteristic Techniques for Adsorption

2.15.1 X – ray diffractometry (XRD) analysis

According to Oshagbemi (2016), XRD is used to determine the crystallinity of a solid sample by measuring the diffraction pattern which provides detailed information about the electronic distribution of atoms in the solid structure. Furthermore, the author reported that unlike the high intensity peaks generated when the x-rays come in contact with the crystalline compounds in the sample, diffuse peaks distributed in a wide 2 theta (θ) range are produced when the x-rays strike the amorphous compounds in the sample. Thus, this analysis can be applied to determine the crystallinity of the sample with the produced X ray diffractions corresponding to electron density distribution within the crystals.

2.15.2 Fourier transform infrared (FTIR)

Fourier transform infrared spectroscopy (FTIR) was used to investigate the surface functional group of the different clay types. The samples were prepared with KBr, and their functional groups were demonstrated by subjecting their tablets or pellets to chemical or physical forces. (Nwosu *et al*., 2018). This technique is often utilised in determining the characteristic functional groups that are responsible for adsorption. (Liu *et al.,* 2012). FTIR analysis provides spectral information which is a molecular fingerprint for organic, polymeric and inorganic materials. (Davis *et al*., 2010).

2.15.3 Scanning electron microscope (SEM)

This is an electron microscope that produces images of each clay type by scanning with a focused beam of electrons. The interaction between atoms in clay and electrons give signals that can be interpreted to reveal important details about the surface morphology and constituents of the clay type being studied. SEM typically produce resolutions greater than 1nm (Nwosu *et al*., 2018).

2.15.4 Brunnauer, Emmet and Teller (BET)

The BET analysis gives the surface area, pore size and pore volume of the sample. This information determines the adsorption capacity of adsorbents as it gives information of the availability of active sites for adsorption and availability of pore spaces onto which pollutants can be adsorbed.

2.16 Adsorption Studies

2.16.1 Adsorption isotherms

Adsorption is a mass transfer process where substances accessible in a fluid phase are stored onto, or assembled on a solid phase and in this way removed from the fluid (Foo and Hameed, 2010). An adsorption isotherm is an important curve depicting the phenomenon governing the retention (or discharge) or mobility of a substance from the

aqueous permeable media or aquatic environments to a solid phase at a steady temperature and pH (Srivastava *et al*., 2019). Adsorption equilibrium (the ratio between the adsorbed amount with the remaining in the solution) is established when an adsorbate containing phase has been contacted with the adsorbent for sufficient time, with its adsorbate concentration in the bulk solution is in a dynamic balance with the interface concentration (Abdullah *et al*., 2009) a wide variety of equilibrium isotherm models (Langmuir, Freundlich, Brunauer–Emmett–Teller, Redlich– Peterson, Dubinin–Radushkevich, Temkin, Toth, Koble–Corrigan, Sips, Khan, Hill, Flory–Huggins and Radke–Prausnitz isotherm), have been formulated in terms of three fundamental approaches, namely; kinetic consideration, thermodynamics and potential theory (Foo and Hameed, 2010).

2.16.1.1 *Langmuir isotherm*

Langmuir adsorption isotherm, initially designed to depict gas–solid-phase adsorption onto activated carbon, has generally been utilised to measure and differentiate the capacity of various bio-sorbents (Elmorsi *et al.,* 2009). In its formulation, this empirical model assumes monolayer adsorption (the adsorbed layer is one molecule in thickness), with adsorption can only occur at a finite (fixed) number of definite localised sites, that are identical and equivalent, with no lateral interaction and steric hindrance between the adsorbed molecules, even on adjacent sites (Elmorsi *et al.,* 2009). In its derivation, Langmuir isotherm refers to homogeneous adsorption, which every molecule has steady enthalpies and sorption activated energy (all sites have equivalent reactivity for the adsorbate), with no transmigration of the adsorbate in the plane of the surface (Elmorsi *et al.,* 2009). The mathematical expression of Langmuir isotherm is given by;

$$q_e = \frac{q_{max} KlCe}{1 + KlCe} \quad (2.1)$$

Where q_e is the equilibrium adsorbent-phase concentration of the adsorbate (mg g^{-1}), K_L is the langmuir's constant which is related to the energy of adsorption, C_e is equilibrium adsorbent-phase concentration of adsorbate in solution (mg L^{-1}), q_m is maximum adsorbent-phase concentration of adsorbate when surface sites are saturated with adsorbate, (mg adsorbate g^{-1} adsorbent).

The equation can be re-arranged in its linear form as:

$$\frac{1}{qe} = \frac{1}{q_{max}} \frac{1}{Ce} + \frac{Kl}{qmax} \quad (2.2)$$

The plot of $\frac{1}{\mathrm{qe}}$ and $\frac{1}{\mathrm{Ce}}$ gives the representation of the model. K_L and q_{max} values are obtained from the slope and intercept of the curve.

2.16.1.2 *Freundlich isotherm*

This model gives an empirical relationship that describes the adsorption of solutes from a liquid to a solid surface and assumes that different sites with several adsorption energies are involved. (Ayawei *et al.,* 2017) In other words, the Freundlich adsorption isotherm is the relationship between the amounts of contaminant adsorbed per unit mass of adsorbent, q_e and the concentration of the contaminant at equilibrium, C_e.

The Freundlich adsorption isotherm models could either be linear or non-linear model. The non-linear Freundlich isotherm is expressed in Equation 2.3 while the linear form is shown in Equation 2.4 (Gai *et al.,* 2015).

$$q_t = K_f C_e^{\frac{1}{n}} \quad (2.3)$$

$$log_{q_e} = log_{h_f} + \frac{1}{n} log_{c_e} \quad (2.4)$$

where K_f is Freundlich adsorption capacity parameter, (mg/g) $(L/mg)^{1/n}$ and 1/n is Freundlich adsorption intensity parameter.

2.16.1.3 *Temkin isotherm*

Temkin and Pyzhev suggested that, because of the existence of adsorbent–adsorbate interactions, the heat of adsorption should decrease linearly with the surface coverage (Awala and El-Jamal, 2011).

The corresponding adsorption isotherm can thus be adjusted by the following equation:

$$qe = k_1 * lnk_2 + k_1 ln(Ce) \quad (2.5)$$

where k_L is related to the heat of adsorption (L/g), and k_2 is the dimensionless Temkin isotherm constant.

2.16.2 Adsorption kinetics

In adsorption, kinetic study is to an extraordinary degree fundamental; this is to procure bits of knowledge about the performance and mechanism of the adsorption. The solute take-up rate which chooses the residence time required for the consummation of adsorption can be acquired from kinetic analysis (Yazdani *et al.*, 2013). The kinetic models are;

a. Pseudo-first order model
b. Pseudo-second order model
c. Elovich model

These are utilised to look at the adsorption system.

2.16.2.1 *Pseudo-first order kinetic model*

Pseudo-first order response is portrayed by equations 2.6 and 2.7 (Gai *et al.*, 2015).

$$\frac{dq_t}{dt} = k_1(Qe - Qt) \tag{2.6}$$

After integration by applying conditions, $q_t = 0$ at $t = 0$ and $q_t = q_t$ at $t = t$ the equation becomes

$$\log(q_e - q_t) = logq_e \frac{k_i}{2.303} t \tag{2.7}$$

Where q_e and q_t are the amounts adsorbed (mg/g) at equilibrium and at time t respectively, and k_1 is the adsorption rate constant, which can be determined from slope of the linear plot of log ($q_e - q_t$) versus t.

2.16.2.2 *Pseudo-second order kinetic model*

The pseudo – second order kinetic equation is expressed as;

$$\frac{dq_t}{dt} = k_2(q_e - q_t)^2 \tag{2.8}$$

Where q_e and q_t are the adsorption capacity at equilibrium and at time t (mg g^{-1}) respectively and k_2 is the rate constant of the pseudo-second order equation (g mg^{-1} min^1). For the boundary condition $t = 0$ to $t = t$ and $q_t = 0$ to $q_t = q_t$, the integration of equation 2.3 gives the linearised form (Gai *et al.*, 2015).

$$\frac{t}{q_t} = \frac{1}{k_2 q_e 2} + \left(\frac{1}{q_e}\right) t \tag{2.9}$$

Where k_2 is the adsorption rate constant, which can be determined by plotting $\frac{t}{q_t}$ versus t.

2.16.2.3 *Elovich kinetic model*

The Elovich model is used to describe the kinetic nature of a chemisorption process. The model is represented by the equation 2.10.

$$\mathrm{qt} = \frac{1}{\beta e}\ln(\alpha\beta e) - \frac{1}{\beta e} lnt \qquad (2.10)$$

Where q_t is the sorption capacity at time t (mg/min), α is the initial sorption rate (mg g^{-1} min^{-1}) and βe is the desorption constant (g mg^{-1}) during any one experiment (Yu *et al.*, 2013).

2.16.2.4 *Inter particle diffusion model*

The sorption kinetics may alternatively be described from a mechanistic point of view. The overall adsorption process may indeed be controlled either by one or more steps, e.g. film or external diffusion, pore diffusion, surface diffusion and adsorption on the pore surface, or a combination of more than one step. In a rapidly stirred batch, the diffusive mass transfer can be related by an apparent diffusion coefficient, which will fit the experimental sorption rate data. Generally, a process is diffusion-controlled if its rate depends on the rate at which components diffuse towards one another. The possibility of intra-particle diffusion was explored by using the intra-particle diffusion model (Fierro *et al.*, 2008), according to which the amount adsorbed at time t, qt, reads:

$$qt = k_{id}.t^{0.5} + \theta \qquad (2.11)$$

where k_{id} is the intra-particle diffusion rate constant (mg/(g$min^{1/2}$), and θ (mg/g) is a constant related to the thickness of the boundary layer: the larger is the value of θ, the greater is the boundary layer effect.

2.16.3 Thermodynamics study

The thermodynamics study gives data about the spontaneous nature of the adsorption process by deciding the thermodynamic parameters i.e the standard enthalpy (ΔH^o), Gibbs free energy (ΔG^o) and entropy (ΔS^o). These parameters are calculated using Equations 2.12 and 2.13 (Hefne *et al*., 2012).

$$\text{Ln } K_c = \frac{\Delta S}{R} - \frac{\Delta H}{RT} \quad (2.12)$$

$$\Delta G^o = \Delta H^o - T\Delta S^o \quad (2.13)$$

Where K_c is the equilibrium constant, R is the universal gas constant (8.314J/molK) and T is the absolute temperature in Kelvin.

CHAPTER THREE

3.0 METHODOLOGY

3.1 Materials and Chemicals

This research work was carried out in the Quality Control Laboratory of Wupa Waste Water Treatment Plant Abuja, Nigeria.

Influent (raw sewage) just as it was discharged into the manhole of the sewage treatment plant, at latitude N 9 º 11’ 30 longitude E 7 º 24’ 37 at an altitude of 430.98 m and the samples were collected in the morning.

The list of materials/equipment/apparatus used are tabulated in Tables 3.1 and 3.2

Table 3.1: List of clay materials and reagents used

Material and Reagents	Source
Feldspar Clay	Kutigi, Niger State, Nigeria
Plastic Clay	Agaie, Niger State, Nigeria
Barite	Azara, Nassarawa State Nigeria
Red clay	Kujuru, Kaduna State, Nigeria
0.1M Hydrochloric acid (HCl)	WUPA Laboratory
Distilled water	WUPA Laboratory
Influents	WUPA Treatment Plant

The study area for feldspar is situated in Kutigi, in Lavun Local Government Area of Niger State. It lies between longitude 5^{o} 35^{1} E and 5^{o} 39^{1} E and latitude 9^{o} 10^{1} N and 9^{o} 13^{1} N and covers an area of about 39.88 km^{2}. The various tests conducted on the clay as reported by Akhirevbulu *et al*. (2010) showed that Kutigi clay occur as residual clay due

to the weathering of feldspar from feldspathic sandstone. The method of investigation involved an intensive fieldwork, detailed field mapping.

Barite samples were collected from different locations in the area of Wuse in Nasarawa state, Nigeria. The characterization of these samples was carried out using the SEM/EDS (Olugbemi, 2019).

Plastic clay was sourced locally from Agaie, Niger state and identified by (Adejo *et al*., 2018). This involved series of processes whereby the chemical and physical properties and characteristics of raw materials were tested. The Red clay samples were collected and their physico-chemical properties were analysed, (Shuaib-Babata *et al.*, 2016),

Table 3.2: List of equipment and apparatus

Equipment/Apparatus		Model	Manufacture
Muffle furnace	-	Apex 43850	Gallenkamp, England
Oven	-	Memmert 600	Gallenkamp, England
pH meter	-	330i	W T W
Spectrophotometer	-	Spectroquant	Merck, Germany
Heating Mantle	-	EM, 250	Thermo Scientific Uk
Magnetic stirrer	-	Model 300	Gallenkamp, England
Weighing balance	-	ELE	ELE International
Crucible	-		Pyrex, England
Conical flask	0-250 ml	-	Pyrex, England
Beakers	0-250 ml	-	Pyrex, England
Measuring Cylinder	50-250 ml	-	Gallenkamp, England
Mortar and Pestle	0-100 ml	3D model	WUPA Laboratory

3.2 Experimental Procedure

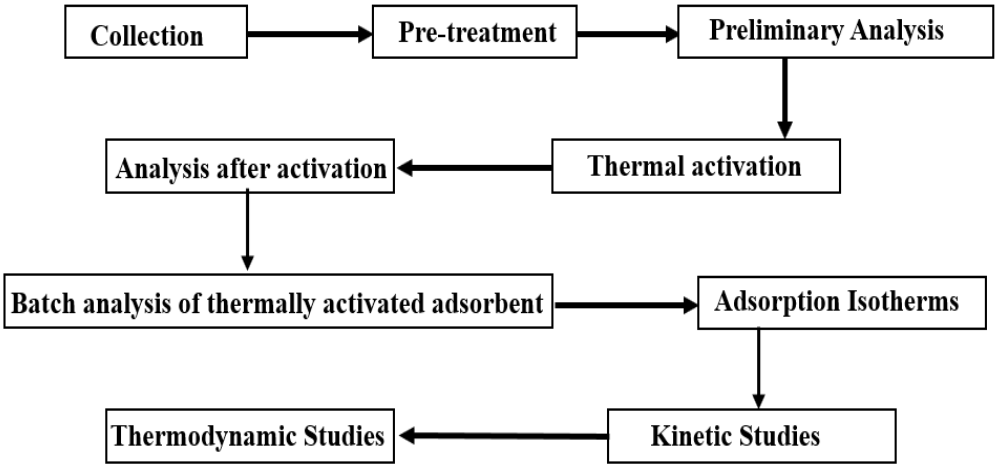

Figure 3.1: Summary of the experimental procedure

3.2.1 Sample collection method

Grab method of sampling was used; sterile sample bottle was dipped into the wastewater at a depth of 30cm, and placed in the direction of the flow of water. The cork was removed and the sample taken, leaving space for agitation. The sample was stored in a cooler and transferred to the laboratory for analysis.

3.2.2 Raw material collection

The raw clay was collected from Kagara (Niger State), Agaie (Niger State), Kaduna State and Plateau state.

3.2.3 Pretreatment of the clay minerals

The raw clay was treated by hand picking to remove dirt and other foreign bodies and after which it was sieved with a 60µm mesh sieve. It was used without any further purification (Awala and El-Jamal, 2011).

3.2.4 Preliminary investigation on different clay minerals

Raw sewage (influent) just as it was discharged in the channel that receives raw wastewater from different homes was collected using a sterile sample bottle and placed in the direction of the flow of water. The sample was properly labeled, then stored in a cooler and transferred to the laboratory for analysis 2 g of each of the four clay minerals were added to 100 ml of the wastewater. Each of the conical flasks was kept in water bath for 24 h after which the content was filtered and analysed using AAS.

3.2.5 Thermal activation of feldspar

As reported by Ali *et al*., 2012 adsorption capacity of natural bentonite was improved by thermal treatment but decreased by acid treatment. The powdered sample was oven dried at 100 ℃ for 24 hours, grounded with mortar to fine particle sizes and screened to 60 µm size. The sieved samples were then calcined in a muffle furnace at temperature of 500, 600 and 700 ℃ for 1 h. The calcination process was done in order to reduce the volatile matter content of the raw clay sample (Bijeljić *et al*., 2017).

3.3 Determination of Physicochemical Parameters of the Water Samples

The physical and chemical properties of the domestic wastewater were characterised in other to determine the constituents and nature of the wastewater. Properties such as pH, Total Dissolved Solids, Conductivity, Chemical Oxygen Demand, Biological Oxygen Demand, Dissolved Oxygen, phosphate and Ammonium were all determined.

The pH and temperature were measured using the standard pH electrode meter (Hanna HI 98129 pH EC/TDS Waterproof Combo Tester/Meter) as reported by Muriuki (2015). Similarly, the Total dissolved solids (TDS), Total suspended solids (TSS), Electrical conductivity (EC), ammonium and phosphate were analyzed.

3.3.1 Determination of biochemical oxygen demand (BOD_5)

This was carried out using respirometric method, the standard method recognised by U.S. EPA and a labeled Method 5210B in the Standard Methods for Examining water and waste water. The BOD bottles were rinsed with the appropriate samples and labelled. The samples were measured and saturated for 10 min. The adequate volume of sample (164 mL) to be used was measured using the measuring flask. It was then poured into the BOD bottle, immediately the quiver was dropped, 2 pellets of NaOH (sodium hydroxide) was added. After that, it was covered with the readout and labelled properly. The BOD bottle was then placed on a magnetic stirring tray and stirred before it was taken for storage in an incubator for 5 days at 30 ºC before the final reading was taken. The dissolved oxygen (DO) for the final solution and incubated samples at the end of the 5^{th} day were determined.

3.3.2 Determination of chemical oxygen demand (COD)

This was carried out using closed reflux colorimetric method and was determined using a COD reactor (HACH company) by Merck KGaA kit, 64271 Darmstadt, Germany, according to the manufacturer's instruction. The bottom sediment in the reaction cell (test tube) was suspended by swirling 3 mL of the sample was pipette and carefully allowed to run from the pipette down the inside of the tilted test tube (reaction cell) on the reagent (potassium dichromate, silver sulphate and sulphuric acid). Then the screw cap was tightly attached to the cell. The cell was only held by the screw cap and the content of the reaction cell was vigorously mixed. After that, the cell was heated at 148 ºC in the preheated thermo reactor for 2 h. The hot cell was then removed from the thermo reactor and allowed to cool in a test tube rack. After 10 min the cell was swirled and returned to the rack for complete cooling to room temperature (cooling time at least 30 minutes). The COD concentration was then measured in the spectrophotometer.

3.3.3 Determination of total suspended solid analysis (TSS)

This was carried out using gravimetric method. Two micro filter papers were pre-treated using distilled water and suction pump, which were then flood until the proposed volume of distilled water was exhausted. The filter paper was taken to the hot air oven and subjected to heat at 105 ℃ for 2 h. The desiccator was taken out and weighted using a weighing balance. 200 mL of each of the samples were measured in two separate beakers. Label properly (beaker A-Influent, beaker B-effluent) and run the process consecutively for each of the samples. Stir the sample for some minutes using each of the magnetic stirrers with a stirrer inside each of the samples.

Insert the filter papers into the suction pump and carefully pour the samples (being concentrated at the center of the filter paper for easy accumulation of residue), shake until the sample is exhausted in the beakers. Dry the fitter papers in the hot air oven for 2 h at 105℃ cool the desiccator for 10-15 minutes and weigh the filter papers using the weighing balance. Record as A (weight of filter paper + residue)

TSS = (A-B/sample volume) * 1000 mg/L (3.1)

3.3.4 Determination of phosphate (PO_4^{3-})

This was carried out using colorimetric method and was determined using photometer (Palintest Photometer 7100). 5 ml of pre-treated sample was pipette into a test tube. 5 drops of PO_4^{3-} was added and mixed. 1 level blue micro spoon of PO_4^{3-} was added. It was then shaken vigorously until the reagent was completely dissolved. After that, it was left to stand for 5 min. Then the sample was filled into the cell and measured in the photometer.

3.3.5 Determination of ammonium (NH_4^+)

This was carried out using colorimetric method and was determined using photometer (Palintest Photometer 7100). 5 mL of reagent NH_4^+ was pipette into a test tube. 0.20 mL of pre-treated sample was added and mixed. 1 level blue micro spoon of reagent NH_4^+ was added and shaken vigorously until the reagent was completely dissolved. It was then left to stand for 15 min. Then the sample was filled into a cell and measured in the photometer.

3.4 Atomic Absorption Spectroscopy (AAS)

Atomic absorption spectroscopy (AAS) is described as one of the analytical techniques that give reliable result for the metal concentration of a sample (Bashir, 2012). AAS makes use of the amount of light that passes through a cloud of atoms (absorbance). This gives a quantitative determination of the amount of element present as each element has its own unique pattern of wavelength.

3.5 Batch Adsorption Study

In the batch adsorption 0.5 g of the thermally activated feldspar at 600 ℃ was placed in a set of 250 mL conical flasks containing 50 mL. The flasks were placed in a water bath at 30 ℃ at a shaker speed of 200 rpm and at 0 - 60 min. The effects of initial pH, contact time, initial concentration and contact temperature were investigated. The solid was separated from liquid by centrifuging the mixture at 103 rpm for 2 min. The ultimate content was used to evaluate the adsorption capacity and efficiency. Each experiment was repeated five times. The solution was determined using Atomic Absorption Spectroscopy (Li *et al.*, 2014).

3.5.1 Determination of removal efficiency

The removal efficiency of the adsorbents on the ion adsorption was determined using Equation 3.2

$$\text{Removal efficiency}(\%) = \frac{(C_0 - C_e)}{C_0} \times 100 \quad (3.2)$$

where C_o and C_e (mL) are the initial and final concentrations of ions.

3.5.2 Determination of effect of pH on removal efficiency

The pH of the solution is one of the most critical parameters in the adsorption process; it affects surface charge of the adsorbent material and the degree of ionization and specification of adsorbate. The effect of pH on the removal efficiency was studied at different pH values ranging from 2.0 to 10.0. Samples of 50 mL of working solution containing 12 mg/L of phosphate ion and 35 mg/L of ammonium ion were maintained at different pH of 2, 4, 7, 8, and 10. The pH of each solution was adjusted with 0.1M HCl solution with the aid of pH meter. To each sample was added dose of 0.5 g thermally activated feldspar in 250 ml Pyrex flasks. The content of each flask was subjected to agitation at constant speed of 150 rpm for 30 min. Thereafter, the filtrates were individually collected and analysed using AAS.

3.5.3 Effect of initial concentration and contact time on adsorption of phosphate ion and ammonium ion.

The concentration increases the accessibility of pores for adsorbate molecules and increases interactions at solid–liquid interface. In studying the effect of initial concentrations of the ions (impurities) and contact time with the adsorbent (feldspar), different initial concentrations of phosphate ions (4 mg/L, 6 mg/L, 8 mg/L and 12 mg/L) and ammonium ions (15 mg/L, 20 mg/L, 25 mg/L and 35 mg/L) in a 50 mL solutions of

pH 6.2 were separately contained in 250 mL pyrex flasks. 0.5 g of the feldspar adsorbent was separately added to the solutions. The contents were then subjected to constant agitation for 5 min at ambient temperature of 30 ^{0}C. The different filtrates were thereafter collected and analysed using AAS. This procedure was then repeated for an increasing contact time of 10, 20, 30, and 60 min separately.

3.5.4 Determination of effect of adsorbent dose

Precise measurements of 0.4, 0.8, 1.2, 1.6 and 2.0 g of thermally activated feldspar were dispensed separately into five 250 mL conical flasks. Then, 50mL of the working solution of 12 and 35 mg/L of phosphate and ammonium ion were added to the content of the five flasks in turn (Behera *et al.,* 2012). This was followed by agitation at constant speed of 200 rpm, for a contact time of 30 min. The mixtures in each flask were filtered by the use of filter papers and the different filtrates were collected and analysed.

3.5.5 Effect of temperature

In order to examine the effect of temperature on the adsorption process, 1.2 g of the feldspar adsorbent (optimum dosage) was poured into 100 mL of the domestic wastewater and set in a water bath shaker set at 30˚C at a steady contact time of 30 min. The mixtures in each flask were then filtered by the use of filter papers and the different filtrates were collected and analysed using the AAS. The methodology was repeated for varying temperatures of 30, 40, 50, 60 and 70 ˚C.

3.6 Characterization of the Raw and Activated Clay

The effect of raw and activated clay minerals was analysed with various characterization methods such as Thermo-gravimetric Analysis (TGA), Fourier Transformed Infrared Spectroscopy (FTI-R), Brunauer- Emmett- Teller (BET), Scanning Electron Microscope (SEM), X-ray fluorescence (XRF) spectrometry.

3.6.1 Thermo-gravimetric Analysis (TGA)

The TGA of the sample was conducted using Perkin Elmer TGA 4000 instrument. 0.5 g of the sample was placed into the instrument via the top loading pan and covered. Nitrogen gas supplied to the instrument and its flow rate was set to 50 mL/min before analysis was conducted. Data generated were captured and reported accordingly (Enyeribe *et al*., 2017).

3.6.2 Fourier Transformed Infrared Spectroscopy (FTIR)

The infra-red spectrometer analysis of the adsorbent was performed using Bruker Alpha II infra-red spectrometer. In carrying out the analysis, the spectrometer was powered and allowed to warm up for 5 min after which sample was mixed with alkali halide potassium bromide (KBr) and compressed into a thin transparent pellet using a hydraulic press, before being placed in the standard sample compartment of the spectrometer. The transmission spectra of composite films were recorded at ambient temperature and the sample was scanned from 4000 to 400 cm^{-1} with resolution of 0.4 cm^{-1} (Jose and Kuriakose, 2017).

3.6.3 Brunauer- Emmett- Teller (BET)

The BET was carried out by nitrogen adsorption-desorption method using nitrogen with an autosorb BET apparatus, Micrometrics ASAP 2020, surface area and porosity analyzer. These were carried out to determine the surface area and porosity of the adsorbent before and after activation.

3.6.4 X-ray fluorescence (XRF) spectrometry (specification)

X-rays fluorescent (XRF) analysis was carried out using PAN analytical XRF spectrometer (MiniPal 4). X-RF analysis was carried out by placing 2 g of 100 µm size of the sample on a clean stainless steel lid which was placed in the cubicle of the

spectrometer to determine its elemental composition. When X-rays irradiated the sample, the system software measures the individual component wavelengths of the fluorescent emission produced by atoms in the sample and compares to standard wavelengths of atoms of known elements.

3.6.5 Determination of Scanning Electron Microscopy (SEM)

This was carried out according to the method in which a ASPEX 3020 scanning electron microscope, model SIRIUS50/3.8 with an attached energy dispersive X-ray spectroscopy (SEM/EDX) machine is used to generate images of the sample. The machine is operated at an accelerated voltage of 5 to 15 kV to determine the samples elemental composition.

3.7 Adsorption Studies

3.7.1 Adsorption isotherm

The equilibrium characteristic of the adsorption process was investigated using the Langmuir Freundlich and Temkin isotherm models.

The Langmuir isotherm model is based on number of active sites. The Langmuir equations are as expressed in Equations 3.3 and 3.4

$$q_e = \frac{\mathrm{qmaxKlCe}}{1 + \mathrm{KlCe}} \tag{3.3}$$

$$\frac{1}{\mathrm{qe}} = \frac{1}{\mathrm{qmax}}\ \frac{1}{\mathrm{Ce}} + \frac{\mathrm{Kl}}{\mathrm{qmax}} \tag{3.4}$$

Where q_e is the equilibrium adsorbent-phase concentration of the adsorbate (mg g^{-1}), K_l is the langmuir's constant which is related to the energy of adsorption, C_e is equilibrium adsorbent-phase concentration of adsorbate in solution (mg L^{-1}), q_{max} is maximum

adsorbent-phase concentration of adsorbate when surface sites are saturated with adsorbate, (mg adsorbate g^{-1} adsorbent) (Yazdani *et al*., 2013).

The plot of $\frac{1}{qe}$ and $\frac{1}{Ce}$ gives the representation of the model. K_l and a_l values are obtained from the slope and intercept of the curve.

The Freundlich isotherm endorses the heterogeneity of the surface and assumes that the adsorption occurs at sites with different energy of adsorption. Freundlich isotherm is expressed in Equation 3.5 as;

$$\log q_e = \log k_f + \frac{1}{n} \log C_e \quad (3.5)$$

Where K_f ($mg^{1-1/n}L^{1/n}g$) and n is the Freundlich constant, q_e and Ce are the uptake capacity and equilibrium concentration. (Ayawei *et al*., 2017)

The Temkin isotherm examines the adsorbent-adsorbate interactions and gives the relationship between heat of adsorption and active sites availability. The model is represented by Equation 3.6;

$$Qe = k_1 * lnk_2 + k_1 \ln(Ce) \quad (3.6)$$

where k_1 is related to the heat of adsorption (L/g), and k_2 is the dimensionless Temkin isotherm constant. These isotherms were studied to determine the model that best fits for the adsorption of phosphate ion and ammonium ion from the wastewater.

3.7.2 Adsorption kinetics studies

To carry out adsorption study, the study of the kinetics of the process is fundamental to a very large extent. The kinetic models of pseudo-first order model, pseudo-second order model and Elovich model were utilised to study the adsorption system.

The Pseudo-first order response is represented by the Equation 3.7;

$$\frac{dq_t}{dt} = k_1(Qe - Qt) \quad (3.7)$$

After integration by applying conditions, $q_t = 0$ at $t = 0$ and $q_t = q_t$ at $t = t$ the equation becomes

$$Log\ (q_e - q_t) = log q_e - \frac{k_i t}{2.303} \quad (3.8)$$

Where q_e and q_t are the amounts adsorbed (mg/g) at equilibrium and at time t respectively, and k_1 is the adsorption rate constant, which can be determined from the slope of the linear plot of log ($q_e - q_t$) versus t

The graph of log (q_e- q_t) against t was plotted from which q_e , k_1 and R^2 values were obtained.

The pseudo – second order kinetic equation is expressed as

$$\frac{dq_t}{dt} = k_2(q_e - q_t)^2 \quad (3.9)$$

Where q_e and q_t are the adsorption capacity at equilibrium and at time t (mg g^{-1}) respectively and k_2 is the rate constant of the pseudo-second order equation ($gmg^{-1}min^1$). For the boundary condition $t = 0$ to $t = t$ and $q_t = 0$ to $q_t = q_t$, after integration, the equation becomes

$$\frac{t}{q_t} = \frac{1}{k_2 q_e 2} + \left(\frac{t}{q_e}\right) t \quad (3.10)$$

The graph was obtained by plotting $\frac{t}{q_t}$ versus t from which q_e, k_2 and R^2 were calculated and obtained.

The Elovich model is represented by the Equation 3.11

$$\mathrm{qt} = \frac{1}{\beta e}\ln(\alpha\beta e) - \frac{1}{\beta e} lnt \qquad (3.11)$$

Where q_t is the sorption capacity at time t (mg/min), α is the initial sorption rate (mg g^{-1} min^{-1}) and βe is the desorption constant (g mg^{-1}) during any one experiment (Yu *et al.*, 2013). The graph of q_t against lnt was plotted from which the α, βe and R^2 values were calculated and obtained.

The parameters obtained from the three kinetic models tested were analysed and compared to determine the model that best fits the experimental data obtained.

3.7.3 Thermodynamics of adsorption

Standard free energy (Δ*G*°) was calculated from the Equations 3.12 and 3.13 given in chapter two.

ln

$$K_c = \frac{\Delta \mathrm{S}}{R} - \frac{\Delta \mathrm{H}}{RT} \qquad (3.12)$$

$$\Delta \mathrm{G}^{O} = \Delta \mathrm{H}^{0} - \mathrm{T}\Delta \mathrm{S}^{0} \qquad (3.13)$$

Where K_c is the equilibrium constant, R is the universal gas constant (8.314J/molK), T is the absolute temperature in Kelvin, ΔS°S standard entropy, G standard free energy and H standard enthalpy.

The graph of ln K_c against 1/T was plotted from which ΔG^o, ΔH^o, ΔS^o and K_c were calculated to determine the spontaneity and enthalpy of the adsorption process.

3.8 Statistical Error Validity of Adsorption Model

Sum of square error and chi square error expressed by equation 3.7 and 3.8 was used to validate isotherm and kinetic model (Foo and Hameed 2010)

$$SSE = \sum_{i=1}^{n} (q_{cal} - q_{exp})^2 \quad (3.14)$$

$$X^2 = \sum_{i=1}^{n} \frac{(q_{exp} - q_{cal})}{q_{cal}} \quad (3.15)$$

CHAPTER FOUR

4.0 RESULTS AND DISCUSSION

4.1 Preliminary Analysis on the Clays Minerals

Akhirevbulu *et al*. (2010) reported that the soil exposures were observed and described based on their colour, texture, structural elements and mode of occurrences. Barite occurs as white, reddish brown and clear varieties with specific gravity ranging between 3.5 and 4.4 (Falade and Adeyeye, 2016). Barite occur in Nigeria as vein infilling materials associated with lead-zinc lodes and veins in both the pre-cambrain basement and Cretaceous sedimentary rocks of lower and middle Benue valley. The barite showed

distinct specific gravities ranging between 4.38 and of 4.11 Olugbemi, (2019), which met the API standard.

The mineral composition of plastic clay as revealed from the characterization of the sample with X-ray flurescence, consists mainly of silica 58.75 % and alumina 27.6 % with metallic oxides present in trace or small amount (Adejo *et al*., 2018).

Shuai-Babata *et al*, (2016) reported that the soil in the upland areas are rich in red clay and sand but poor in organic matter. The results showed that the tested clay samples belong to alumino-silicate group.

The wastewater samples were properly labeled, then stored in a cooler and transferred to the laboratory for analysis; 2 g of each of the four clay minerals were added to 100 mL of the wastewater at 40 ℃ for 24 h. The results of the physiochemical analysis of the clay minerals are as shown in Table 4.1a. The percentage reduction and removal efficiency of the different clay minerals were also calculated and the results shown in Table 4.1b.

Table 4.1a: The physicochemical analysis of raw domestic wastewater using clay minerals

Parameter	Raw wastewater	Plastic Clay	Red clay	Barite	Feldspar	WHO'S Limit for effluent	F.M.Envlimit for effluent
pH	6.689	7.443	7.49	7.601	7.527	6.5-8.5	06-Sep
Temp (^{0}C)	26.1	24.4	24	23.7	23.3	< 40	<40
Conductivity (µS/cm)	580	548	570	672	643	1250	
NH_4^+(mg/L)	50	15	25	25	5	10	10
PO_4^{3-}(mg/L)	14.4	3	2.2	0.6	3.75	5	5
Fe_2^+(mg/L)	2	1.15	0.8	0.25	1.05	1	
COD	750	120	300	200	280	80	80
BOD	350	40	120	80	120	30	50
TSS	1000	40.5	40	12	41	30	30

Table 4.1b: The analysis of raw domestic wastewater in percentage removal using clay minerals

Parameter	Raw Sample	Plastic Clay	Red clay	Barite	Feldspar
NH_4^+	50	70.00%	50.00%	50.00%	90.00%
PO_4^{3-}	14.40	79.17%	84.72%	95.83%	73.96%
Fe^{2+}	2.00	42.50%	60.00%	87.50%	47.50%
COD	750.00	84.00%	60.00%	73.33%	62.67%
BOD	350.00	88.57%	65.71%	77.14%	65.71%
TSS	1000.00	95.95%	60.00%	95.95%	95.90%

As clearly observed from the Tables 4.1a-4.1b, comparing the removal efficiencies of the different clay minerals tested in the removal of the pollutants, it was observed that the feldspar clay gave a better result (higher removal efficiency) in ammonium than the other clay minerals especially in the removal of the pollutants under study (ammonium ion). Hence, the feldspar was selected for use as adsorbent in the removal of ammonium and phosphate ions from domestic wastewater.

4.2 Characterization of Raw and Thermal Activated Clay Minerals

4.2.1 Brunauer Emmet Teller (BET) analysis of the clay minerals

The surface area, pore size and pore volume of the clay minerals were determined by Brunauer Emmet Teller (BET) surface area analysis and the results are shown in Table 4.2.

Table 4.2: BET of the clay minerals

Sample	Surface Area m^2/g	Pore Volume cc/g	Pore size nm
Plastic clay	110.9	0.0519	2.096
Feldspar	332.8	0.2123	2.433
Barite	329.0	0.1775	2.452

As shown in Table 4.2, the feldspar adsorbent is seen to be higher in surface area, pore volume and pore size than plastic clay by 66.7 %, 75.5 % and 13.9 % respectively. The feldspar adsorbent was similarly seen to be higher in surface area and pore volume than barite by 1.14 % and 7.8 % respectively. This implies that feldspar adsorbent will provide more active sites for adsorption compared to plastic clay and barite, hence its selection for use in the adsorption study (Awala and El-Jamal, 2011).

4.2.2 XRF analysis of feldspar

The mineral constituents of Feldspar were analysed with XRF machine to ascertain the chemical composition of the clay samples and the results are presented the Table 4.3.

The Table 4.3 shows that the mineral composition of feldspar clay as revealed from the characterization of the sample with X-ray flurescence, the clay mineral consists mainly of silica and alumina, with metallic oxides present in trace or small amount. This results agrees with (Al-Anber, 2015) although the silica content of the clay mineral was higher which could be due to the origin of formation of the feldspar clay.

Table 4.3: XRF analysis of feldspar clay sample

Element	Concentration	Peak (CPS/MA)
Fe_2O_3	0.99%	3027
SiO_2	80.48%	4586
Al_2O^3	14.16%	211
MgO	2.78%	3
P_2O_5	0.20%	49
SO_3	0.07%	35
TiO_2	0.03%	123
MnO	0.05%	510
CaO	0.53%	861
K2O	5.20%	5106
CuO	0.00%	7
ZnO	0.00%	27
Cr_2O_3	0.00%	7
V_2O_5	0.00%	7
As_2O_3	0%	0
PbO	0.02%	10

4.2.3 Thermogravimetric Analysis of Raw Feldspar (TGA)

Figure 4.1 shows the Thermogravimetric Analysis (TGA) of raw feldspar. Clay calcination leads to changed physical and chemical properties (Li *et al.*, 2014). The weight variance is categorised into 3 regions (phases). In Phase I (25 ℃ - 280 ℃) correspond to the loss of moisture content in the raw feldspar. Phase II which corresponds

to temperature range of 280 ℃ - 470 ℃ gave a sharp drop in the weight of the feldspar. This could be attributed to the loss of volatile content present. Phase III which starts from the temperature of 470 ℃ depicts the genesis of thermal decomposition whereby the calcium carbonate in powder is converted to calcium oxide due to the liberation of carbon (IV) oxide. Process of dehydration is completed when an atomic structure is destroyed, heating up to the temperature higher that it's needed for observed material, effects of sintering and formation of non-active mullite are always expected (Bijeljić *et al*, 2017).

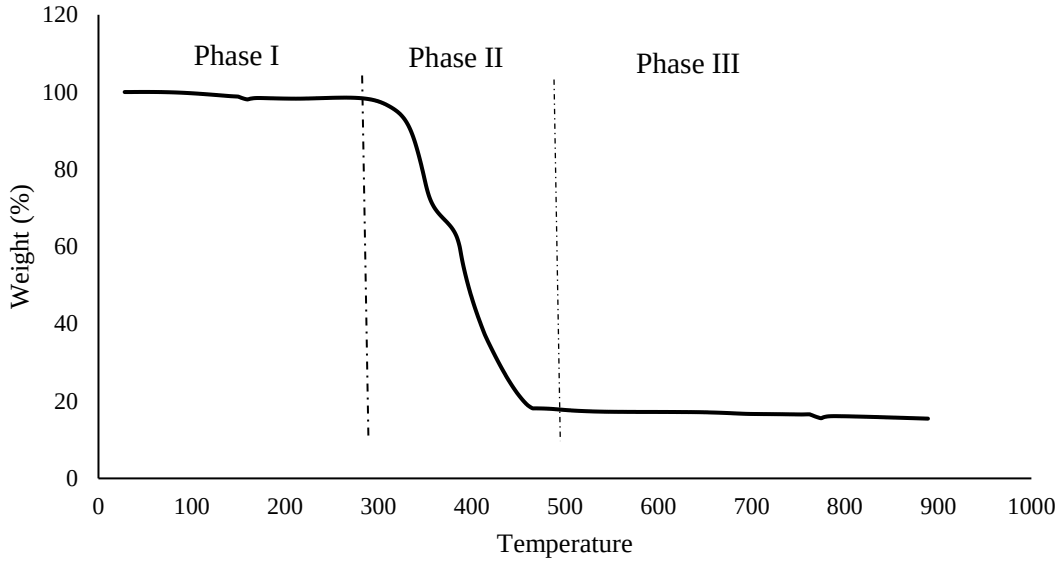

Figure 4.1: Thermo-gravimetric analysis (TGA) plot of feldspar adsorbent

4.2.4 Thermal activation of feldspar

Heat treatment was carried out on 80 g samples in the laboratory furnace at different temperatures (500, 600, and 700 ℃) for 60 min. The samples were quenched at room temperatures on heating at ambient conditions to avoid crystallization. The samples were used to adsorb pollutant ions and the optimum temperature was determined (Ilić *et al.*, 2010).

The effect of the calcination temperature on the adsorption efficiency of the calcinated feldspar was investigated, and the results are shown in Tables 4.4. The BET result shown in Table 4.4 shows that increasing temperature increases the surface area and pore volume of the adsorbent up till 600 ℃. It was observed that from Tables 4.5a and 4.5b that the adsorption efficiency gradually increased when calcination temperature increased from 500 to 600 ℃, however, the adsorption efficiency reduced a bit when the calcination temperature was increased to 700 ℃. The main reason for this is that increasing calcination temperature helps to increase the specific surface area and develop cracks from the surface of the mineral to its center (Kerisit and Liu, 2012). The slight negative effect of the calcination temperature observed at 700 ℃ indicated that the optimum calcination temperature is between 600 ℃ and 700 ℃. Studies have shown that thermal treatment generates more adsorption sites for pollutants.

Table 4.4: BET of Thermally Activated Feldspar

Sample	Surface Area m^2/g	Pore Volume cc/g	Pore width nm
Raw Feldspar	332.8	0.218	2.433
Feldspar at 500 ℃	352.5	0.216	2.433
Feldspar at 600℃	533.9	0.272	2.105
Feldspar at 700℃	418.3	0.211	2.100

Table 4.5a: Effect of calcination temperature on removal efficiency

Temperature		500 ^{0}C			600 ^{0}C			700 ^{0}C		
Time (mins)	RAW	10	30	60	10	30	60	10	30	60
Phosphate	12	8	7.3	5.1	4.7	4.4	4.2	6.9	7	5.9
Ammonium	20	16	14.4	9.8	9.8	8.1	7	10.9	11	11.9

Table 4.5b: Effect of calcination temperature on removal efficiency (in percentage)

Temperature	500 ^{0}C			600 ^{0}C			700 ^{0}C		
Time (mins)	10	30	60	10	30	60	10	30	60
Phosphate removal (%)	33.30	39.20	57.50	60.80	63.30	65.00	42.50	41.70	50.80
Ammonium ion removal (%)	20.00	28.00	51.00	51.00	59.50	65.00	45.50	45.00	40.50

4.2.5 Fourier transform infrared spectra (FTIR) analysis of feldspar

The FTIR spectroscopy analysis was used to study the appearance and disappearance of some bands associated with functionalization reactions on the feldspar sample. The FTIR pattern for the raw feldspar is as presented in Figures 4.2a while the raman spectra for the treated and used feldspar adsorbent are as presented in Figures 4.2b and 4.2c respectively**.**

The FTIR spectra for the raw felspar as shown in Figure 4.2a gave a characteristic wide band of 3473.91 cm^{-1} which corresponded to the O-H strech,free hydroxyl group. Likewise, the band observed at 2360.95 cm^{-1} corresponded to the amine (N-H) group streching . The bands at 2000.25 cm^{-1}, 1803.5 cm^{-1} , 1639.55 cm^{-1} and 534.30 cm^{-1} corresponded to carbonyl(C-O), alkene (C=C), carbonyl (C=O) and M-O groups respectively as reported (Ler and Stanforth., 2013).

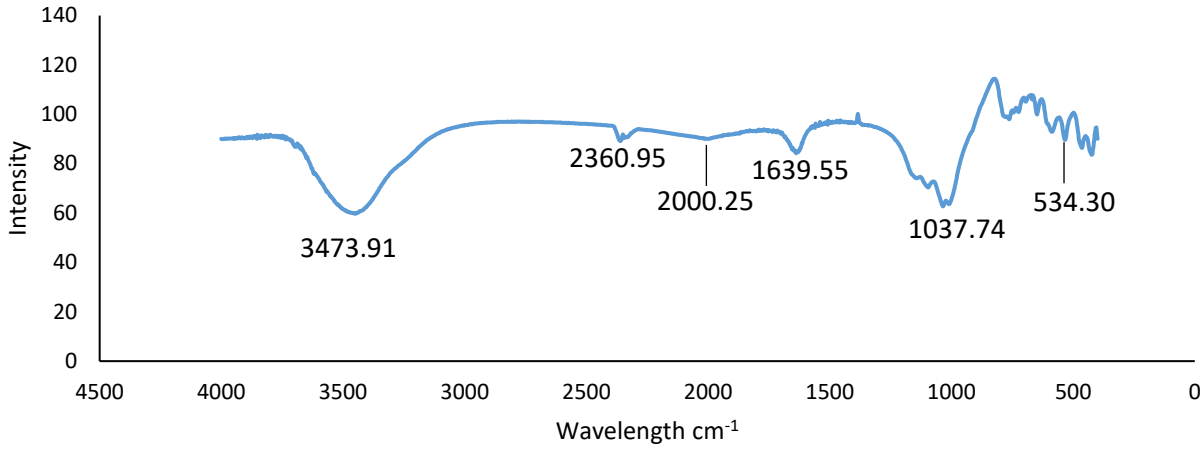

Figure 4.2a: FTIR of Raw feldspar

The raman spectra for the treated felspar as shown in Figure 4.2 gave a characteristic wide double band of 3126 cm^{-1} and 2876 cm^{-1} which corresponded to the N-H group stretching. The bands at 2392 cm^{-1}, 1786 cm^{-1} and 872 cm^{-1} corresponded to C-O, C=O and C-H groups respectively, Likewise, the band observed at 420 cm^{-1} corresponded to the S-S group streching as reported (Awala and El-Jamal, 2011).

Table 4.6a: Bands and suspected bonds in raw feldspar

IR	Band	Bond suspected
4000-3800	3473.91	O-H strech,free hydroxyl
3300-2900	2360.95	N-H group streching
2400-2150	2000.25	C-O
2000-1950	1803.5	C-C
1790-1660	1639.55	C=O
585-570	534.30	M-O

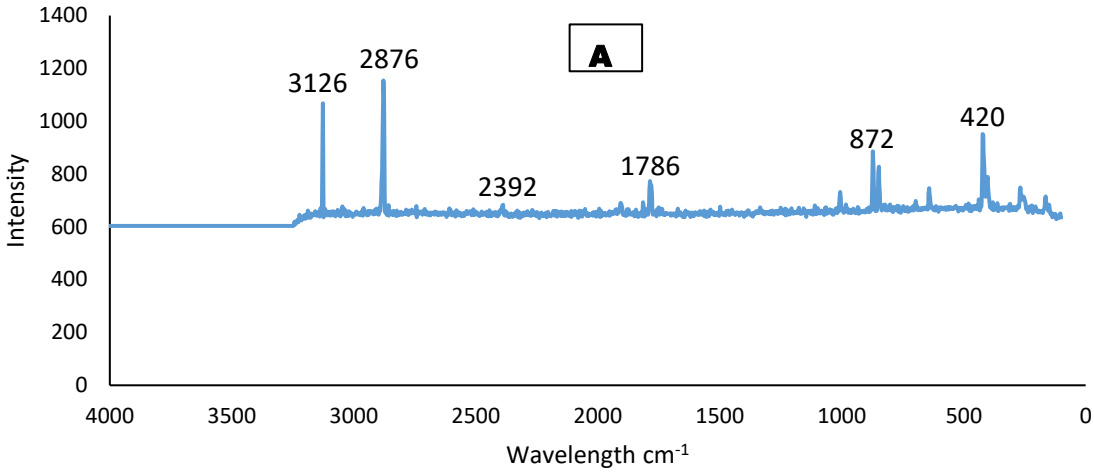

Figure 4.2b: Raman spectra of treated feldspar adsorbent

Table 4.6b: Bands and suspected bonds in treated feldspar

IR	Band	Bond suspected
3300-2900	3126, 2876	N-H group streching
2400-2150	2392	C-O Stretch
1790-1660	1786	C=O Stretch
1615-950	872	N-H wag
500-430	420	S-S Stretch

The raman spectra for the used felspar as shown in Figure 4.2c gave a characteristic triple bands of 3218 cm^{-1}, 2876 cm^{-1} and 2782 cm^{-1} which corresponded to the N-H group stretching. The bands at 2000.25 cm^{-1}, 1803.5 cm^{-1}, 1564 cm^{-1} and 872 cm^{-1} corresponded to C-O, C-C, C=O and C-H groups respectively, Likewise, the band observed at 420 cm^{-1} corresponded to the S-S group streching as reported (Liu *et al.*, 2012)

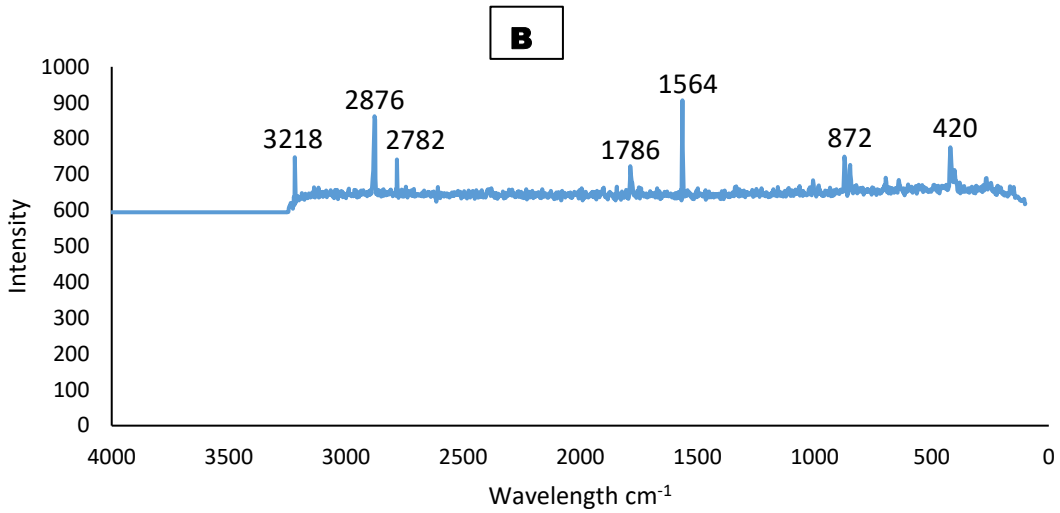

Figure 4.2c: Raman spectra of used feldspar adsorbent

Table 4.6c: Bands and suspected bonds in used feldspar

IR	Band	Bond suspected
3300-2900	3218, 2876, 2782	N-H group stretching
2400-2150	2000.25	C-O
2000-1950	1803.5	C-C
1790-1660	1786, 1564	C=O
1615-950	872	C-H
500-430	420	S-S Stretch

These functional groups identified on the structures of the feldspar adsorbent could act as reaction sites for the adsorption of pollutants (Yazdani *et al.*, 2013).

As shown in Figure 4.2d, the bands of some groups of the treated feldspar had changed in their amplitudes and positions after the treated feldspar was used for adsorption. The N-H and C=O groups had shifted from 3126 cm^{-1} and 1786 cm^{-1} to 3218 cm^{-1} and 1564 cm^{-1} respectively. These shift in bands indicated that the functional groups played an important role in the adsorption process (Awala and El-Jamal, 2011).

Comparing the Figure 4.2c and Figure 4.2d, the intensity of A increased when subjected to the adsorption whereas the wavenumber decreased. Hence, adsorption process leads to increased intensity and decreased wavenumber.

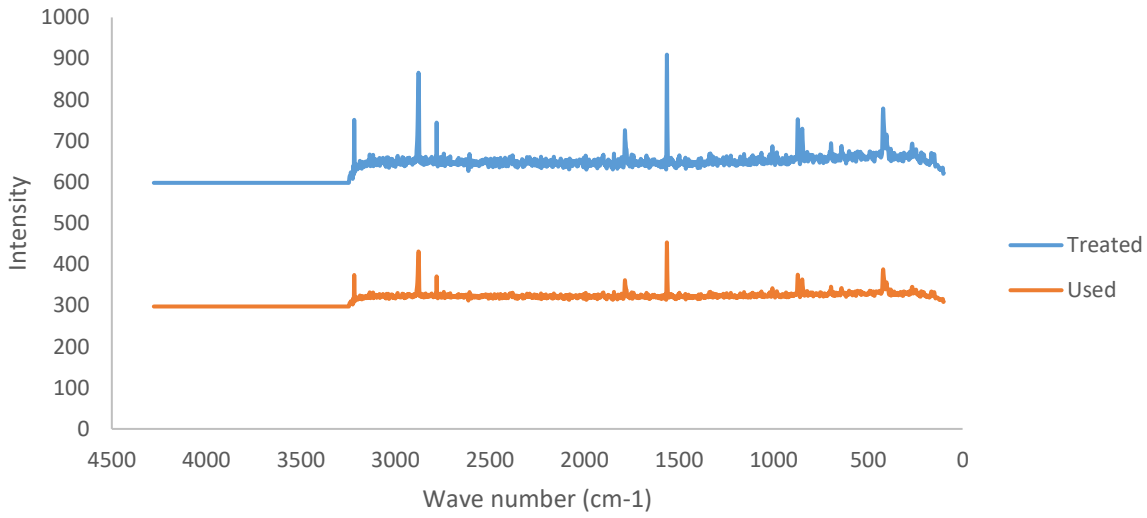

Figure 4.2d: Combined Raman spectra of used and treated feldspar adorbent

4.2.6 Scanning electron microscopy (SEM) analysis of feldspar

The SEM images of the raw and thermally activated feldspar are shown in Figures 4.3 and 4.4 respectively. It was observed that the structure of raw feldspar particles consisted of crystalline and irregular layered structures, whereas the thermally activated feldspar displayed relatively smooth structure with cracks on the surface. The significant difference in the surface morphology confirms the presence of more pores and cracks on the surface which could supply a large surface area for the reaction. (Yazdani, *et al.*, 2013).

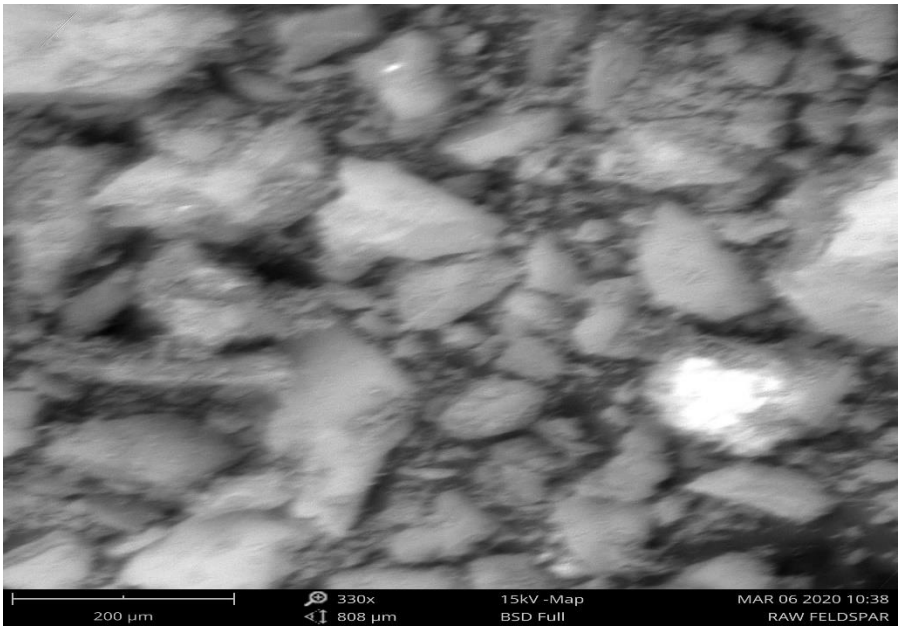

Figure 4.3a: SEM of raw feldspar adsorbent at magnification of (330X)

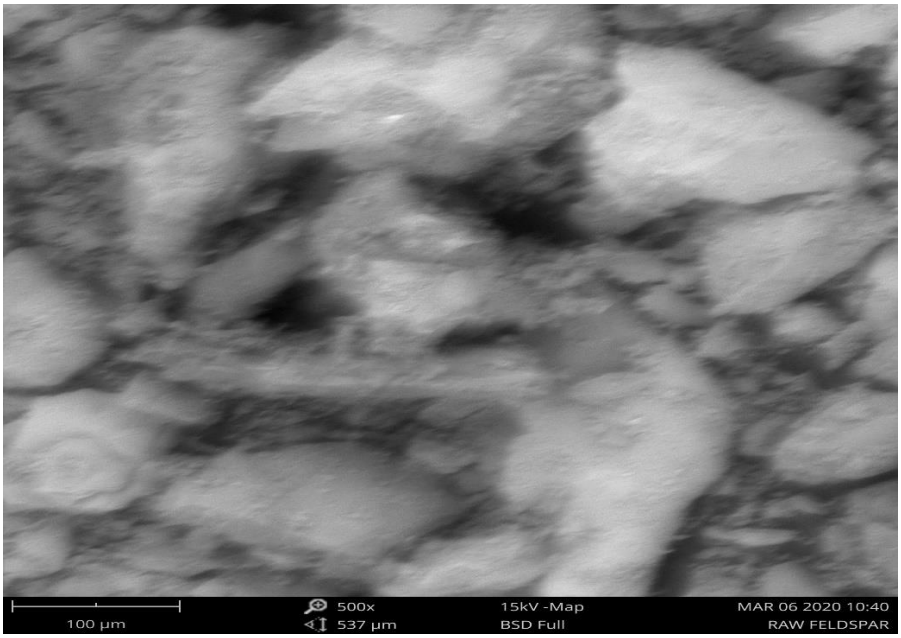

Figure 4.3b: SEM of raw feldspar adsorbent at magnification of (500X)

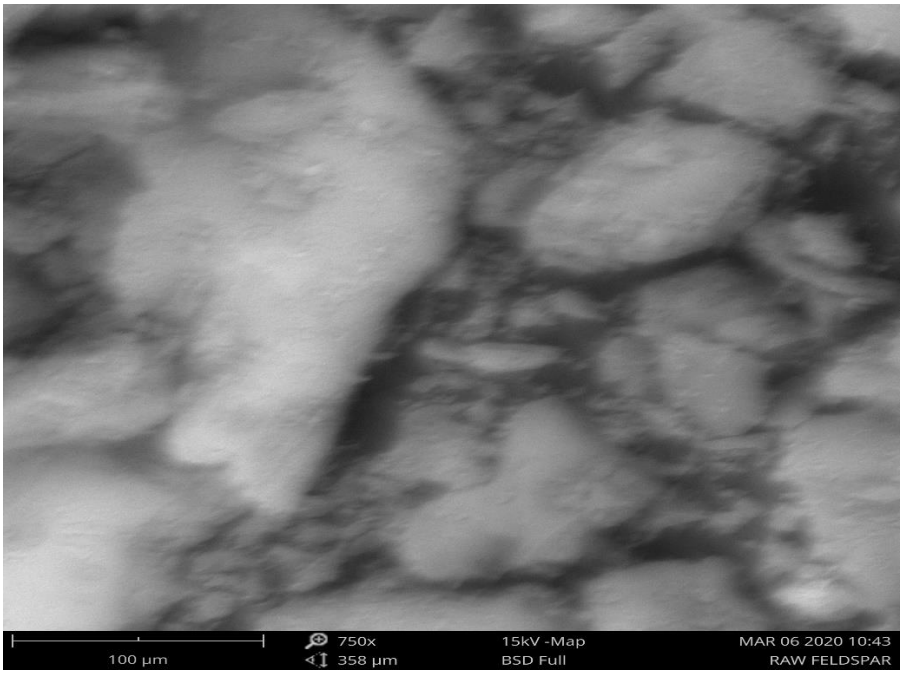

Figure 4.3c: SEM of raw feldspar adsorbent at magnification of (750X)

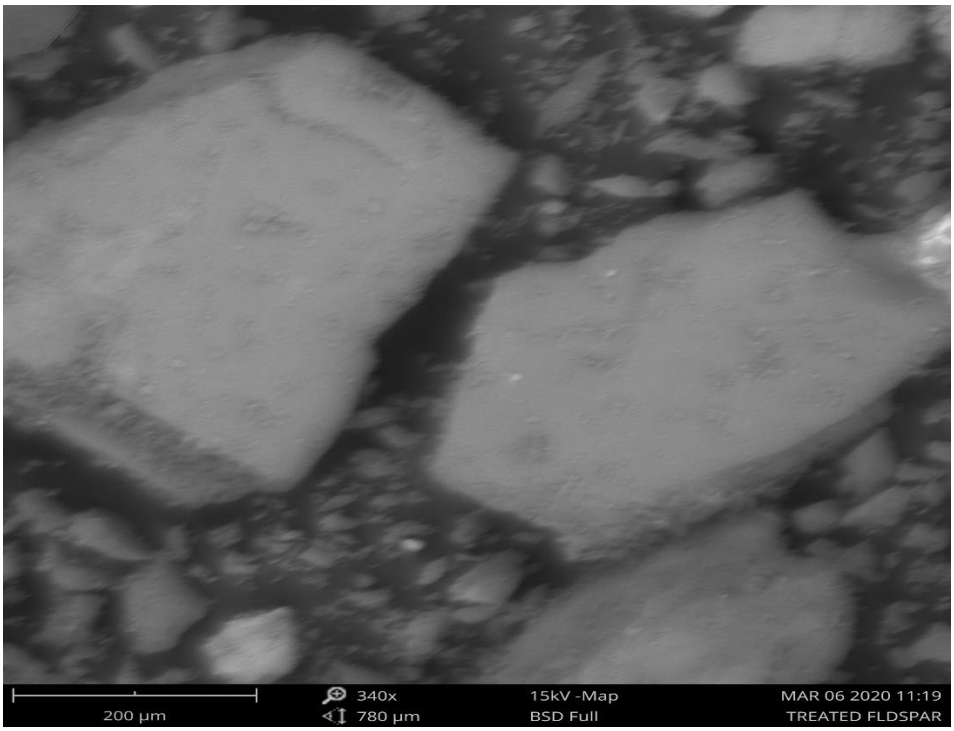

Figure 4.4a: SEM of treated feldspar adsorbent at magnification of (340X)

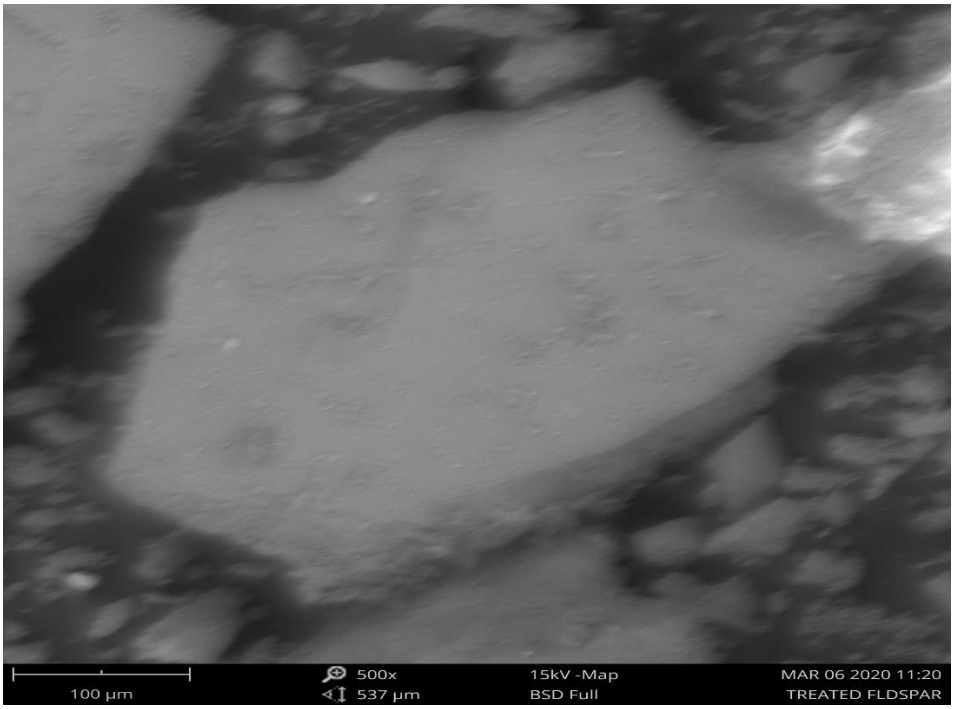

Figure 4.4b: SEM of treated feldspar adsorbent at magnification of (500X)

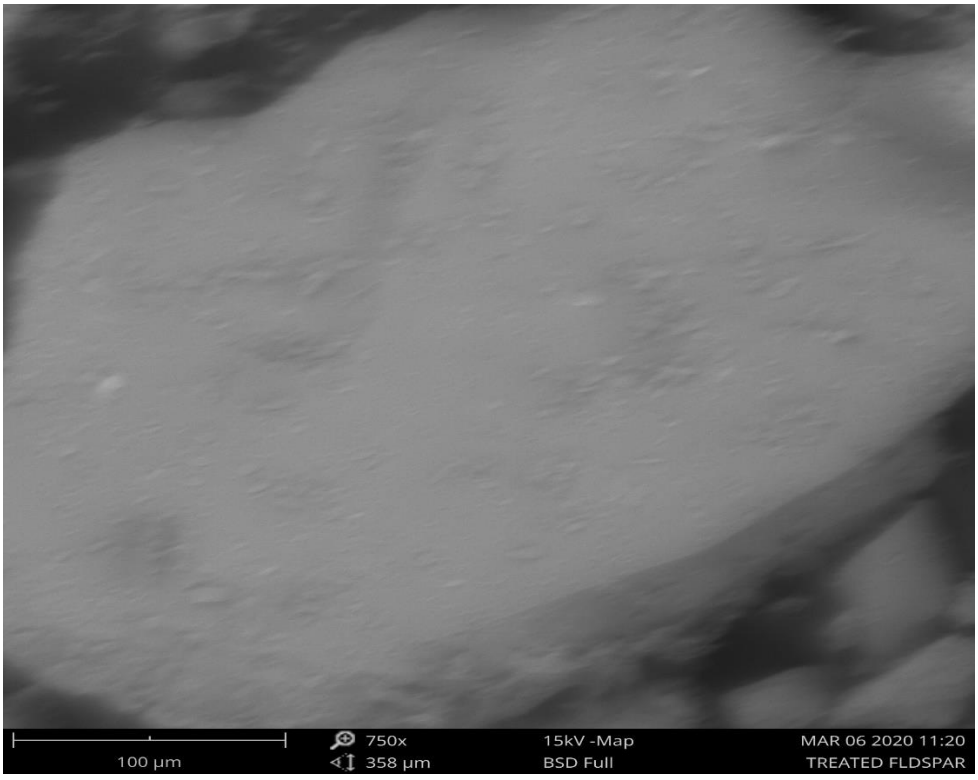

Figure 4.4c: SEM of treated feldspar adsorbent at magnification of (750X)

4.2.7 Electron Dispersive Spectroscopy (EDS)

EDS is an added function of SEM which is used to identify the chemical elements distributed on the sample. The results of the EDS analysis are as represented in Table 4.7 and Figure 4.5. The difference between the raw and activated feldspar shows there as cation exchange, the ions were lynched out and the purity appreciated. The atomic percentages of silicon in raw and thermally activated feldspar were 58.34 and 67.94 respectively and that of aluminum were 12.81 and 12.06 respectively. The openings of pores were probably that the rehydration resulted in the enhancement of the spacing. (Ler and Stanforth., 2013).

Table 4.7a: Elemental composition of raw feldspar

Element Number	Element Symbol	Element Name	Atomic Conc.	Weight Conc.
14	Si	Silicon	58.34	48.67
19	K	Potassium	14.47	16.80
13	Al	Aluminum	12.81	10.27
26	Fe	Iron	5.23	8.68
38	Sr	Strontium	3.09	8.05
20	Ca	Calcium	2.14	2.55
47	Ag	Silver	0.47	1.51
11	Na	Sodium	1.84	1.25
41	Nb	Niobium	0.33	0.90
16	S	Sulfur	0.66	0.63
22	Ti	Titanium	0.31	0.44
15	P	Phosphorus	0.16	0.15
12	Mg	Magnesium	0.15	0.11
39	Y	Yttrium	0.00	0.00

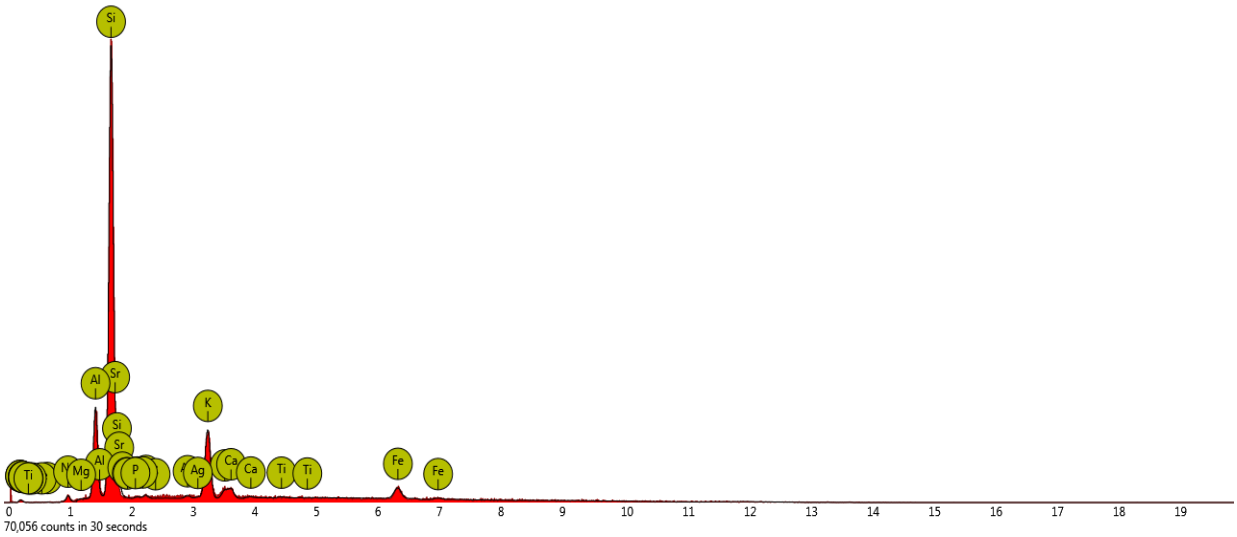

Figure 4.5a: Electron Dispersive Spectra (EDS) of raw feldspar

Table 4.7b: Elemental composition of treated feldspar

Element Number	Element Symbol	Element Name	Atomic Conc.	Weight Conc.
14	Si	Silicon	67.94	59.53
13	Al	Aluminum	12.06	10.15
19	K	Potassium	7.29	8.89
26	Fe	Iron	4.11	7.17
38	Sr	Strontium	2.21	6.03
20	Ca	Calcium	1.59	1.99
11	Na	Sodium	2.18	1.57
47	Ag	Silver	0.46	1.55
41	Nb	Niobium	0.50	1.46
16	S	Sulfur	0.69	0.69
15	P	Phosphorus	0.58	0.56
22	Ti	Titanium	0.18	0.27
12	Mg	Magnesium	0.21	0.16

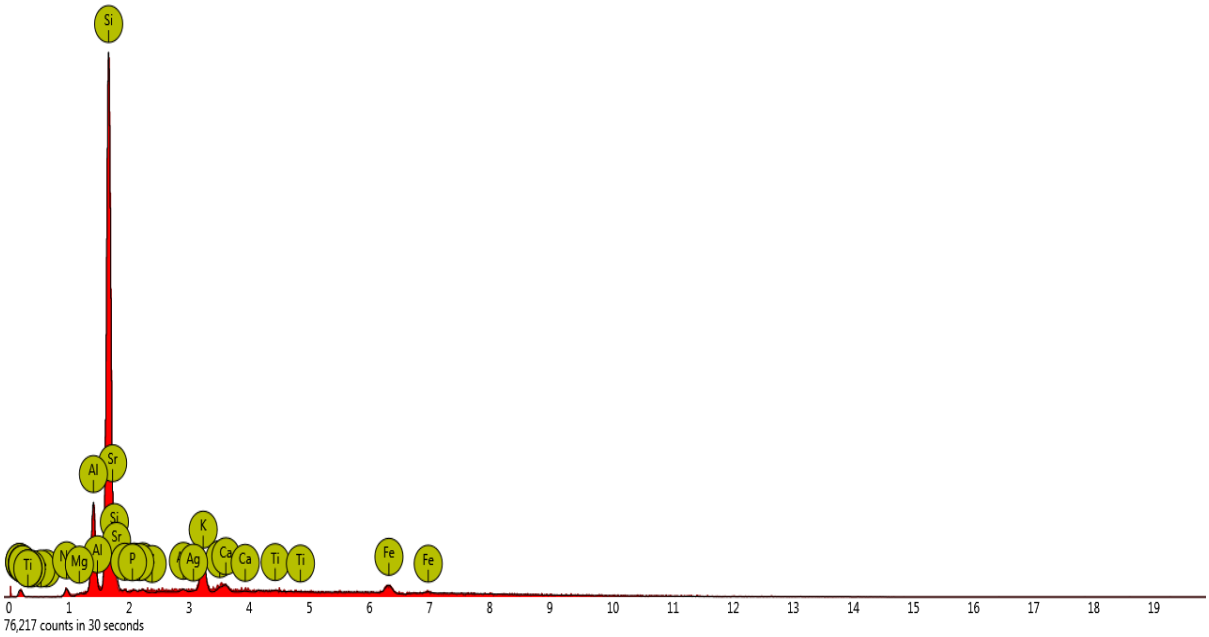

Figure 4.5b: Electron Dispersive Spectra (EDS) of treated feldspar

4.2.8 X-ray Diffractometry Analysis (XRD) of feldspar clay sample.

The XRD analysis was conducted on the raw and thermally activated feldspar to determine the effect of the thermal treatment on it and the patterns are presented in Figures 4.6a and 4.6b. The XRD patterns revealed presence of crystalline peaks of microcline at 2 theta of 27.26 and 27.48 on both raw and thermally activated mineral samples respectively which corresponded to that reported by Yazdani *et al.* (2013). Other peaks were also revealed such as quartz and albite as indicated in the Figures 4.6a and 4.6b. The treated feldspar showed a higher crystal structure which was reflected in a higher diffraction pattern of intensity 21162 at 27.48^{o} (2 Theta), with the raw feldspar having a lower intensity (14802) when compared to the treated. This agrees with the work reported by Ler and Stanforth., 2013. These differences indicated that the feldspar had changed in its basic structure and its primary crystal structure after the calcination treatment. These alterations may be due to the burning and the evaporation of the organic substances and other channel impurities in the feldspar. Therefore, calcination treatment

may increase the specific surface area of activated feldspar and improve its properties for adsorption. (Ler and Stanforth., 2013).

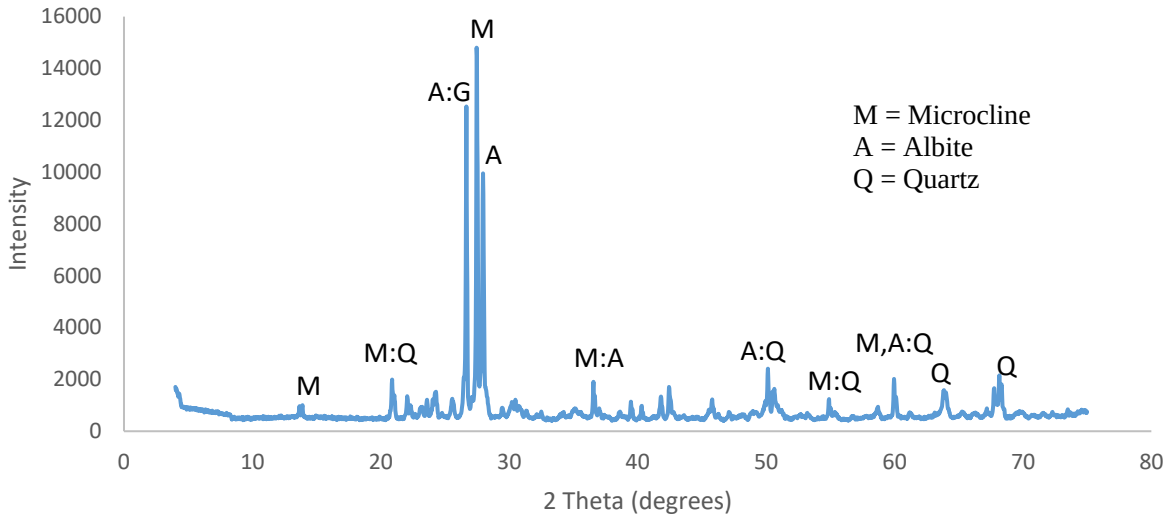

Figure 4.6a: XRD of raw feldspar adsorbent

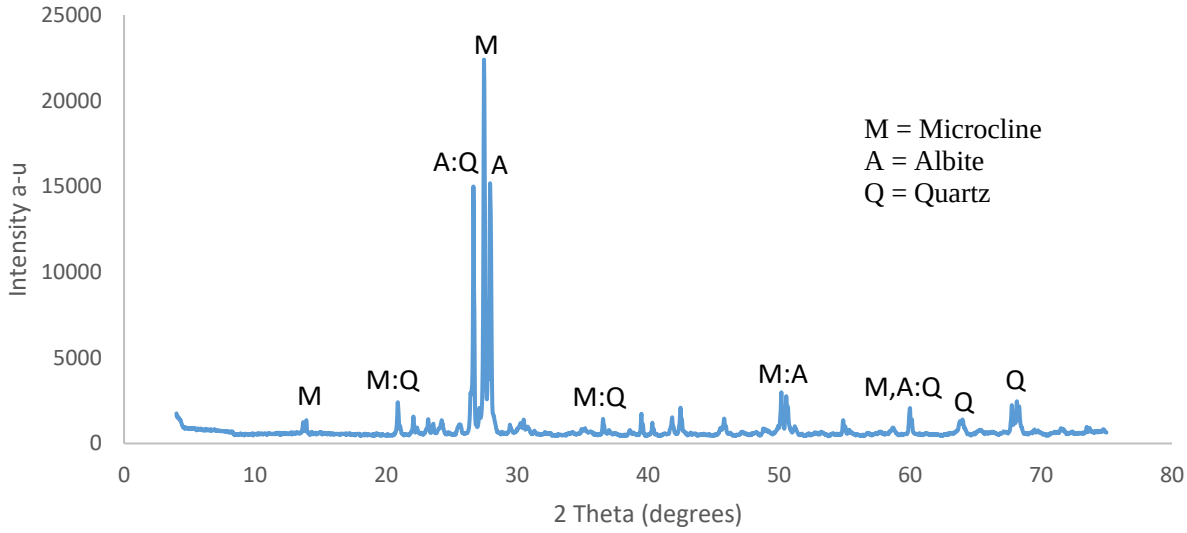

Figure 4.6b: XRD of treated feldspar adsorbent

4.3 Batch Adsorption Study

The batch adsorption study was carried out where the parameters investigated include the adsorbent dosage, pH, adsorption temperature and initial ion concentration were analysed

at various conditions. The investigation of these parameters revealed their effect on the adsorption capacity of the adsorbent.

Table 4.8: The AAS Analysis of Phosphate and Ammonium ion

Run/Order	Temp (℃)	Time (min)	Dosage (g)	PO_4^{3-} removal efficiency (%)	NH_4^+ removal efficiency (%)
1	30	10	0.5	42.92	73.54
2	30	30	0.5	59.50	80.26
3	30	60	0.5	59.25	79.89
4	70	40	0.4	34.33	67.22
5	45	60	0.5	36.39	70.24
6	80	50	0.9	48.54	70.57
7	30	10	0.8	32.50	64.24
8	30	30	0.8	37.50	68.77
9	30	70	2.2	45.08	75.29
10	30	40	1.3	46.67	76.56
11	70	60	2.0	54.28	70.54
12	40	50	1.0	55.65	72.51
13	40	20	1.0	52.67	73.34
14	60	50	0.8	49.21	71.33
15	72	30	2.0	57.75	71.74
16	50	45	1.2	57.54	72.32
17	50	10	1.2	42.65	61.24
18	65	30	2.0	54.75	69.84
19	40	60	1.6	55.58	72.42
20	40	50	1.6	56.00	73.98

4.3.1 Effect of initial concentration and contact time on adsorption of phosphate ion and ammonium ion.

In order to study the effects of initial concentrations of the impurities and contact time with the adsorbent on the adsorption of phosphate ion and ammonium ion, the initial

concentrations of the phosphate ions and ammonium ions were varied from 4-12 mg/L and 15-35 mg/L respectively. The contact time was varied from 5-60 min keeping other parameters, pH (6.2), adsorbent dosage (0.5 g) in 50 ml of sample and temperature (30 ℃) constant. The results obtained are as depicted in the figures 4.7a and 4.7b. At initial phosphate ion concentration of 4 mg/L in figure 4.9a, the percentage removal of the ion increased as the contact time increases. There was a rapid adsorption at 5 min followed by a marginal increase in the adsorption rate from 5-20 min after which the adsorption equilibrates (optimum point) from 30 min, with are percentage removal of 83.25 %. Similar trends were noticed with the other initial concentrations. However, the adsorption efficiency was observed to be decreasing with increasing initial concentration of the phosphate ion as the optimum percentage removal at 12 mg/L initial concentration (59.5 %) was lower than that obtained at 4 mg/L initial concentration (83.25 %).

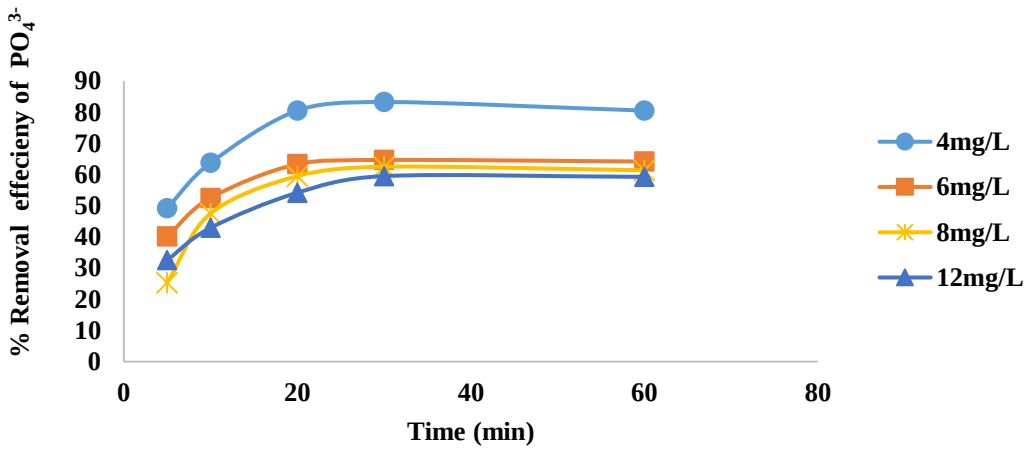

Figure 4.7a: Effect of initial concentration of PO_4^{3-} and contact time

Similarly, in figure 4.7b, as contact time increases, the percentage removal of the ammonium ion increased also, being rapid initially then slowing down till it reached equilibrium at 30 min. The rate of adsorption was also seen to reduce with increasing initial ammonium ion concentration, yielding 91 % removal at 15 mg/L initial

concentration and reducing to 80 % removal at 35 mg/L initial concentration of the ammonium ion.

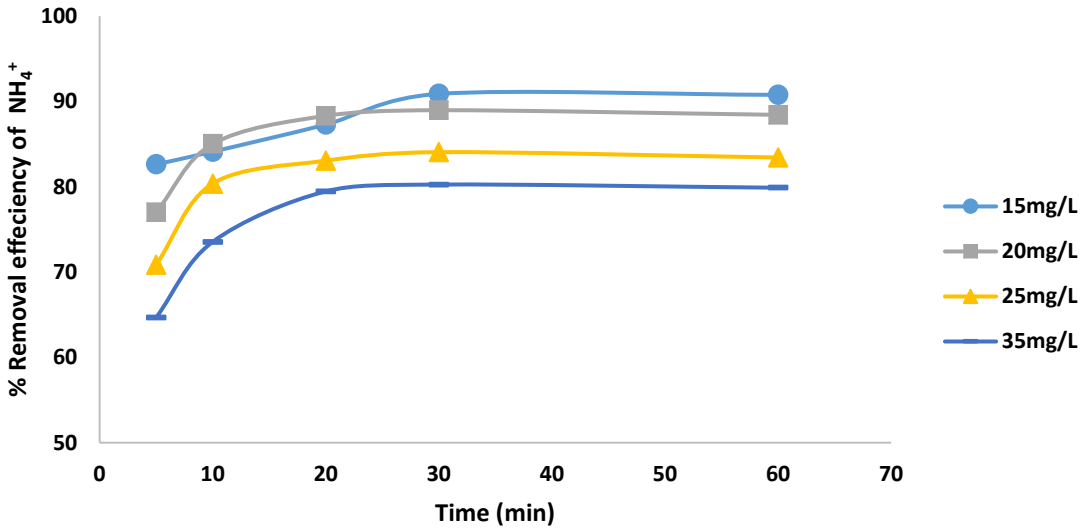

Figure 4.7b: Effect of initial concentration of NH_4^+ and contact time

In all the curves obtained, it was observed that the optimum percentage removal of the ammonium ions was obtained at 30 min contact time, which implies that a quasi-state equilibrium is reached at 30 min for all initial concentrations, hence, no significant change in the adsorption of the ions could be observed. The rapid adsorption observed initially was due to accessible adsorption sites present in the adsorbent at the underlying contact time (Yu *et al*., 2016). However, with time the vacant active sites get occupied with adsorbed phosphate and ammonium ion which reduces the rate of further adsorption of the ions.

4.3.2 Effect of pH on adsorption of phosphate ion and ammonium ion

The effect of the pH of the solution was studied due to its significant effect on the adsorption process of the phosphate and ammonium ions. The solution's pH is significant to adsorption because of the ion-exchange nature of adsorption process (Awala and El-Jamal, 2011). The outcome of the solution's pH on the removal of both the phosphate and

ammonium ions was studied at initial concentration, adsorbent dosage and temperature of 12 mg/L, 0.5 g and 30 ℃ (for phosphate ion) and 35 mg/L, 0.5 g and 30 ℃ (for ammonium ion) respectively while varying the pH in the range of 2-10. The result as depicted in Figure 4.8 showed that in the pH range of 2-4, the phosphate and ammonium ion adsorption increased rapidly, and for pH > 4, the percentage removal efficiency remained similar (70.67% and 70.08% for phosphate ion removal; 76.49% and 76. 37% for ammonium ion removal). This result agrees with that reported by Awala and El-Jamal (2011) who worked on the adsorption of dyes onto feldspar. The increase in the adsorbate removal is due to the electrostatic interactions between the adsorbent and the adsorbate in acidic medium than in the basic medium.

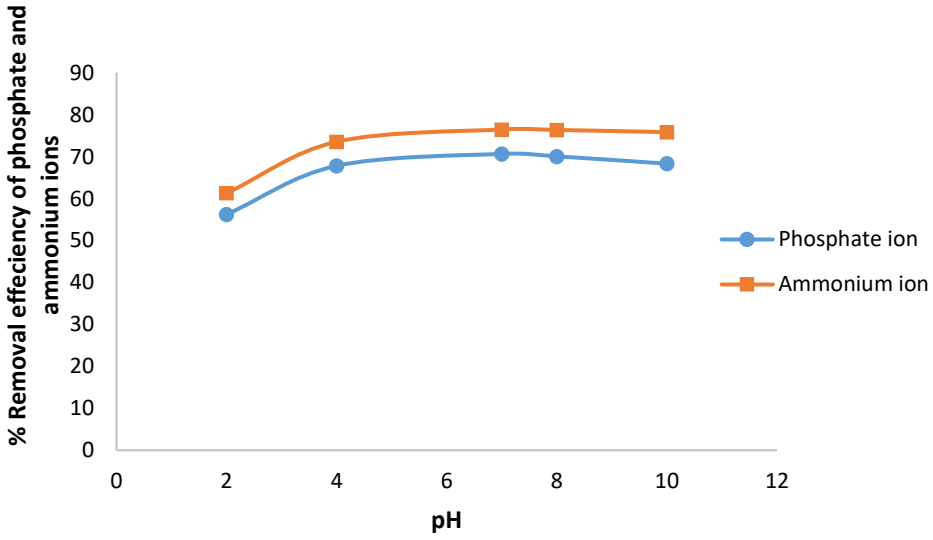

Figure 4.8: Effect of pH on adsorption of phosphate ion and ammonium ion

4.3.3 Effect of adsorbent dosage on adsorption of phosphate ion and ammonium ion

The effect of adsorbent dosage on the removal of the phosphate ion and ammonium ion was studied with initial phosphate and ammonium ions concentrations of 12 mg/L and 35 mg/L respectively. The temperature was kept constant at 30 ℃ while varying the adsorbent dosage from 0.4-2.0 g. The results obtained as depicted in Figure 4.9 showed

that as the adsorbent dosage increases, the rate of adsorption of the phosphate ion and ammonium ion increased also, yielding optimum percentage removal 47% for phosphate ion and 77% for ammonium ion removal. This is because more adsorbent dosage causes increment in adsorption limit of the adsorbent (more extensive surface area of dynamic locales) thereby enhancing more adsorption. These optimum adsorptions were achieved at adsorbent dosage of 1.2 g for both the phosphate and ammonium ion removal. The adsorption rate was observed to be decrease progressively after the optimum dosage of 1.2 g was exceeded, indicating that adsorption rate increases with dosage till the optimum dosage is reached after which further adsorption is not possible due to overlapping of the pores as a result of overcrowding of the adsorbent particles (Gai *et al.*, 2015).

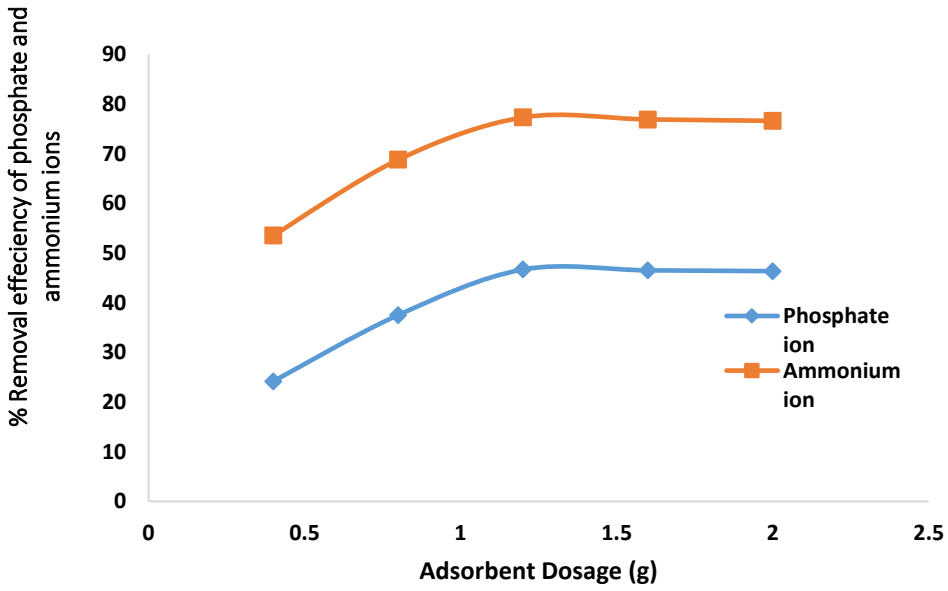

Figure 4.9: Effect of adsorbent dosage on adsorption of phosphate ion and ammonium ion

4.3.4 Effect of Temperature on adsorption of phosphate ion and ammonium ion

The effect of temperature on the adsorption process was studied by varying the temperatures from 30℃ to 70℃ at intervals of 10℃, keeping pH, contact time and

adsorbent dosage constant at their optimum values of 6.2, 30 min and 1.2 g respectively. The result as depicted in Figure 4.10 shows that phosphate ion and ammonium ion adsorption rate increases with temperature rise from 30 ℃ to 50 ℃ after which it equilibrates, indicating that optimum adsorption is reached.

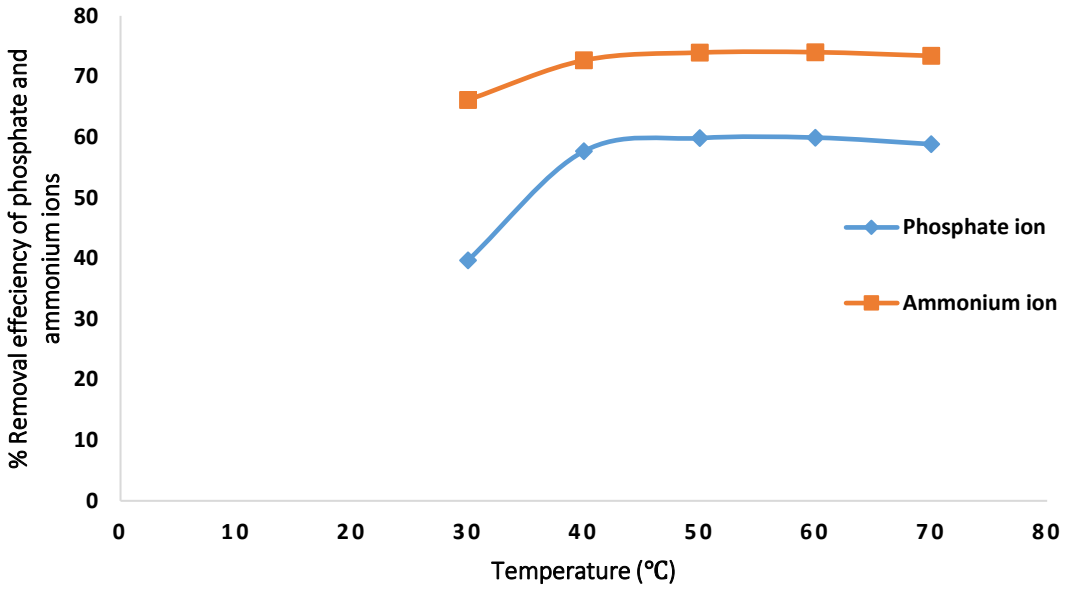

Figure 4.10: Effect of Temperature on adsorption of phosphate ion and ammonium ion

A rapid adsorption was noticed at 30 ℃ (with 40% removal of phosphate ions and 66% removal of ammonium ions) followed by a proportional increase till 50℃ after which equilibrium was reached. The optimum temperature for the adsorption is 50℃, here 59.8% of the phosphate ion and 73.9% of the ammonium ions were removed from the wastewater respectively. The increment in the adsorption rate with temperature was possible because increase in temperature facilitates the ionization of the functional groups (adsorption sites) which also increases their movement towards the adsorption of the selected impurities (Yu *et al.*, 2016).

4.4 Domestic Wastewater Analysis

The domestic wastewater was analysed to determine the physiochemical properties pH, Turbidity, Total Dissolved Solids, Conductivity, Chlorine, Total hardness, Phosphate ion and Ammonium ion. The results are as shown in Table 4.9.

Table 4.9: Physicochemical properties of the well water after treatment

Physicochemical Parameters	**Wastewater Before Treatment**	**Wastewater after Treatment**	**WHO limit for effluent**
P^H	8.22	4.21	6.5-8.5
Conductivity (µS/cm)		783	<1250
Turbidity (NTU)	185	120	
TDS (mg/L)	1338.16	255.85	
Total hardness	230	135	2000
Chlorine (mg/L)	330.75	232.75	
Calcium (mg/L)	132.2	39.94	
Magnesium (mg/L)	52.15	16.25	
Phosphate(mg/L)	12	4.2	5
Ammonium (mg/L)	35	6	10

4.5 Adsorption Isotherm Studies

The adsorption isotherms for phosphate ion and ammonium ion removal were studied using initial concentrations of 12 mg/L and 35 mg/L of phosphate ion and ammonium ion respectively at the varied adsorbent dosage levels of 0.4 g to 2.0 g for 30 ℃, 40 ℃ and 50 ℃. Three adsorption isotherm (Langmuir, Freundlich and Temkin isotherms) models were adopted to investigate the adsorption behavior of feldspar on the removal of the phosphate and ammonium ions. The parameters obtained for the isotherms are tabulated in Table 4.10.

The results obtained for the three isotherms tested are as shown in the Table 4.10. The Langmuir's model showed that the adsorption for both PO_4^{3-} and NH_4^+ was favorable due to the K_l values of less than 1 obtained for all the temperatures (Yazdani *et al.*, 2013). The adsorption process was observed to be most favourable at 50 ℃ giving the lowest Kl values of 0.48 (for PO_4^{3-}) and 0.23 (for NH_4^+); particularly more favorable towards NH_4^+ than PO_4^{3-} in that the Kl value of the former is much lower than that of the latter. However, lower correlation coefficient (R^2) values were obtained for langmuir's model compared to the other models tested. The R^2 values obtained for phosphate ion adsorption was 0.6155 (at 30 ℃), 0.4567 (at 40 ℃) and 0.5933 (at 50 ℃) while those for ammonium ion adsorptions were 0.683 (at 30 ℃), 0.4693 (at 40 ℃) and 0.4908 (at 50 ℃).

The values for the Freundlich isotherm as shown in the Table 4.10 shows that the adsorption capacity (k_f) and adsorption intensity (1/n) are influenced by temperature. When the temperature is increased from 30 ℃ to 40 ℃, the values of k_f decreased (from 8.4283 to 4.3593 for PO_4^{3-} and from 1.1735 to 0.0085 for NH_4^+. The values of 1/n also decreased from 2.0965 to 1.6269 for PO_4^{3-} and increased from 1.4423 to 6.1518 for NH_4^+. The decrease in both the adsorption capacity and intensity with increasing temperature implies that the adsorption process was exothermic in nature. Furthermore, the n values which varied between 0 and 1, implies that the adsorption process was favourable (Yazdani *et al.*, 2013). The R^2 values obtained ranges from 0.5689 to 0.7377 for PO_4^{3-} and from 0.675 to 0.8221 for NH_4^+.

Table 4.10: Isotherm parameters for removal of PO_4^{3-} and NH_4^+ from wastewater using feldspar adsorbent

Isotherms		**PO_4^{3-}**			**NH_4^+**	
	30 ℃	**40 ℃**	**50 ℃**	**30 ℃**	**40 ℃**	**50 ℃**
Langmuir						

Q_{max}	33.946	17.062	18.548	6.1966	20.854	39.349
R^2	0.6155	0.4567	0.5933	0.683	0.4693	0.4908
K_l	0.5337	0.5514	0.4814	0.4905	0.2599	0.2305
SSE	3.0821	4.9878	3.1725	2.7586	3.8112	2.9712
χ^2	1.2009	1.3458	1.2151	2.4227	1.9586	1.3670
Freunlich						
log k_f	2.1316	1.4723	1.7308	0.16	-4.7692	1.908
K_f	8.4283	4.3592	5.6451	1.1735	0.0084	6.7395
1/n	2.0965	1.6269	2.0559	1.4423	6.1518	12.58
n	0.4769	0.6146	0.4864	0.6933	0.1625	0.0794
R^2	0.7271	0.5689	0.7377	0.8221	0.675	0.7057
SSE	1.0057	1.7249	0.9826	0.9218	1.2767	1.1690
χ^2	0.2783	0.8121	0.2275	0.2119	0.3863	0.2473
Temkin isotherm						
Qe (mg/g)	1.5792	1.2655	1.8679	6.8612	45.831	6.8612
K_1	1.0485	1.08	1.4905	4.1296	21.466	4.1296
K_2	3.0440	1.5385	1.8468	3.9746	7.8583	3.9746
R^2	0.836	0.6931	0.8685	0.9222	0.8483	0.9222
SSE	0.1985	0.3416	0.1575	0.1357	0.1751	0.1341
χ^2	0.1053	0.2715	0.1219	0.0826	0.7349	0.1201

Finally, the Temkin model shows the highest values of the correlation coefficient (R^2) compared to the Langmuir and Freundlich isotherm models, ranging from 0.6931 to 0.8685 for PO_4^{3-} and 0.8483 to 0.9222 for NH_4^+. This result implies that the heat of adsorption decreases with the degree of adsorption process.

The sum of square error (SSE) and non-linear-chi square test (χ^2) were employed to determine the model to further justify the suitability of the best isotherm model. The low value suggested that termkin best fitted the adsorption process**.**

4.6 Adsorption Kinetics Study

In order to study the underlying mechanism of phosphate ion and ammonium ion adsorption onto the surface of feldspar adsorbent, the pseudo-first order, pseudo-second order, Elovich kinetic models were fitted with the kinetic data at different initial phosphate ion and ammonium ion concentrations. The values of the different model parameters are shown in Tables 4.11a and 4.11b for phosphate ion removal and ammonium ion removal respectively.

Table 4.11a: Pseudo-Kinetic parameters for removal of PO_4^{3-}

Pseudo-Kinetic Parameters	**4 mg/L**	**6 mg/L**	**8 mg/L**	**12 mg/L**
First order				
q_e,exp (mg/g)	33.3	38.8	50	51.4
q_e,cal (mg/g)	7.5805	9.8673	16.7725	36.7790
k_1 (min^{-1})	0.0421	0.0656	0.0518	0.0758
R^2	0.5337	0.7734	0.7006	0.9165
SSE	1.8349	1.2816	1.5272	0.9473
χ^2	1.0173	0.7954	0.9934	0.0471
Second order				
q_e,exp (mg/g)	33.3	38.8	50	51.4

q_e,cal (mg/g)	34.1296	40.4858	54.6448	59.8802
H	13.5318	16.6944	10.7411	7.2463
k_2 (min^{-1})	0.0116	0.0101	0.0035	0.0020
R^2	0.9958	0.9979	0.9870	0.9875
SSE	0.5891	0.4711	0.4667	0.4681
χ^2	0.5133	0.5751	0.0995	0.3513
Elovich				
β	0.1823	0.1651	0.0853	0.0720
α	56.3609	96.0343	21.6981	13.5186
R^2	0.8152	0.8321	0.806	0.9083
SSE	1.0089	1.1935	1.1279	1.0715
χ^2	0.7893	1.0631	1.1325	0.9878

Table 4.11b: Kinetic parameters for removal of NH_4^+

Kinetic Parameters	**15 mg/L**	**20 mg/L**	**25 mg/L**	**35 mg/L**
First order				
q_e,exp (mg/g)	118.1	161.4	194.2	280.9
q_e,cal (mg/g)	41.5910	1.5183	28.086	34.889
k_1 (min^{-1})	0.0840	0.0594	0.0506	55.5023
R^2	0.8739	0.751	0.7427	0.7117
SSE	0.3592	0.5734	0.8229	0.7515
χ^2	0.2854	0.4996	0.8543	0.5619
Second order				
q_e,exp (mg/g)	118.1	161.4	194.2	280.9

q_e,cal (mg/g)	123.4568	163.9344	196.0784	285.7143
H	50.7614	151.5152	208.3333	312.5
k_2 (min^{-1})	0.0033	0.0056	0.0054	0.0038
R^2	0.9985	0.9992	0.9994	0.9997
SSE	0.5526	0.5165	0.4119	0.4892
χ^2	0.5113	0.5399	0.3681	0.3457
Elovich				
β	0.0764	0.0633	0.0587	0.0457
α	2241.406	11410.67	40140.12	221972.8
R^2	0.9128	0.7508	0.7269	0.8096
SSE	0.4915	0.8137	0.9987	0.5189
χ^2	0.3219	0.5529	0.8776	0.3875

The results showed that comparatively lower values of the correlation coefficient were obtained for pseudo-first order and Elovich models. On the other hand, the pseudo-second order kinetic model represents a better fit of experimental data with correlation coefficient values within the range of 0.9985 to 0.9997. It was further observed from Tables 4.11a and 4.11b that in case of pseudo second order kinetic model, the phosphate ion and ammonium ion adsorption capacity (qt) was highest at initial concentration of 12 mg/L and 35 mg/L for phosphate ion and ammonium ion respectively. This report agrees with the report of Song *et al*. (2014). The plots show that the adsorption rate varies linearly with the difference between q_e and adsorption at any time (q_t) (Song *et al.,* 2014).

Determination of best fitting relationship and validating the best kinetics studies have always been through the use of linear correlation coefficient (R^2) values. Due to the inherent bias from transformation, sum of square error (SSE) and non-linear-chi square test (χ^2) were used. The low values further indicated the pseudo-second order kinetic model represents a better fit of experimental data (Foo and Hameed 2010).

4.7 Adsorption thermodynamics study

The thermodynamics parameters enhance the study of the feasibility of the adsorption process (Saad and Fares, 2014). The thermodynamics parameters of the adsorption, that is the standard enthalpy ΔH^o, Gibbs free energy ΔG^o and entropy ΔS^o were obtained and tabulated in Table 4.12 in order to study the thermodynamics of the adsorption process.

Table 4.12: Thermodynamic parameters of PO_4^{3-} and NH_4^+ removal from wastewater by using feldspar

Adsorbate	**Temp.(K)**	**K_c (Lg^{-1})**	**ΔH ($kJmol^{-1}$)**	**ΔS (J/mol.k)**	**ΔG ($kJmol^{-1}$)**
PO_4	303	0.011505	-6857.64	14.48964	-11248
	313	0.01255			-11392.9
	323	0.013617			-11537.8
	333	0.014702			-11682.7
	343	0.015803			-11827.6
NH_4^+	303	0.115596	-4463.04	3.209204	-5435.43
	313	0.12233			-5467.52
	323	0.129			-5499.61
	333	0.1356			-5531.7
	343	0.14213			-5563.8

From the results obtained, the negative values of the Gibbs free energy for both phosphate ion and ammonium ion adsorption shows that the adsorption process is spontaneous,

hence, feasible. The increasing negative values of the ΔG^o shows that the degree of spontaneity of the reaction increases as the temperature increases (Dias *et al*., 2015). The positive values of ΔS^o for both phosphate ion and ammonium ion adsorption is due to the redistribution of energy between the adsorbate and the adsorbent as the temperature is being increased, which increases the spontaneity of the system (Hefne *et al.*, 2012). The reaction is said to be exothermic due to the negative values of ΔH^o for both phosphate ion and ammonium ion removal, which means energy was released during the adsorption.

CHAPTER FIVE

5.0 CONCLUSION AND RECOMMENDATIONS

5.1 Conclusion

At the end of the study, thermally activated feldspar at 600 ℃ was seen to be a good and efficient adsorbent for the removal of phosphate ions and ammonium ions from domestic wastewater compared to the other clay minerals investigated. The Fourier Transform

Infrared (FTIR) analysis indicated the presence of O-H, N-H and C-O groups which were responsible for the adsorption of the phosphate and ammonium ions from the wastewater. The BET results of the thermally activated feldspar revealed surface area and pore volume of 533.9 m^2/g and 0.272 cc/g respectively which provided the active sites for the adsorption of the ions. The adsorption process extremely depends on the contact time, pH, adsorbent dosage, initial pollutant concentration and temperature. The adsorption of the phosphate and ammonium ions increased with increasing contact time, temperature and adsorbent dosage, the removal of the ions were higher in the acidic medium (lower pH) than in basic medium. The equilibrium time, pH and temperature were 30 min, 6.2 and 30 ℃ respectively.

Maximum adsorption efficiencies of 80.25% and 90.89% were achieved for the removal of phosphate ions and ammonium ions from the domestic wastewater using the activated feldspar adsorbent at initial concentrations of 4 mg/L and 15 mg/L of PO_4^{3-} and NH_4^+ respectively, pH of 6.2, and adsorbent dose of 0.5 g, temperature of 50℃ and contact time of 30 min.

The adsorption isotherm model under study were Langmuir, Freundlich and Temkim. However, the adsorption process fitted the Temkin isotherm model and the pseudo-second kinetics model.

The thermodynamic parameters for the adsorption process ΔG^o, ΔS^o and ΔH^o suggested that the process was favorable, feasible, exothermic and spontaneous in nature.

5.2 Recommendations

The following recommendations should be considered:

1. The removal of other pollutants harmful in wastewater.

2. Acid treatment is recommended.

3. A sand bed should be attached to the sewage to prevent intake of pollutants.

5.3 Contribution to knowledge

1. Before now there were no locally produced adsorbent. This research work has been able to use thermally activated feldspar at 600 ^{o}C demonstrated an adsorption capacity of 80.25% and 90.89% in the removal of PO_4 and NH_4 respectively from domestic wastewater

2. The 80.25% and 90.89% adsorption of PO_4 and NH_4 by feldspar is fitted to Temkim isotherm and the pseudo-second order kinetic model

3. The thermodynamics parameters enhance the study of the feasibility of the adsorption process. The standard enthalpy ΔH^{o} with the values of -6857.64 for phosphate and -4463.04 for ammonium indicated that the reaction was said to be exothermic due to the negative values

REFERENCES

Adejo, J. A. & Lawal, S. A. (2018). Production and Quality Analysis of Evaporating Dish Using Local Materials. In IOP Conference Series: Materials Science and Engineering: 413(1) 111-121

Adewumi, J. R., & Oguntuase, A. M. (2016). Planning of wastewater reuse programme in Nigeria. *Consilience*, (15): 1-33.

Adeyemo, A. A., Adeoye, I. O., & Bello, O. S. (2017). Adsorption of dyes using different types of clay: a review. *Applied Water Science*, *7*(2): 543-568.

Akhirevbulu, O. E., Amadasun, C. V., Ogunbajo, M. I. & Ujuanbi, O. (2010). The Geology and Mineralogy of Clay Occurrences around Kutigi Central Bida Basin, Nigeria. *Ethiopian Journal of Environmental Studies and Management*, 3(3):67-72

Akpen, G. D., Ekanem, E. J., & Agunwamba, J. C. (2016). The effects of sewage effluent discharges on the water quality of Wupa River in Abuja, Nigeria. *Journal of Science and Technology (Ghana)*, *36*(2): 86-95.

Akpor, O. B., & Munchie, B. (2011). Environmental and public health implications of wastewater quality. *African Journal of Biotechnology*, *10*(13): 2379-2387.

Al-Anber, M. A. (2015). Adsorption of ferric ions onto natural feldspar: kinetic modeling and adsorption isotherm. *International Journal of Environmental Science and Technology*, *12*(1): 139-150.

Ali, I., Asim, M., & Khan, T. A. (2012). Low cost adsorbents for the removal of organic pollutants from wastewater. *Journal of environmental management*, *113*, 170-183.

Allam, K., Gourai, K., El Bouari, A., Belhorma, B., & Bih, L. (2018). Adsorption of Methylene Blue on raw and activated Clay: case study of Bengurir clay. *Journal of Materials and Environmental Science*, *9*: 1750-1761.

Alver, B. E., & Sakızcı, M. (2012). Ethylene adsorption on acid-treated clay minerals. *Adsorption Science & Technology*, *30*(3): 265-273.

Amari, A., Gannouni, H., Khan, M. I., Almesfer, M. K., Elkhaleefa, A. M., & Gannouni, A. (2018). Effect of structure and chemical activation on the adsorption properties of green clay minerals for the removal of cationic dye. *Applied Sciences*, *8*(11): 2302.

Anderson, E. (2013). Economic Geology: Principles and Practice: Metals, Minerals, Coal and Hydrocarbons—Introduction to Formation and Sustainable Exploitation of Mineral Deposits.3 (3): 9-14

Awala, H. A., & El-Jamal, M. M. (2011). Equilibrium and kinetics study of adsorption of some dyes onto feldspar. *Journal of the University of Chemical Technology & Metallurgy*, *46*(1):45-49

Ayawei, N., Ebelegi, A. N., & Wankasi, D. (2017). Modelling and interpretation of adsorption isotherms. *Journal of Chemistry* (5):23-29

Balić-Žunić, T., Piazolo, S., Katerinopoulou, A., and Schmith, J. H. (2013). Full analysis of feldspar texture and crystal structure by combining X-ray and electron techniques. *American Mineralogist*, *98*(1):41-52.

Bashir, F. A., Shuhaimi-Othman, M., and Mazlan, A. G. (2012). Evaluation of trace metal levels in tissues of two commercial fish species in Kapar and Mersing coastal waters, Peninsular Malaysia. *Journal of Environmental and Public Health* (8):45-54

Behera *S*., Ghanty S., Ahmad F., Santra S., Banerjee S. (2012) UV-visible spectrophotometric method development and validation of assay of paracetamol tablet formation, *Journal of analytical and bioanalytical technique,(* 3): 1-6.

Bellir, K., Bencheikh-Lehocine, M., & Meniai, A. H. (2013). Removal of methylene blue from aqueous solutions using an acid activated Algerian bentonite: equilibrium and kinetic studies. *Int Renew Energy Congr*, *2010*:360-367.

Bhatnagar, A., Hogland, W., Marques, M., & Sillanpää, M. (2013). An overview of the modification methods of activated carbon for its water treatment applications. *Chemical Engineering Journal*, *219*:499-511.

Bhutiani, R., Khanna, D. R., & Faheem, A. (2016). Physico-chemical analysis of sewage water treatment plant at Jagjeetpur Haridwar, Uttarakhand. *Environment Conservation Journal*, *17*(3):133-142.

Bieseki, L., Bertell, F., Treichel, H., Penha, F. G., & Pergher, S. B. (2013). Acid treatments of montmorillonite-rich clay for Fe removal using a factorial design method. *Materials Research*, *16*(5): 1122-1127.

Bijeljić, J., Ristić, N., Tošić, N., & Protić, M. (2017) Impact of different thermal activated calcined clays to concrete properties: A Review. 10th International Scientific Conference "Science and Higher Education in Function of Sustainable Development", Mećavnik – Drvengrad, Užice, Serbia(6):89-95

Chen, J. P. (2012). Decontamination of heavy metals: processes, mechanisms, and applications. Crc Press.(9):56-67

Chukwu M.N & Oranu C.N (2018). Performance assessment of biological wastewater treatment at Wupa wastewater treatment plant, Abuja, Nigeria *Nigerian Journal of Environmental Sciences and Technology* (NIJEST), 2(1),:46 – 55.

Crini, G., & Lichtfouse, E. (2019). Advantages and disadvantages of techniques used for wastewater treatment. *Environmental Chemistry Letters*, *17*(1):145-155.

Daneshgar, S., Callegari, A., Capodaglio, A. G., & Vaccari, D. (2018). The potential phosphorus crisis: resource conservation and possible escape technologies: a review. *Resources*, *7*(2): 37-43

Davis, B. W., Niamnont, N., Hare, C. D., Sukwattanasinitt, M., & Cheng, Q. (2010). Nanofibers doped with dendritic fluorophores for protein detection. ACS applied materials & interfaces, 2(7): 1798-1803.

Dawood, S., & Sen, T. (2014). Review on dye removal from its aqueous solution into alternative cost effective and non-conventional adsorbents. *Journal of Chemical and Process Engineering*, *1*(104): 1-11.

De Gisi, S., Lofrano, G., Grassi, M., & Notarnicola, M. (2016). Characteristics and adsorption capacities of low-cost sorbents for wastewater treatment: A review. *Sustainable Materials and Technologies*, *9*:10-40.

Dias, N. C., Steiner, P. A., & VBraga, M. C. B. (2015). Characterization and modification of a clay mineral used in adsorption tests. *Journal of Minerals and Materials Characterization and Engineering*, *3*(04):277-285.

Djedidi, Z., Bouda, M., Souissi, M. A., Cheikh, R. B., Mercier, G., Tyagi, R. D., & Blais, J. F. (2009). Metals removal from soil, fly ash and sewage sludge leachates by precipitation and dewatering properties of the generated sludge. *Journal of Hazardous Materials*, *172*(2-3):1372-1382.

Ekwueme, B. N., Akpeke, G. B., & Ephraim, B. E. (2015). The chemical composition and industrial quality of Barite mineralization in Calabar flank, Oban Massif, Mamfe embayment and Obudu Plateau, southeastern Nigeria. *Global Journal of Geological Sciences*, *13*(1):53-66.

Elmorsi, T. M. (2011). Equilibrium isotherms and kinetic studies of removal of methylene blue dye by adsorption onto miswak leaves as a natural adsorbent. *Journal of Environmental Protection*, 2(06): 817-834

Enyeribe, C. C., Kogo, A. A., & Yakubu, M. K. (2017). Synthesis and Antimicrobial Activities of Cationated Chitosan. Organ Chem: Indian J, 13:113-127.

Falade, M. O. & Adeyeye, P. (2016). A profile of Nigeria's solid minerals a detailed desk review.(6):50-56

Fierro, V., Torné-Fernández, V., Montané, D., & Celzard, A. (2008). Adsorption of phenol onto activated carbons having different textural and surface properties. Microporous and mesoporous materials, 111(1-3):276-284.

Foo, K. Y., & Hameed, B. H. (2010). Insights into the modeling of adsorption isotherm systems. *Chemical engineering journal*, 156(1): 2-10.

Fu, F., & Wang, Q. (2011). Removal of heavy metal ions from wastewaters: a review. *Journal of environmental management*, *92*(3):407-418.

Gai, W. Z., Deng, Z. Y., & Shi, Y. (2015). Fluoride removal from water using high-activity aluminum hydroxide prepared by the ultrasonic method. *RSC Advances*, *5*(102):84223-84231.

Giwa, A. (2014). Sustainable Wastewater Treatment- The way to go. The Nigerian Voice Newspaper (45):34-40

Gupta, V. K., Carrott, P. J. M., Ribeiro Carrott, M. M. L., & Suhas. (2009). Low-cost adsorbents: growing approach to wastewater treatment—a review. *Critical reviews in environmental science and technology*, *39*(10):783-842.

Gupta, V. K., Sadegh, H., Yari, M., Shahryari, G. R., Maazinejad, B., & Chahardori, M. (2015). Removal of ammonium ions from wastewater a short review in development of efficient methods. (9):11-17

Hefne, J. A., Mekhemer, W. K., Alandis, N. M., Aldayel, O. A., & Alajyan, T. (2012). Kinetic and thermodynamic study of the adsorption of Pb (II) from aqueous solution to the natural and treated bentonite. *International Journal of Physical Sciences*, *3*(11): 281-288.

Huggett, J. M., Petroclays, H., Time, I., Space, I., Dating, A., & Illite, F. (2013). Minerals: Glauconites and Green Clays. *Reference Module in Earth Systems and Environmental Sciences; Elsevier: Amsterdam, The Netherlands*,(10):45-56

Idris-Nda, A., Aliyu, H. K., & Dalil, M. (2013). The challenges of domestic wastewater management in Nigeria: A case study of Minna, central Nigeria. *International Journal of Development and Sustainability*, *2*(2): 1169-1182.

Jaya, H., Noriman, N. Z., Dahham, O. S., Muhammad, N., Latip, N. A., Aini, A. K., & Breesem, K. M. (2018, December). Tensile and Physical Properties of Unsaturated Polyester/Potash Feldspar Composites: The Effect of Potash Feldspar Loading. In IOP Conference Series: Materials Science and Engineering (454): 1-17).

Jose, S., & Kuriakose, S. (2017). Synthesis, characterization and thermal studies of silver nanoparticles-β-cyclodextrin inclusion complexes modified with (2E)-3-{3-[(Z)-naphthalen-1-yldiazenyl] phenyl} prop-2-enoic acid. *Journal of Inclusion Phenomena and Macrocyclic Chemistry*, 87(2):127-140.

Kerisit, S., & Liu, C. (2012). Diffusion and adsorption of uranyl carbonate species in nanosized mineral fractures. Environmental science & technology, 46(3):1632-1640.

Kolhe, A. S., & Pawar, V. P. (2011). Physico-chemical analysis of effluents from dairy industry. *Recent Research in Science and Technology*, (5):5-12

Komadel, P. (2016). Acid activated clays: Materials in continuous demand. *Applied Clay Science*, *131*:84-99.

Kura, N. U., Ramli, M. F., Sulaiman, W. N. A, Ibrahim, S., Aris, A. Z & Mustapha, A. (2013). Evaluation of factors influencing the groundwater chemistry in small tropical island of Malaysia. *International journal of environmental research and public health* 10: 1861-1881.

Ler, A., & Stanforth, R. (2003). Evidence for surface precipitation of phosphate on goethite. *Environmental Science and Technology*, *37*(12): 2694-2700.

Li, L., Ding, D., Hu, N., Fu, P., Xin, X., & Wang, Y. (2014). Adsorption of U (VI) ions from low concentration uranium solution by thermally activated sodium feldspar. *Journal of Radioanalytical and Nuclear Chemistry*, *299*(1):681-690.

Liu, X., Liao, Y., & Gao, H. (2012). Enhancement adsorption of hexavalent chromium from aqueous solution on polypyrrole using ethylamine group. *Journal of Dispersion Science and Technology*, *39*(10):1394-1402.

Mara, D. (2013). *Domestic wastewater treatment in developing countries*. Routledge.

Nwosu, F. O., Ajala, O. J., Owoyemi, R. M., & Raheem, B. G. (2018). Preparation and characterization of adsorbents derived from bentonite and kaolin clays. *Applied Water Science*, *8*(7):195-203

Odlare, M. 2013. Introductory chapter for waste water resources.(2):5-7

Olugbemi, M. (2019). Assessment of Barite Deposit in Nassarawa State for Oil Drilling Application (Doctoral dissertation). .(4):8-13

Omosa, I. B., Wang, H., Cheng, S., & Li, F. (2012). Sustainable tertiary wastewater treatment is required for water resources pollution control in Africa.(8):5-10

Oshagbemi, A.A. (2016). Adsorption Study of the Removal of chromium (vi) ion from aqueous solution using developed chitosan – zeolite composite adsorbent. (5):16-23

Rashed, M. N. (2013). Adsorption technique for the removal of organic pollutants from water and wastewater. *Organic pollutants-monitoring, risk and treatment* (7):167-194.

Saminu, A., Chukwujama, I. A., Garba, A. D., & Namadi, M. M (2017). Performance Evaluation of Wupa Waste Water Treatment Plant Abuja, Federal Capital Territory, Nigeria.(9):1-6

Sankpal, S. T., & Naikwade, P. V. (2012). Physicochemical analysis of effluent discharge of fish processing industries in Ratnagiri India. *Bioscience Discovery*, (1):107-111.

Santamaria-Perez, D., Chulia-Jordan, R., Rodriguez-Hernandez, P., & Munoz, A. (2015). Crystal behavior of potassium bromate under compression. *Acta Crystallographica Section B: Structural Science, Crystal Engineering and Materials*, 71(6), 798-804.

Shuaib-Babata, Y. L., Mudaire, E., & Egwim, C. E. (2016). Suitability of using Ado Ekiti, Akerebiata (Ilorin) and Birni Gwari (Kaduna) Clays for Production of Household Ceramic Water Filter. *Journal of Engineering Research*, (2): 11-25.

Song, C., Wu, S., Cheng, M., Tao, P., Shao, M., & Gao, G. (2014). Adsorption studies of coconut shell carbons prepared by KOH activation for removal of lead (II) from aqueous solutions. *Sustainability*, (1): 86-98.

Srivastava, A., Selvaraj, K., & Prasad, K. S. (2019). Nanoparticles based adsorbent for removal of arsenic from aqueous solution. *Asian Journal of Water, Environment and Pollution*, 16(1), 97-103.

Te, B., Wichitsathian, B., & Yossapol, C. (2015). Modification of natural common clays as low cost adsorbents for arsenate adsorption. *International Journal of Environmental Science and Development*, (11):799-805

Toor, M. K. (2011). *Enhancing adsorption capacity of bentonite for dye removal: physiochemical modification and characterization* (Doctoral dissertation). University of Adelaide, School of Chemical Engineering.(6):205-213

Yazdani, M., Bahrami, H., & Arami, M. (2013). Feldspar/titanium dioxide/chitosan as a biophotocatalyst hybrid for the removal of organic dyes from aquatic phases. *Journal of Applied Polymer Science*, (10):38-43

Yu, X., Tong, S., Ge, M., & Zuo, J. (2013). Removal of fluoride from drinking water by cellulose hydroxyapatite nanocomposites. Carbohydrate polymer, (1):269-275.

Yu, C., & Han, X. (2015). Adsorbent Material Used In Water Treatment-A Review. In *2015 2nd International Workshop on Materials Engineering and Computer Sciences*. Atlantis Press.(7):56-70

Yu, F., Sun, S., Han, S., Zheng, J., & Ma, J. (2016). Adsorption removal of ciprofloxacin by multi-walled carbon nanotubes with different oxygen contents from aqueous solutions. *Chemical engineering journal*, *285*:588-595.

Zhao, Y., Qi, W., Chen, G., Ji, M., & Zhang, Z. (2015). Behavior of Cr (VI) removal from wastewater by adsorption onto HCl activated Akadama clay. *Journal of the Taiwan Institute of Chemical Engineers*, *50*:190-197.

Zwain, H. M., Vakili, M., & Dahlan, I. (2014). Waste material adsorbents for zinc removal from wastewater: a comprehensive review. *International Journal of Chemical Engineering*, *2014*.(11):305-318

APPENDIX

Table 1A: Results for effect of initial concentrations of phosphate ion and contact time of feldspar adsorbent on phosphate ion removal from domestic wastewater

Time	**4 mg/L**		**6 mg/L**		**8 mg/L**		**12 mg/L**	
(min)	**C_t**	**% removal**	**C_t**	**% removal**	**C_t**	**% removal**	**C_t**	**% removal**
5	2.03	49.25	3.59	40.17	5.98	25.25	8.09	32.58
10	1.45	63.75	2.85	52.50	4.20	47.50	6.85	42.92
20	0.78	80.50	2.20	63.33	3.24	59.50	5.50	54.17
30	0.67	83.25	2.12	64.67	3.00	62.50	4.86	59.50
60	0.78	80.50	2.15	64.17	3.09	61.38	4.89	59.25

Table 1B: Results for effect of initial concentrations of ammonium ion and contact time of feldspar adsorbent on ammonium ion removal from domestic wastewater

Time (min)	15 mg/L		20 mg/L		25 mg/L		35 mg/L	
	C_t	% removal	C_t	% removal	C_t	% removal	C_t	% removal
5	6.08	82.63	8.04	77.03	10.20	70.86	12.36	64.69
10	5.56	84.11	5.24	85.03	6.87	80.37	9.26	73.54
20	4.45	87.29	4.09	88.31	5.93	83.06	7.19	79.46
30	3.19	90.89	3.86	88.97	5.58	84.06	6.91	80.26
60	3.23	90.77	4.05	88.43	5.80	83.43	7.04	79.89

Table 1C: Results for effect of adsorbent dosage and temperature on phosphate ion removal from domestic wastewater

Dosage (g)	C_t	30 ^{0}C % removal	C_t	40 ^{0}C % removal	C_t	50 ^{0}C % removal
0.4	9.1	24.17	8.13	32.25	7.52	37.33
0.8	7.5	37.50	5.68	52.67	5.65	52.92
1.2	6.4	46.67	5.08	57.67	4.82	59.83
1.6	6.42	46.50	5.09	57.58	4.80	60.00

Table 1D: Results for effect of adsorbent dosage and temperature on ammonium ion removal from domestic wastewater

Dosage (g)	30		40		50	
	C_t	% removal	C_t	% removal	C_t	% removal
0.4	16.27	53.51	11.16	68.11	10.05	71.29
0.8	10.93	68.77	9.33	73.34	9.20	73.71
1.2	7.95	77.29	9.27	73.51	9.12	73.94
1.6	8.09	76.89	9.29	73.46	9.14	73.89
2.0	8.19	76.60	9.35	73.29	9.19	73.74

Table 1E: Results for effect of pH on phosphate ion and ammonium ion removal from domestic wastewater using feldspar

S/N	pH	PO_4^{3-} (mg/L)	NH_4^+ (mg/L)	% Removal (PO_4^{3-})	% Removal (NH_4^+)
1.	2.0	5.25	13.54	56.25	61.31
2.	4.0	3.86	9.25	67.83	73.57
3.	7.0	3.52	8.23	70.67	76.49
4.	8.0	3.59	8.27	70.08	76.37
5.	10.0	3.80	8.45	68.33	75.86

Table 1F: Results for effect of temperature on phosphate ion and ammonium ion removal from domestic wastewater using feldspar

S/N	Temperature (^{0})	PO_4^{3-} (mg/L)	NH_4^+ (mg/L)	% Removal (PO_4^{3-})	% Removal (NH_4^+)
1.	30	7.24	11.85	39.67	66.14
2.	40	5.08	9.57	57.67	72.66
3.	50	4.82	9.12	59.83	73.94
4.	60	4.81	9.10	59.92	74.00
5.	70	4.94	9.31	58.83	73.40

Charts Showing Results for the Physiochemical Analysis of the Domestic Wastewater Using Clay Minerals

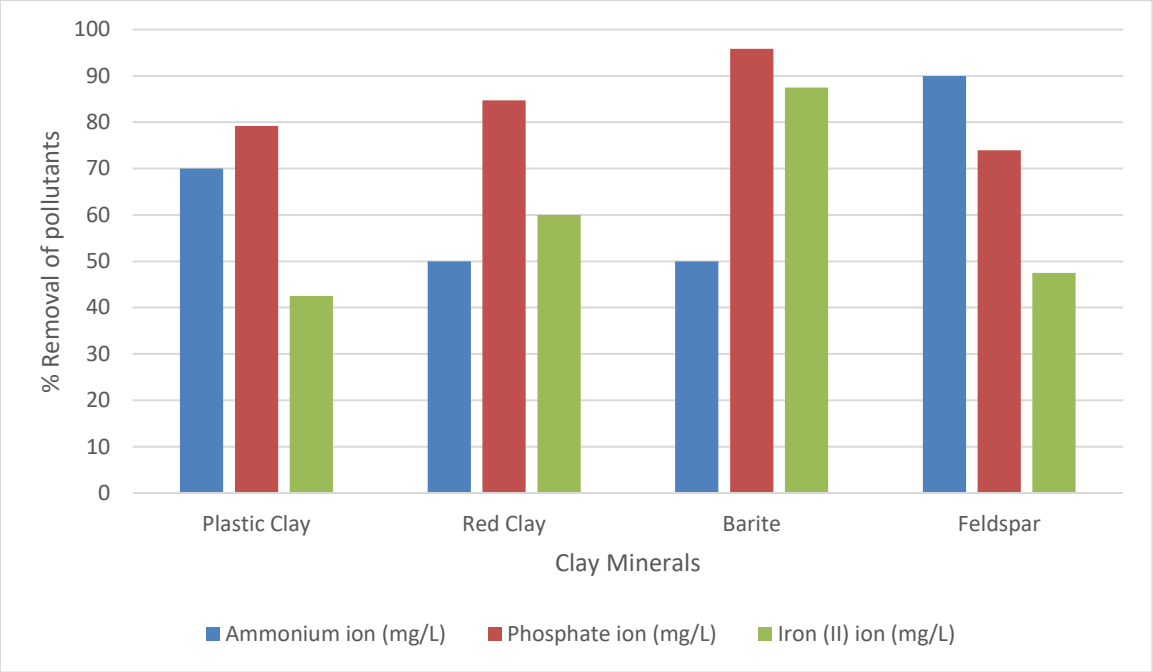

Figure 1a: Percentage removal of pollutants by the different clay minerals

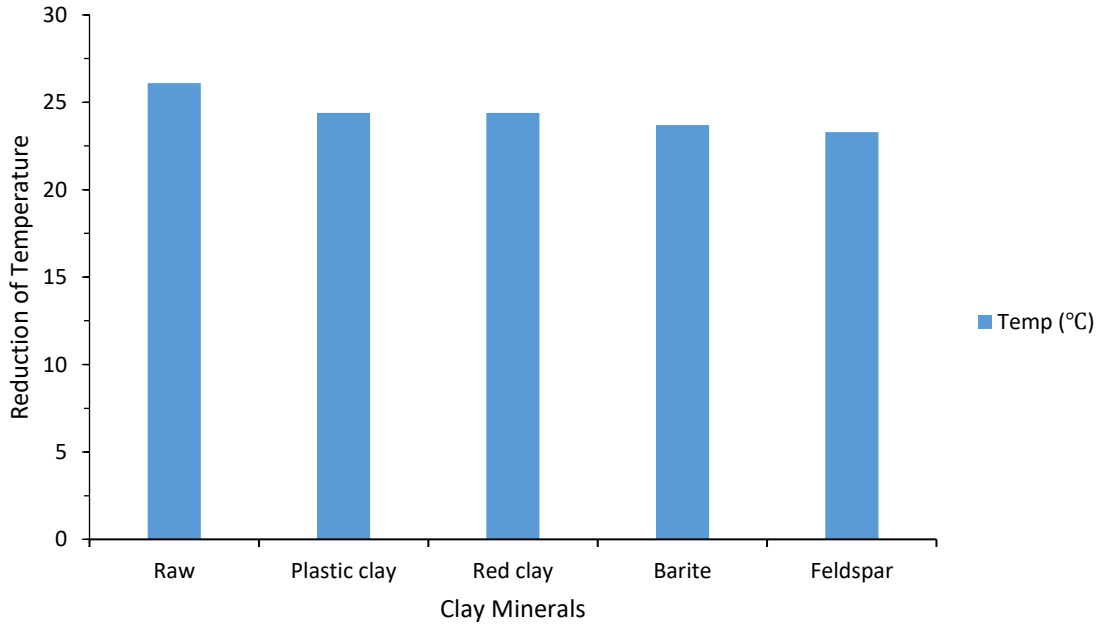

Figure 1b: Reduction of temperature in clay minerals

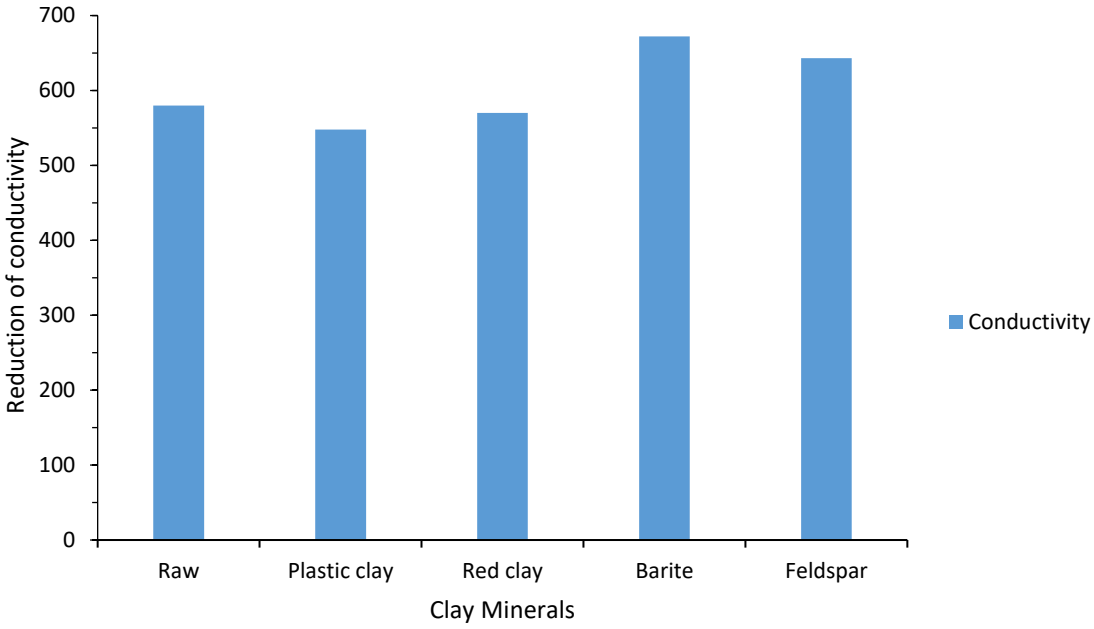

Figure 1c: Reduction of conductivity in clay minerals

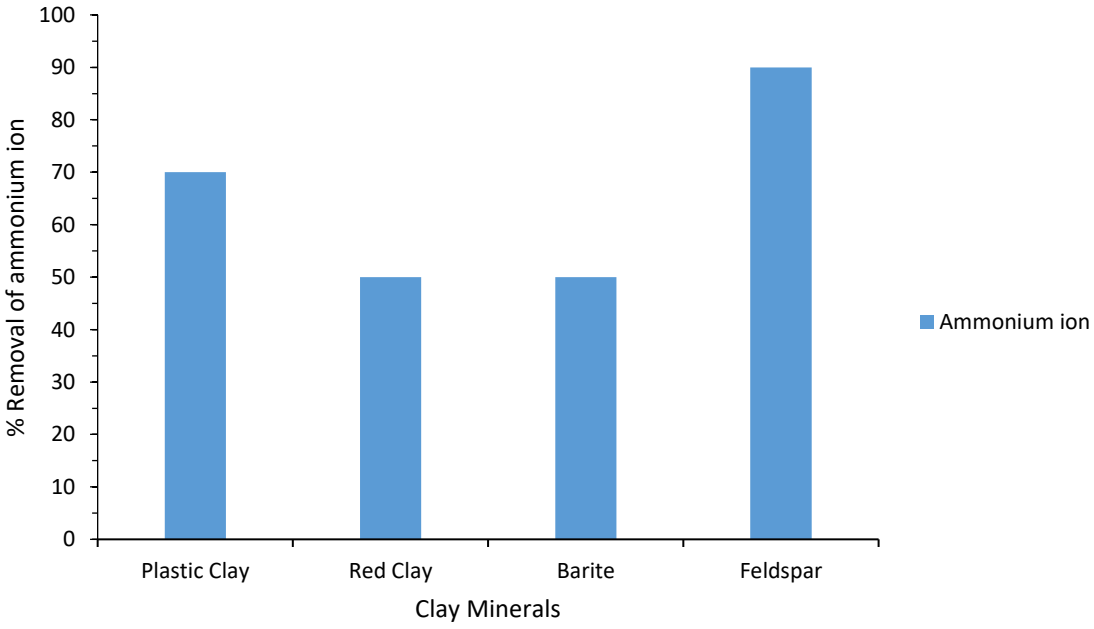

Figure 1d: Percentage reduction of ammonium ion in clay minerals

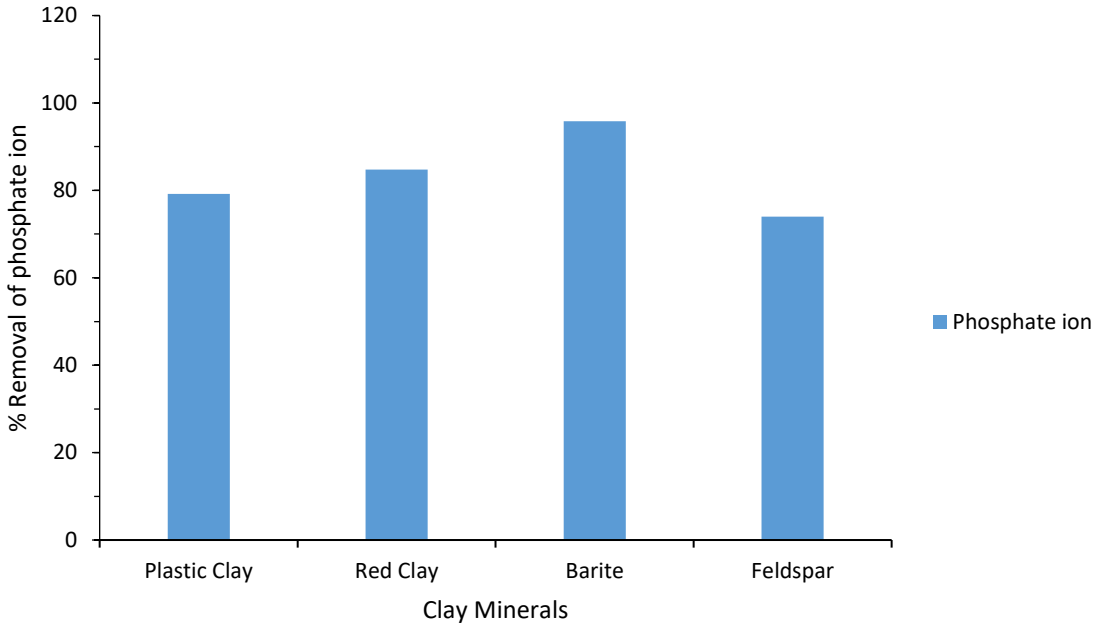

Figure 1e: Percentage reduction of phosphate ion in clay minerals

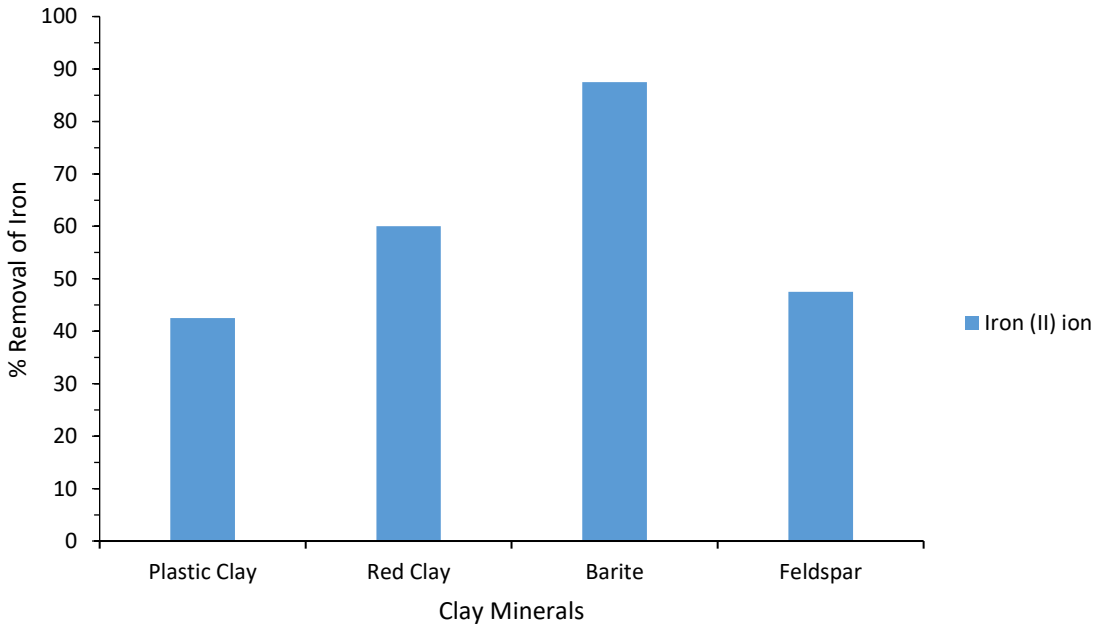

Figure 1f: Percentage reduction of iron in clay minerals

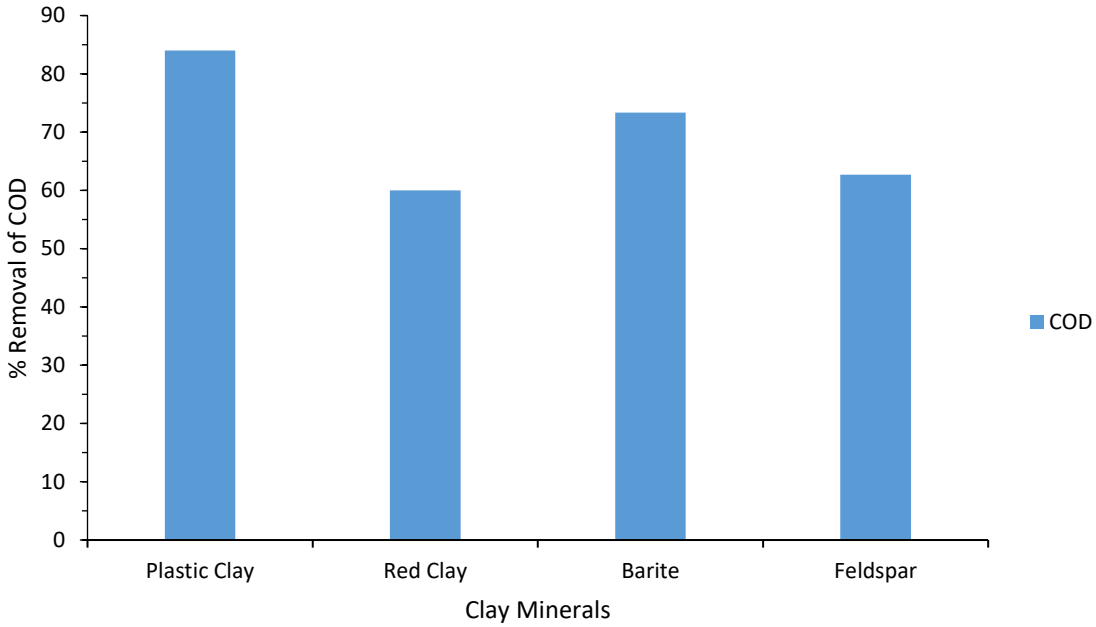

Figure 1g: Percentage reduction of COD in clay minerals

Graphs for effect of calcination temperature on removal efficiency

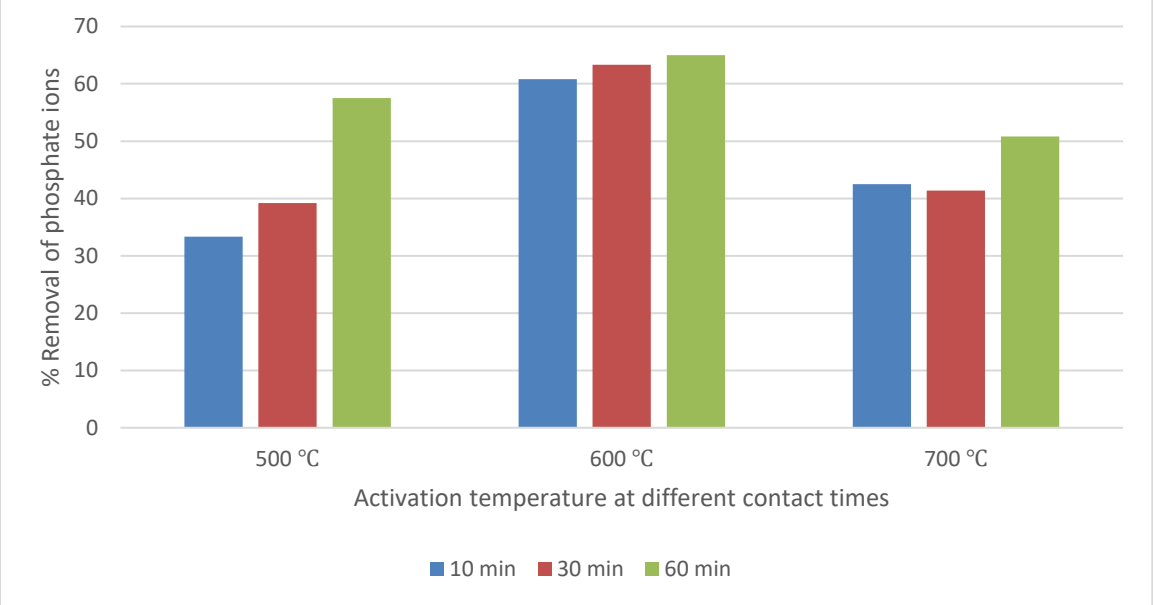

Figure 2a: Percentage removal of phosphate ion at different activation temperatures and contact times

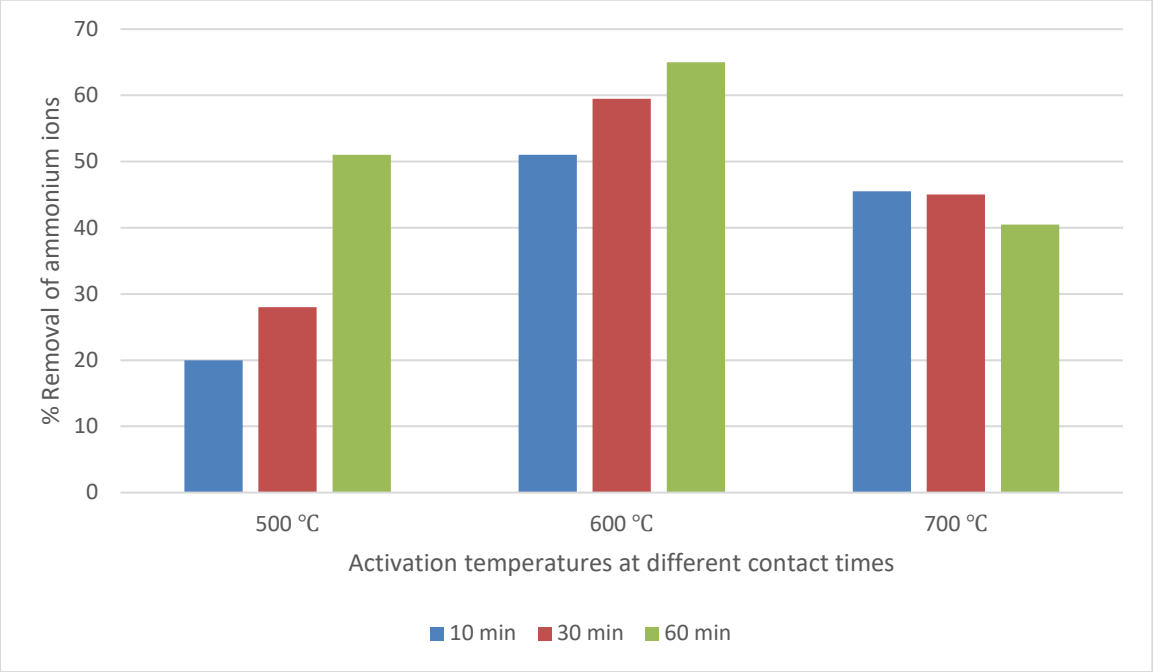

Figure 2b: Percentage removal of ammonium ion at different activation temperatures and contact times

GRAPHS FOR ADSORPTION STUDIES

The graphs for Pseudo-first order kinetics are shown below;

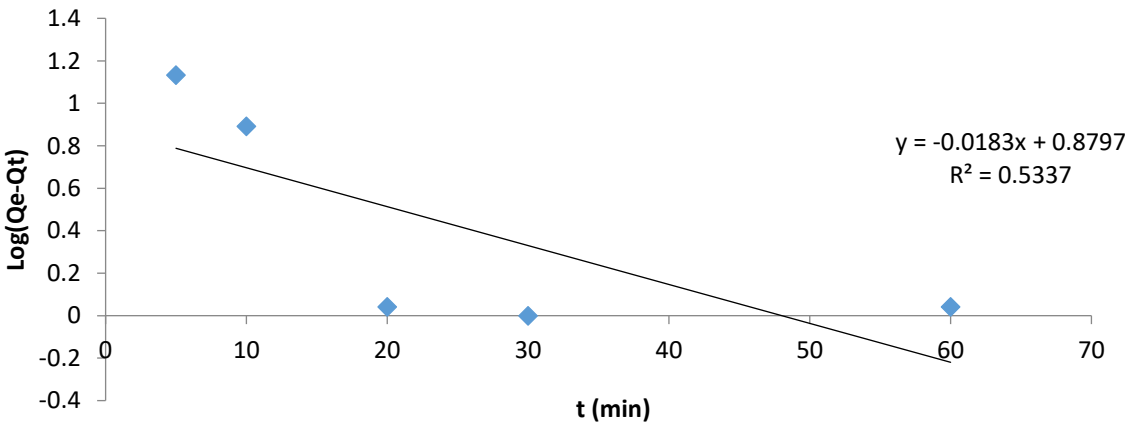

Figure 3Aa: Pseudo-first order plot for PO_4^{3-} removal at 4 mg/L initial concentration

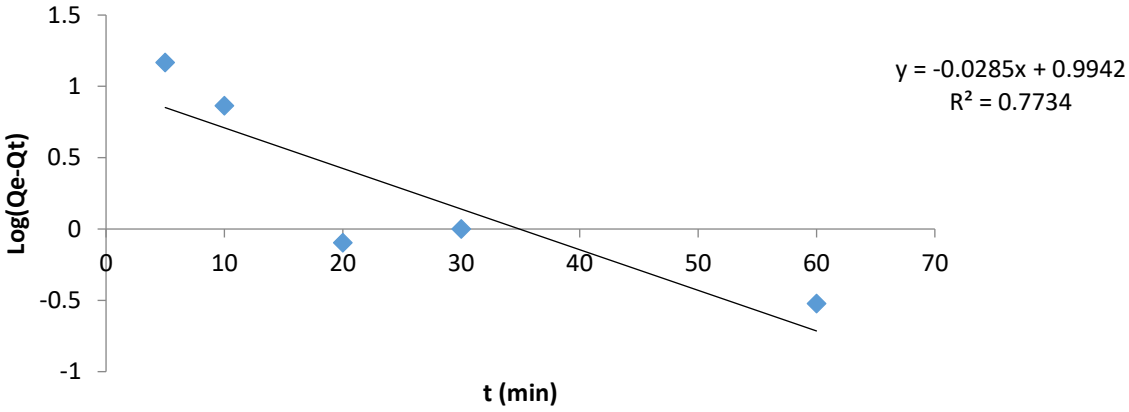

Figure 3Ab: Pseudo-first order plot for PO_4^{3-} removal at 6 mg/L initial concentration

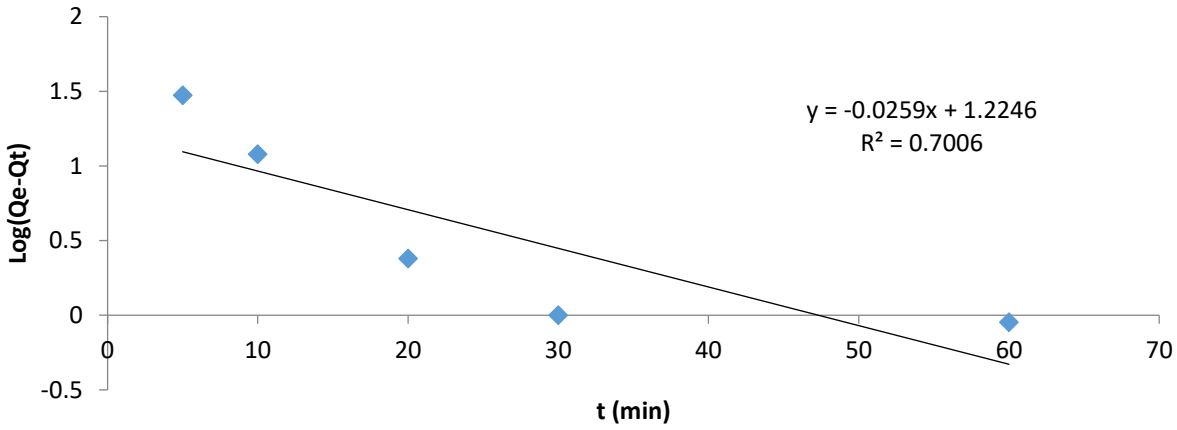

Figure 3Ac: Pseudo-first order plot for PO_4^{3-} removal at 8 mg/L initial concentration

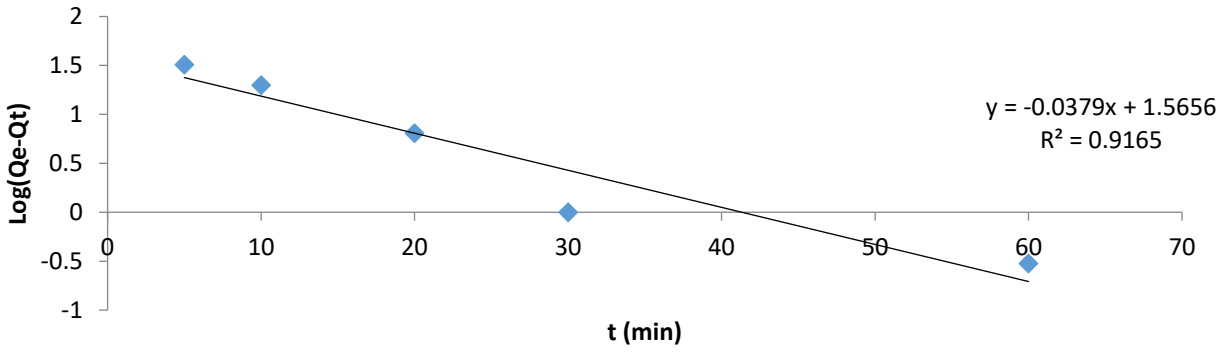

Figure 3Ad: Pseudo-first order plot for PO_4^{3-} removal at 12 mg/L initial concentration

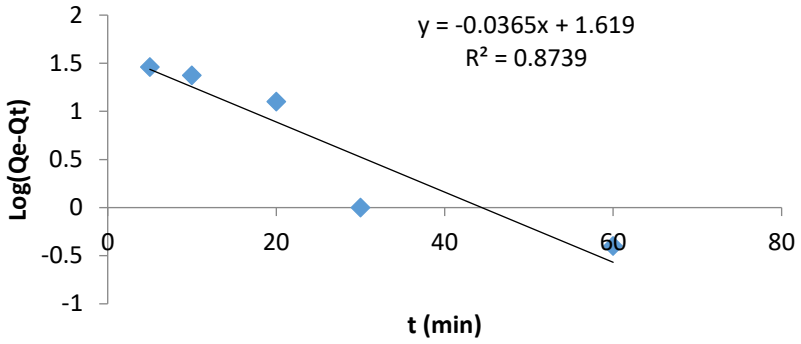

Figure 3Ba: Pseudo-first order plot for NH_4^+ removal at 15 mg/L initial concentration

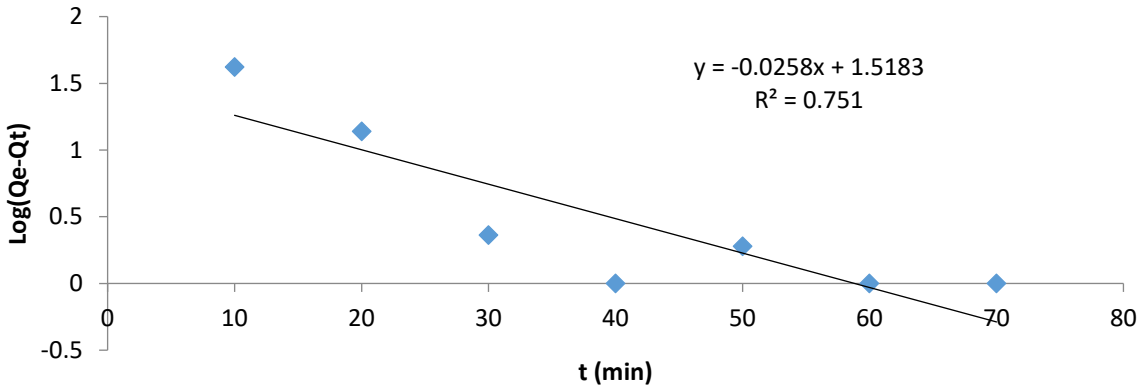

Figure 3Bb: Pseudo-first order plot for NH_4^+ removal at 20 mg/L initial concentration

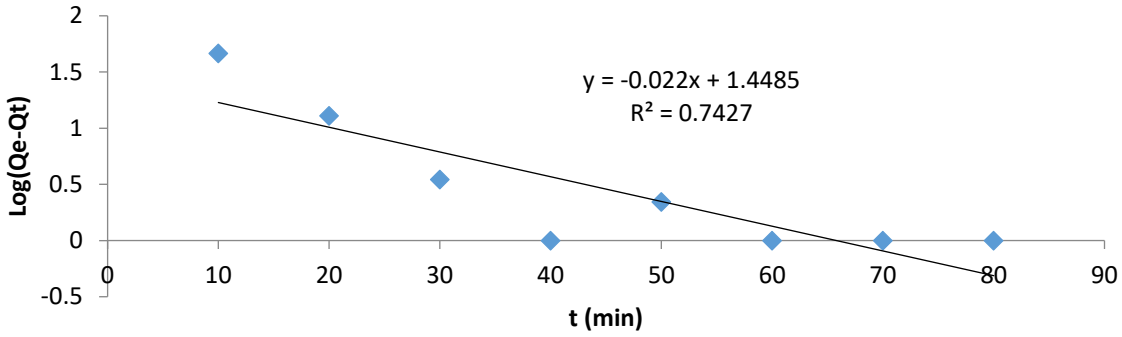

Figure 3Bc: Pseudo-first order plot for NH_4^+ removal at 25 mg/L initial concentration

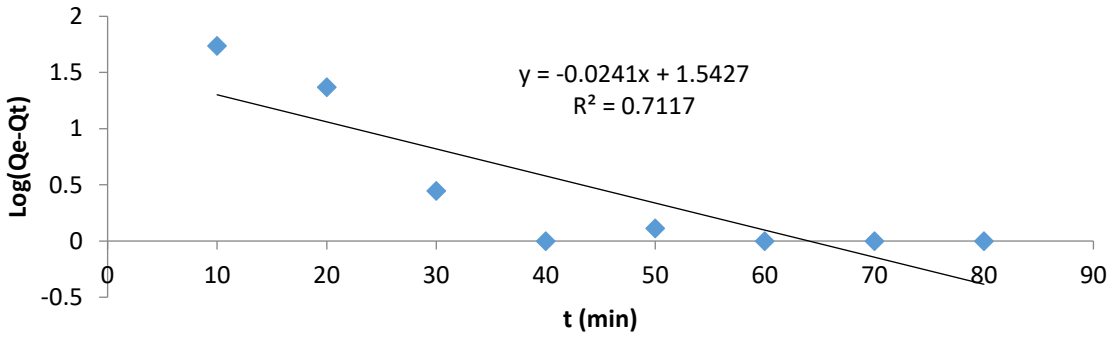

Figure 3Bd: Pseudo-first order plot for NH_4^+ removal at 35 mg/L initial concentration

The graphs for Pseudo-second order kinetics are shown below;

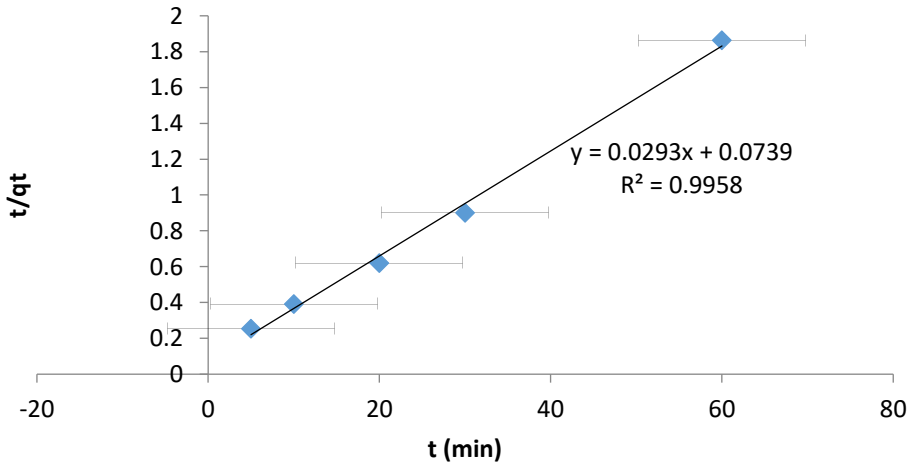

Figure 4Aa: Pseudo-second order plot for PO_4^{3-} removal at 4 mg/L initial concentration

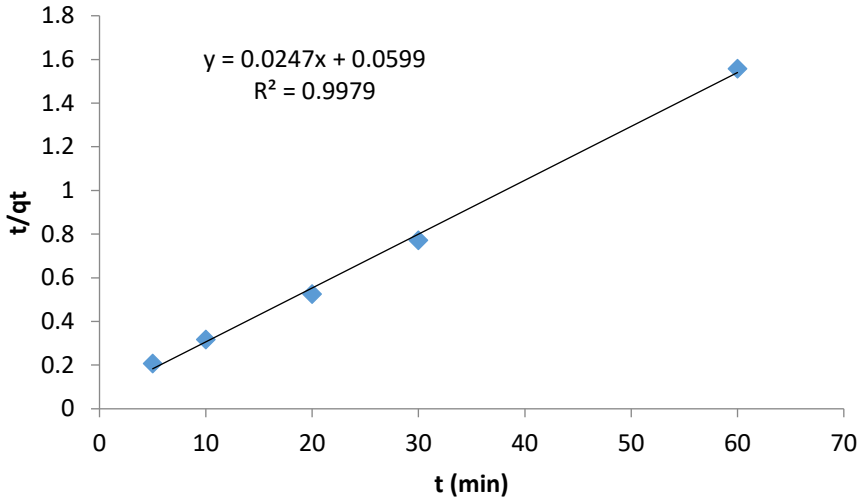

Figure 4Ab: Pseudo-second order plot for PO_4^{3-} removal at 6 mg/L initial concentration

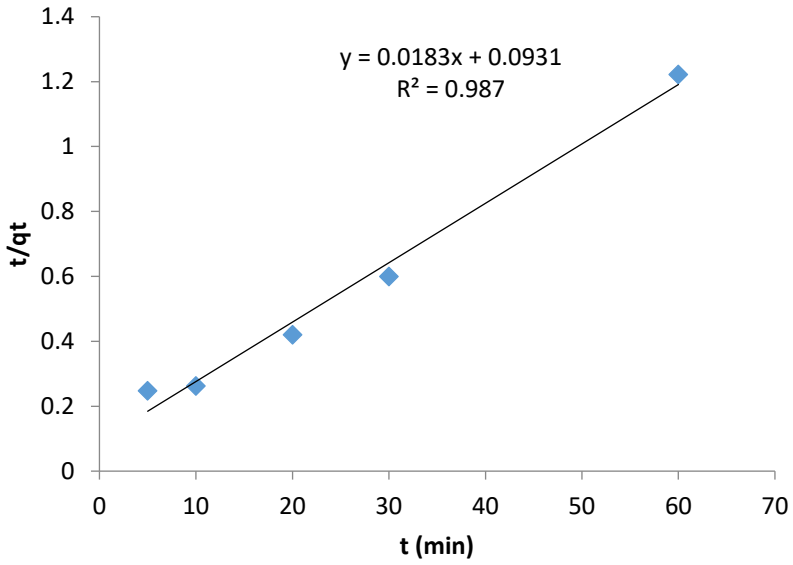

Figure 4Ac: Pseudo-second order plot for PO_4^{3-} removal at 8 mg/L initial concentration

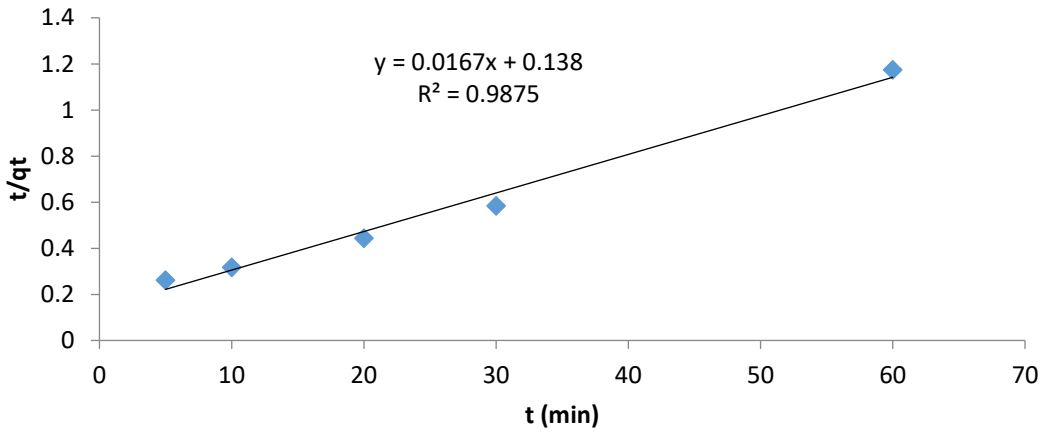

Figure 4Ad: Pseudo-second order plot for PO_4^{3-} removal at 12 mg/L initial concentration

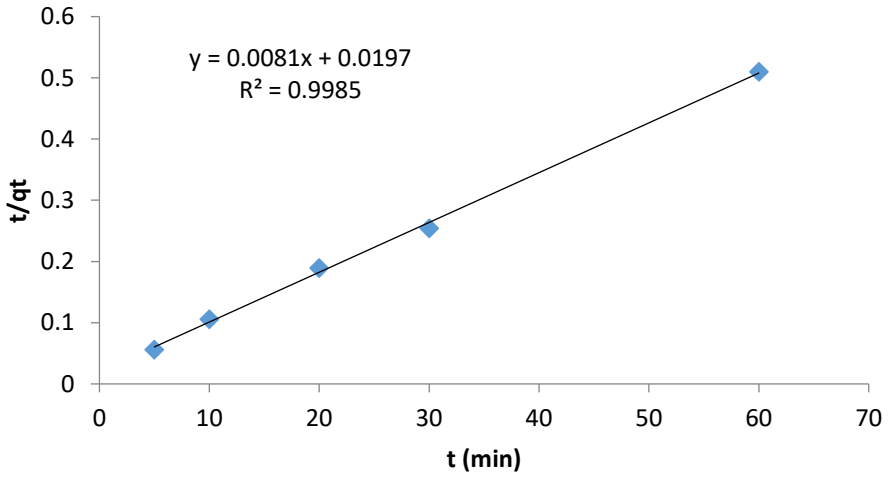

Figure 4Ba: Pseudo-second order plot for NH_4^+ removal at 15 mg/L initial concentration

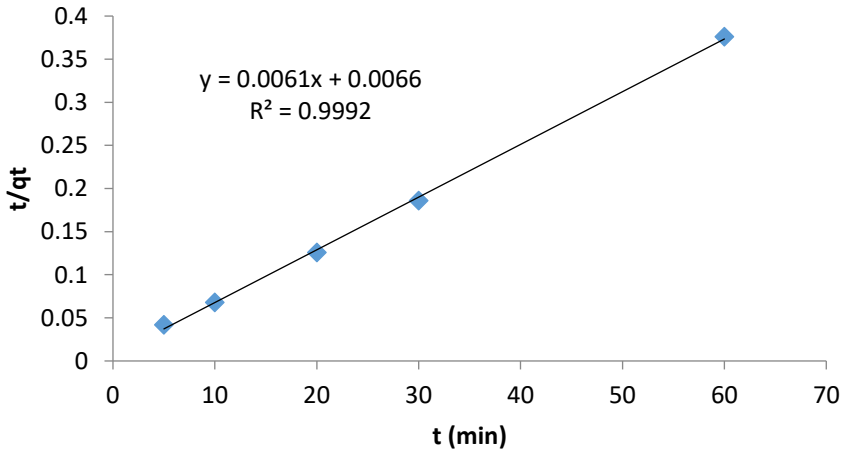

Figure 4Bb: Pseudo-second order plot for NH_4^+ removal at 20 mg/L initial concentration

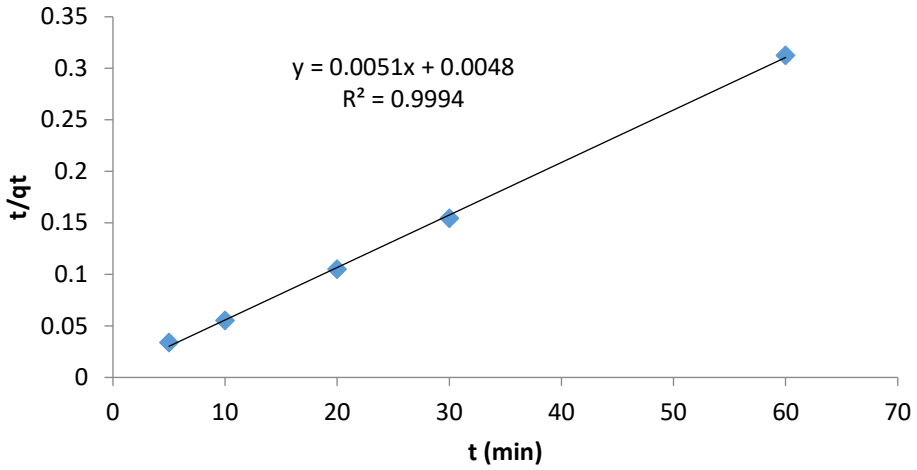

Figure 4Bc: Pseudo-second order plot for NH_4^+ removal at 25 mg/L initial concentration

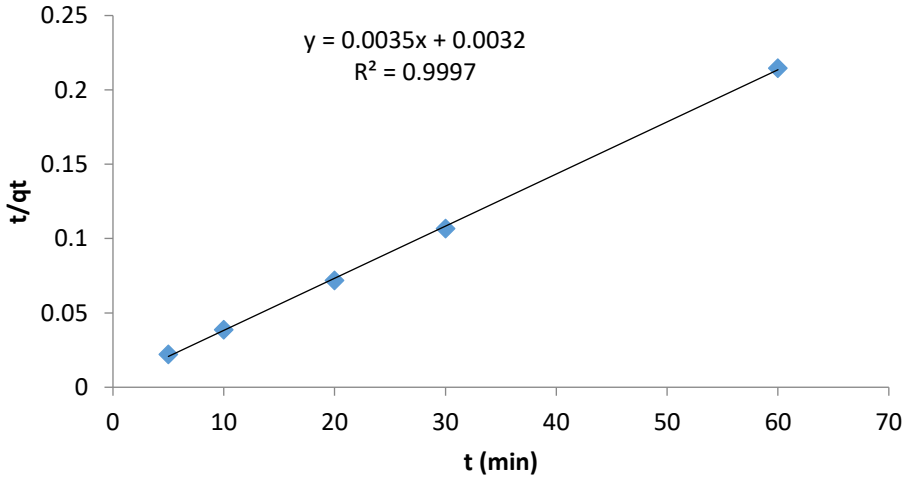

Figure 4Bd: Pseudo-second order plot for NH_4^+ removal at 35 mg/L initial concentration

The graphs for Elovich model are shown below;

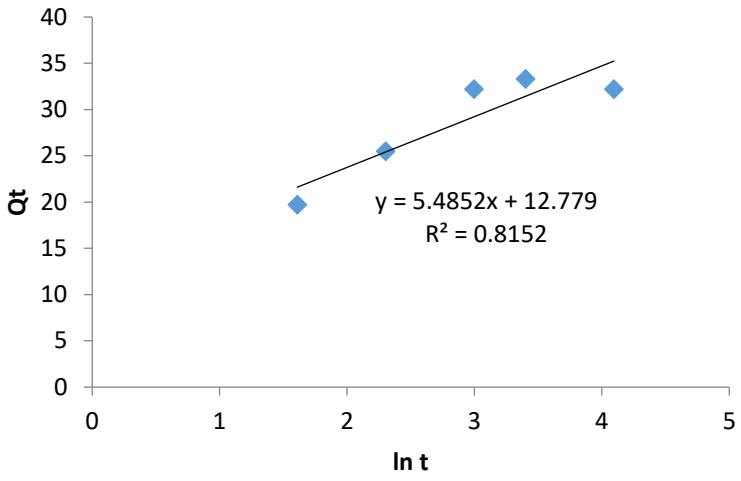

Figure 5Aa: Elovich plot for PO_4^{3-} removal at 4 mg/L initial concentration

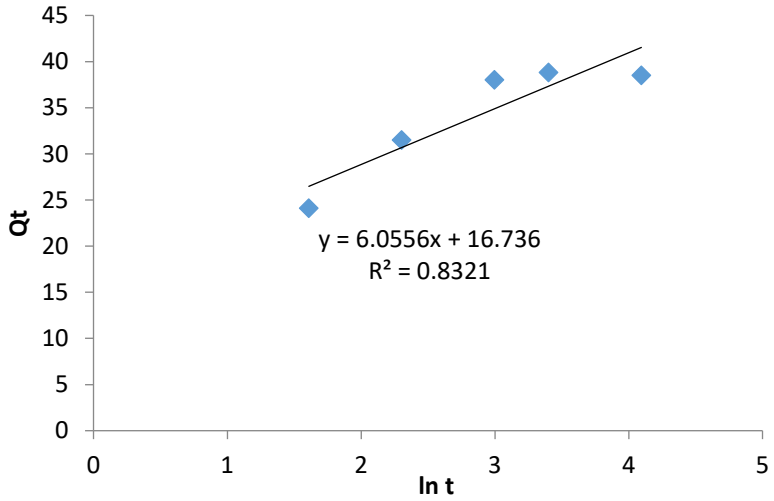

Figure 5Ab: Elovich plot for PO_4^{3-} removal at 6 mg/L initial concentration

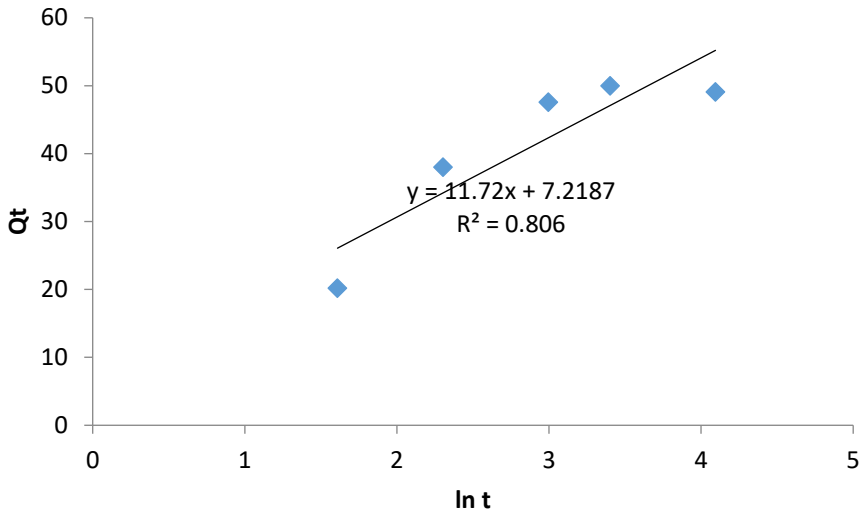

Figure 5Ac: Elovich plot for PO_4^{3-} removal at 8 mg/L initial concentration

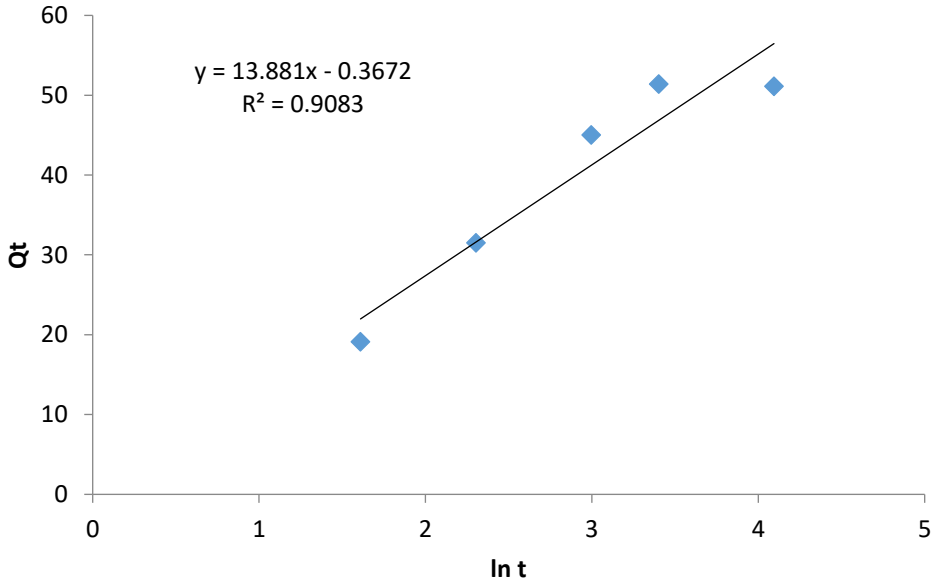

Figure 5Ad: Elovich plot for PO_4^{3-} removal at 12 mg/L initial concentration

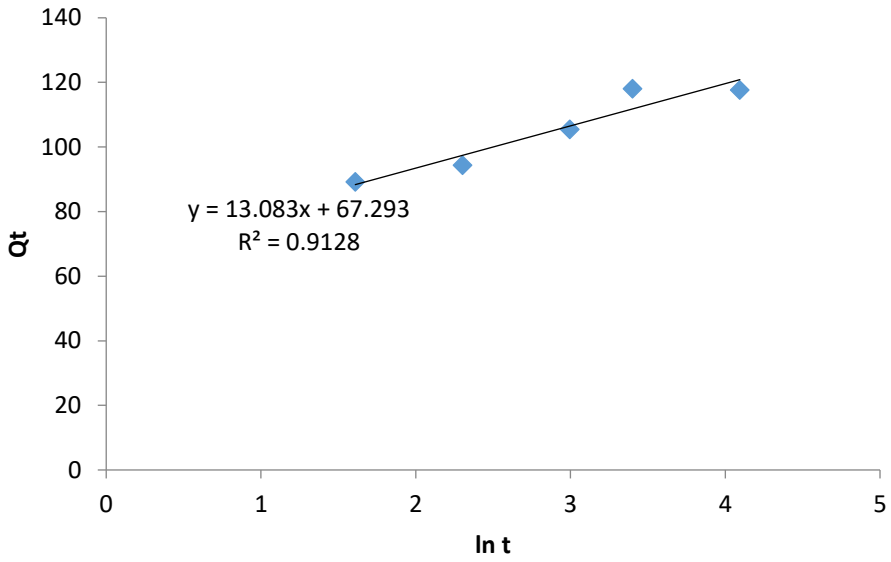

Figure 5Ba: Elovich plot for NH_4^+ removal at 15 mg/L initial concentration

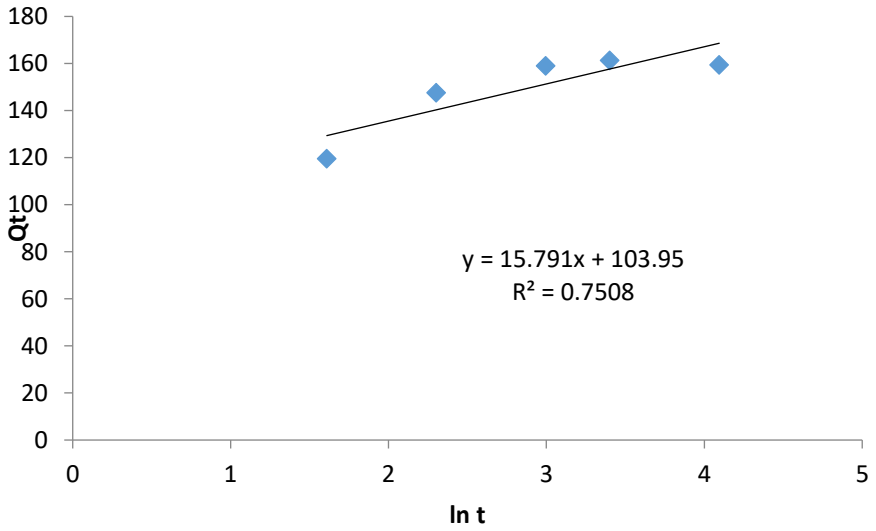

Figure 5Bb: Elovich plot for NH_4^+ removal at 20 mg/L initial concentration

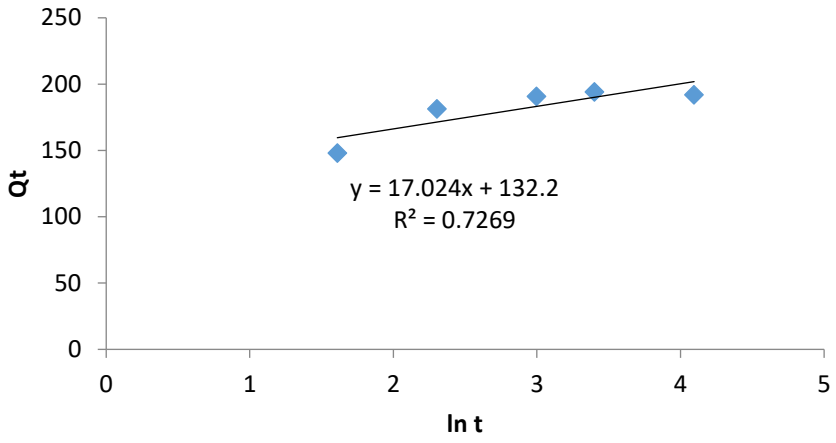

Figure 5Bc: Elovich plot for NH_4^+ removal at 25 mg/L initial concentration

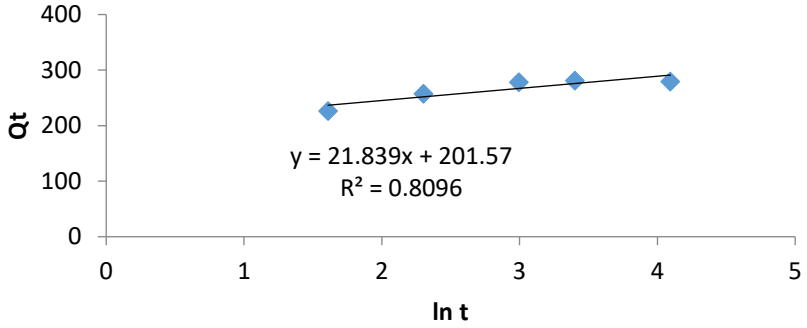

Figure 5Bd: Elovich plot for NH_4^+ removal at 35 mg/L initial concentration

The graphs for Langmuir's isotherm are shown below;

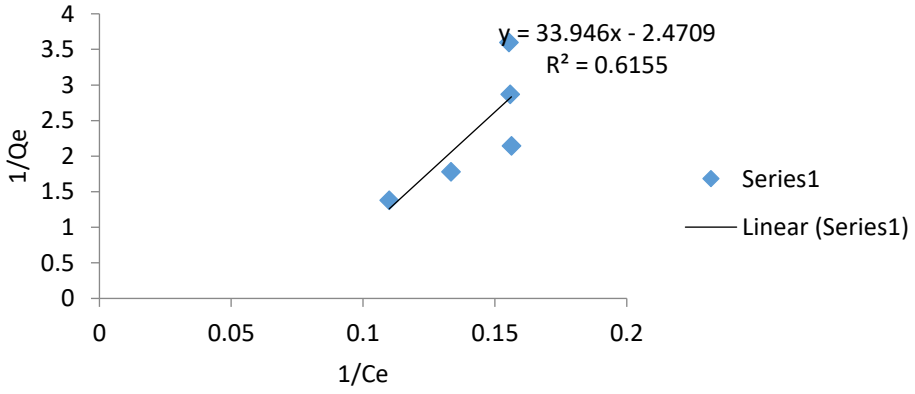

Figure 6Aa: Langmuir's plot for PO_4^{3-} removal at 30^0C

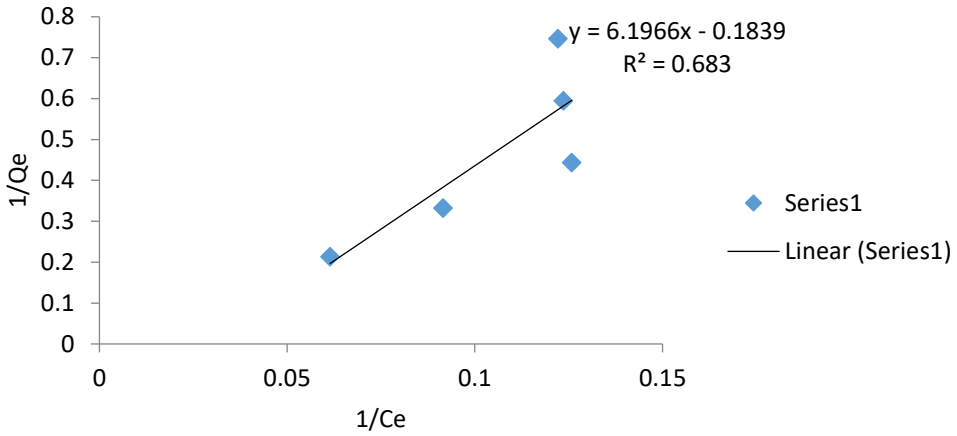

Figure 6Ab: Langmuir's plot for NH_4^+ removal at 30^0C

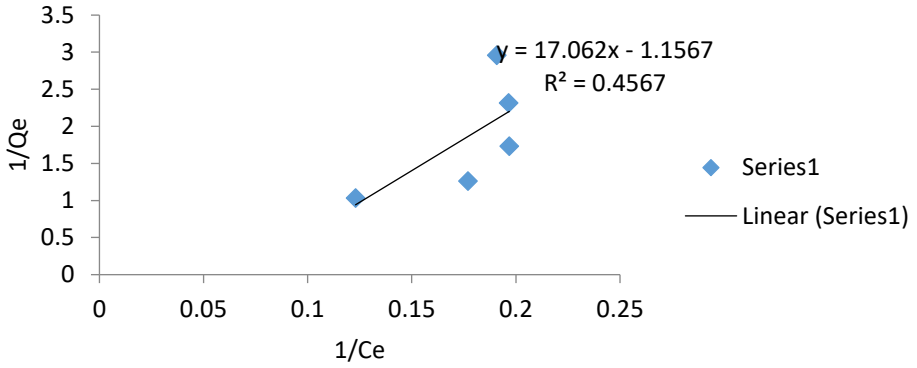

Figure 6Ba: Langmuir's plot for PO_4^{3-} removal at 40^0C

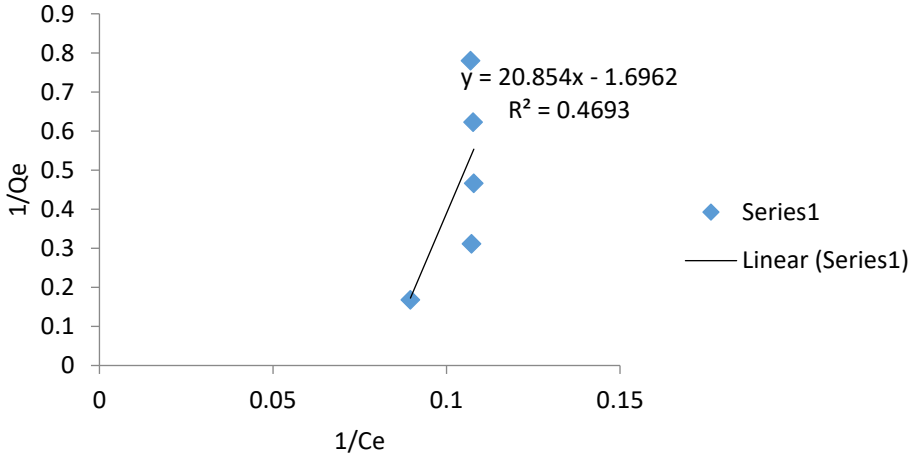

Figure 6Bb: Langmuir's plot for NH_4^+ removal at 40^0C

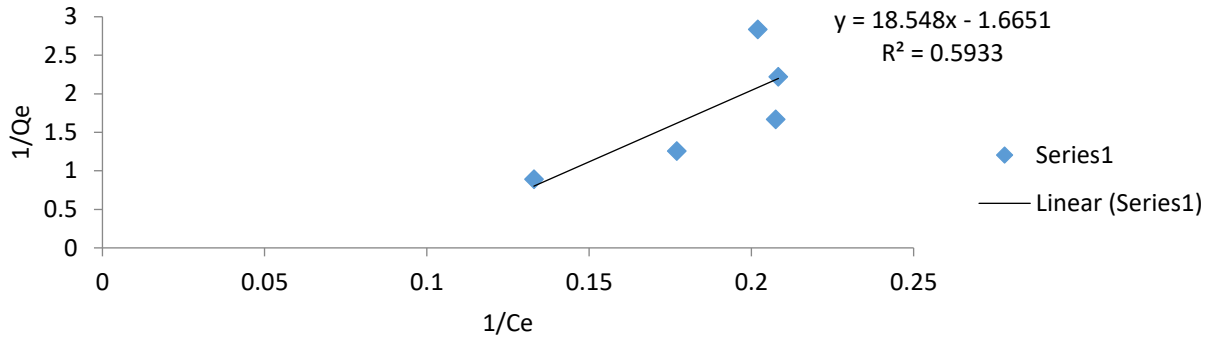

Figure 6Ca: Langmuir's plot for PO_4^{3-} removal at 50^0C

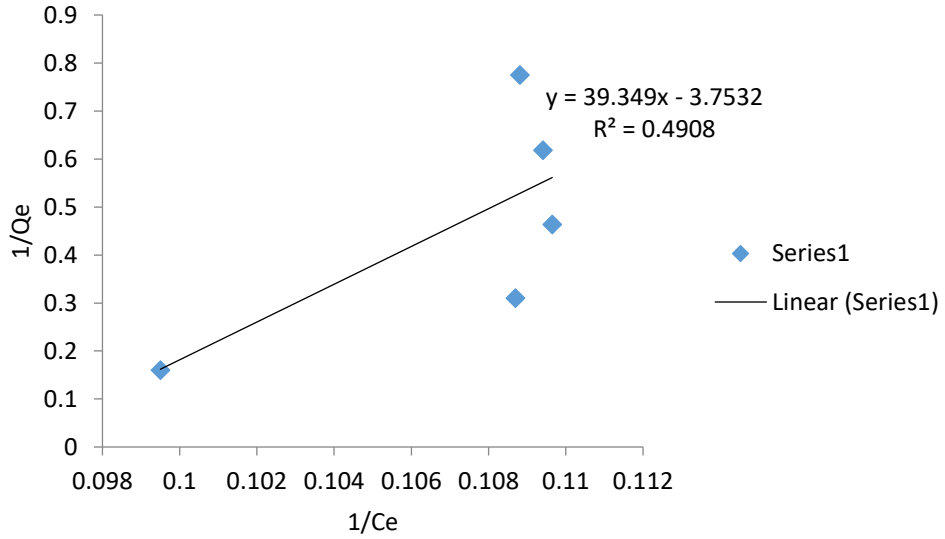

Figure 6Cb: Langmuir's plot for NH_4^+ removal at 50^0C

The graphs for Freundlich isotherm are shown below;

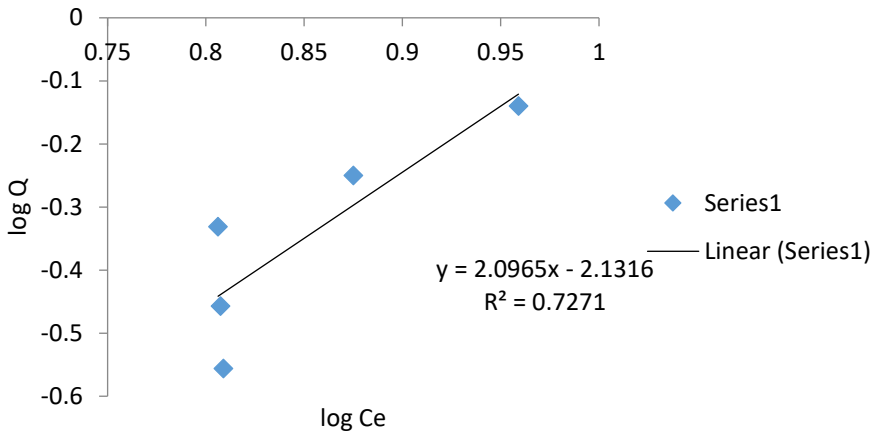

Figure 7Aa: Freundlich plot for PO_4^{3-} removal at 30^0C

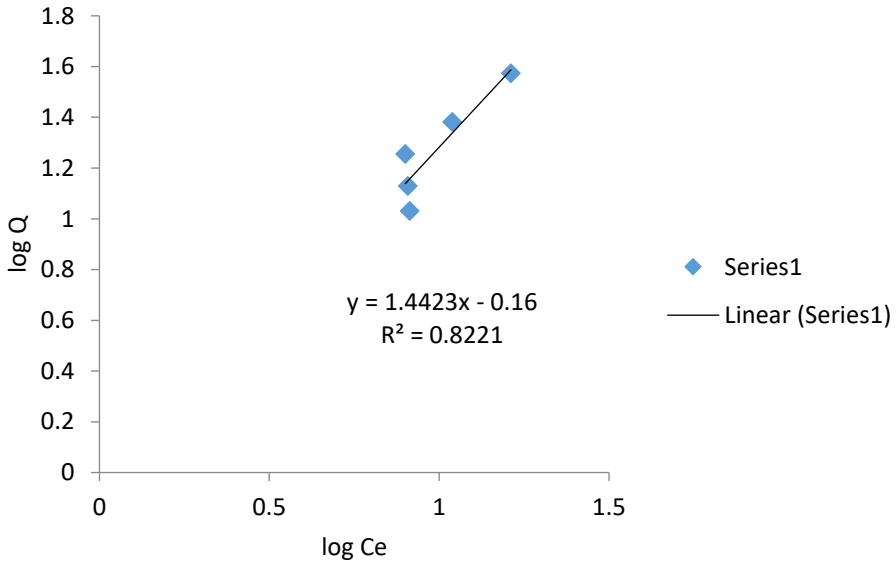

Figure 7Ab: Freundlich plot for NH_4^+ removal at 30^0C

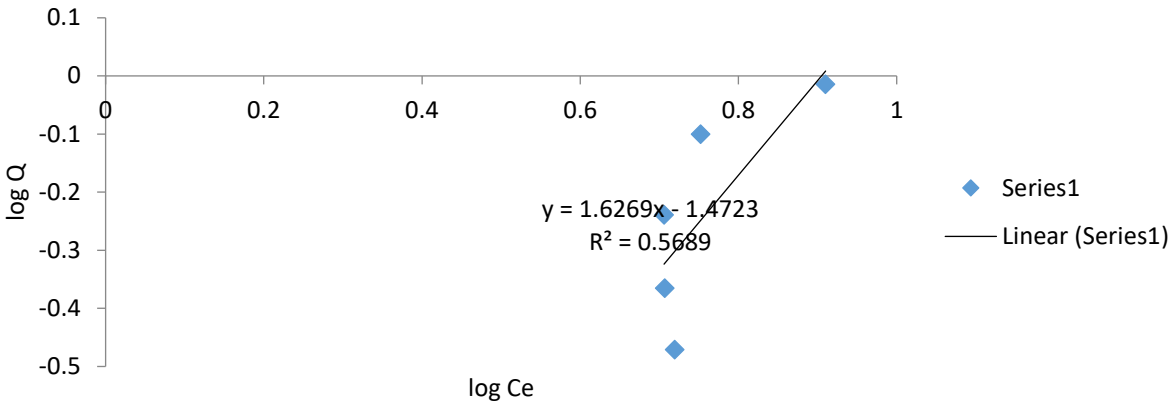

Figure 7Ba: Freundlich plot for PO_4^{3-} removal at 40^0C

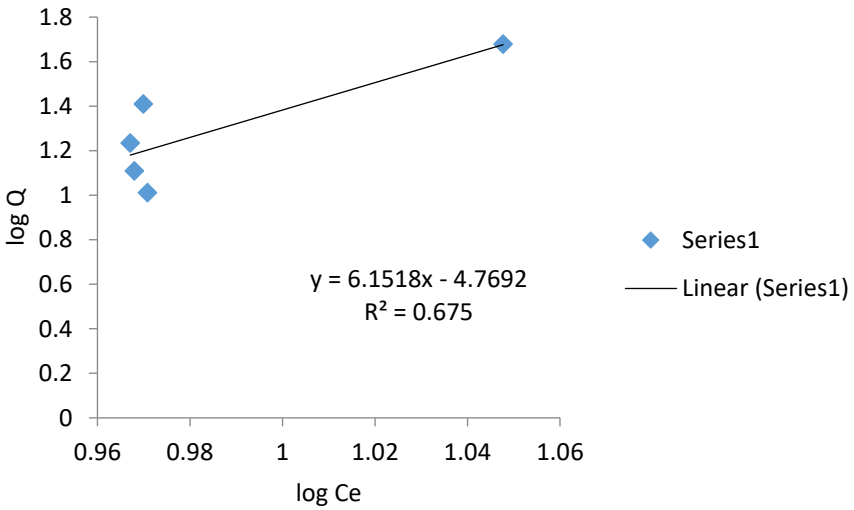

Figure 7Bb: Freundlich plot for NH_4^+ removal at 40^0C

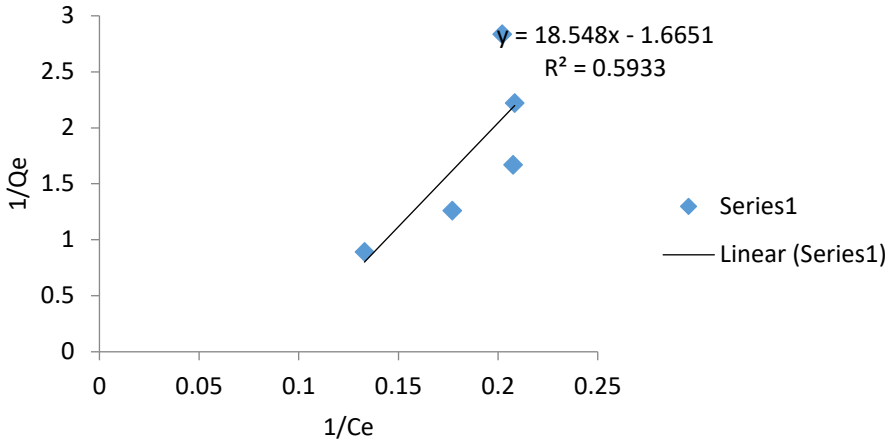

Figure 7Ca: Freundlich plot for PO_4^{3-} removal at 50^0C

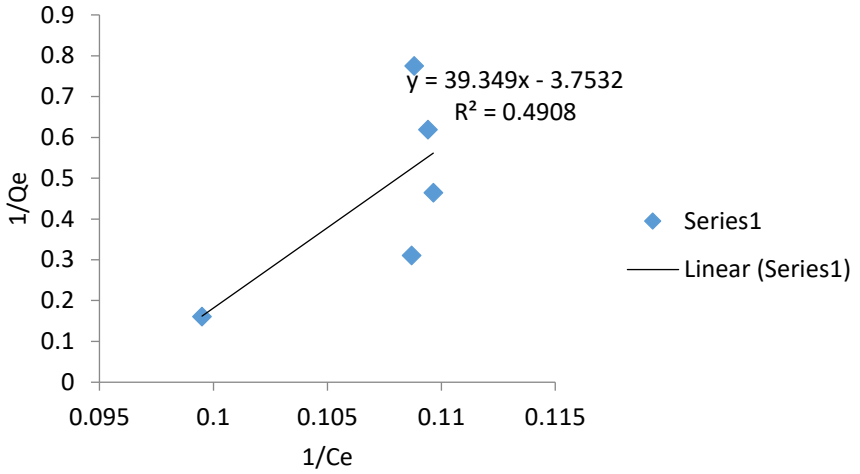

Figure 7Cb: Freundlich plot for NH_4^+ removal at 50^0C

The graphs for Temkin isotherm are shown below;

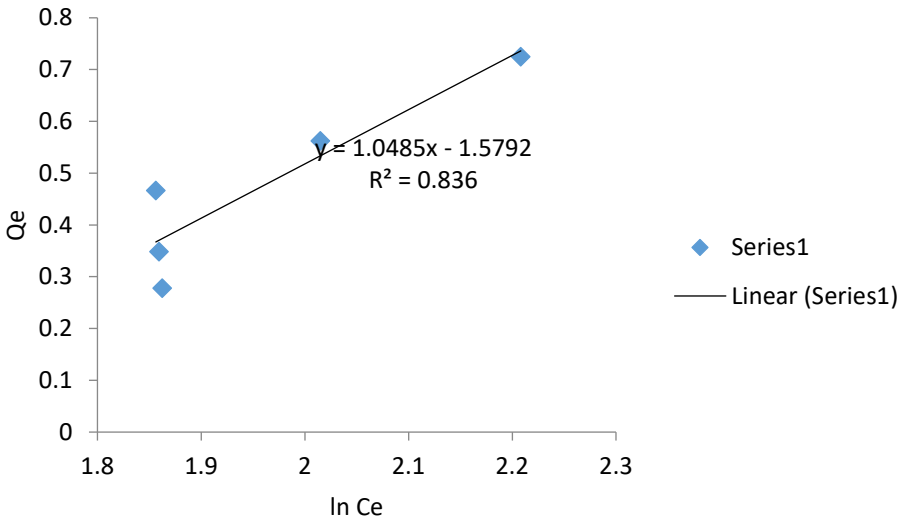

Figure 8Aa: Temkin plot for PO_4^{3-} removal at 30^0C

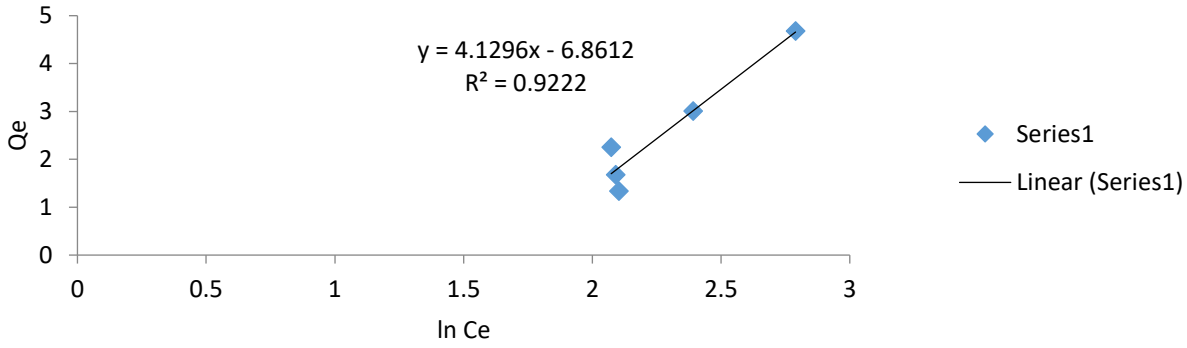

Figure 8Ab: Temkin plot for NH_4^+ removal at 30^0C

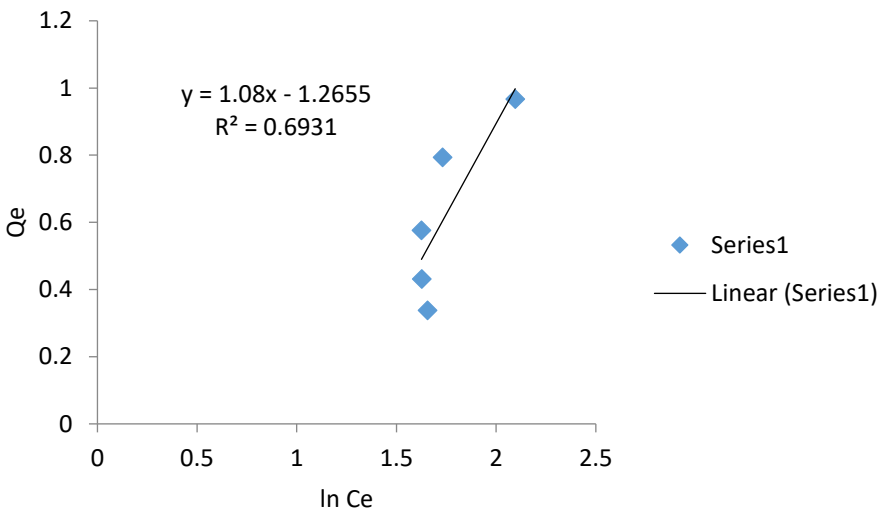

Figure 8Ba: Temkin plot for PO_4^{3-} removal at 40^0C

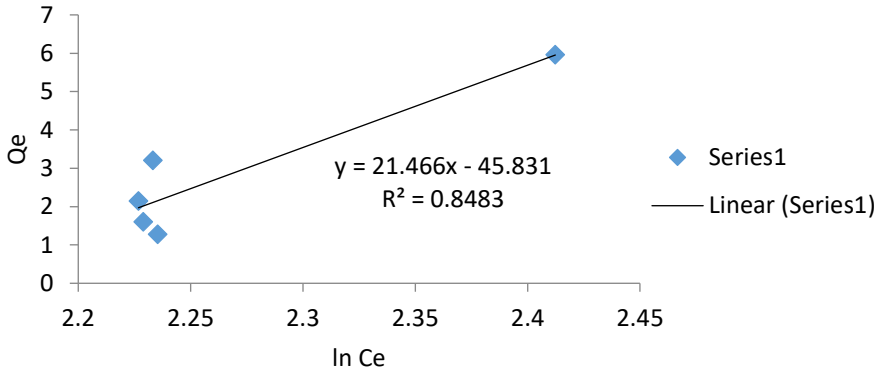

Figure 8Bb: Temkin plot for NH_4^+ removal at 40^0C

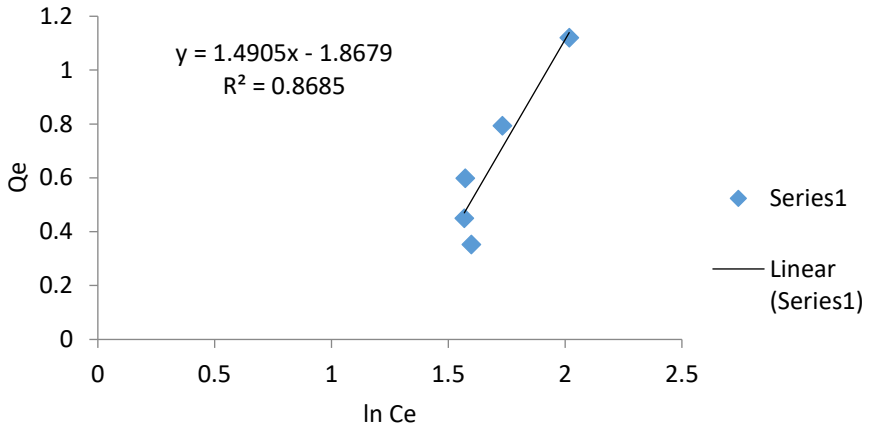

Figure 8Ca: Temkin plot for PO_4^{3-} removal at 50^0C

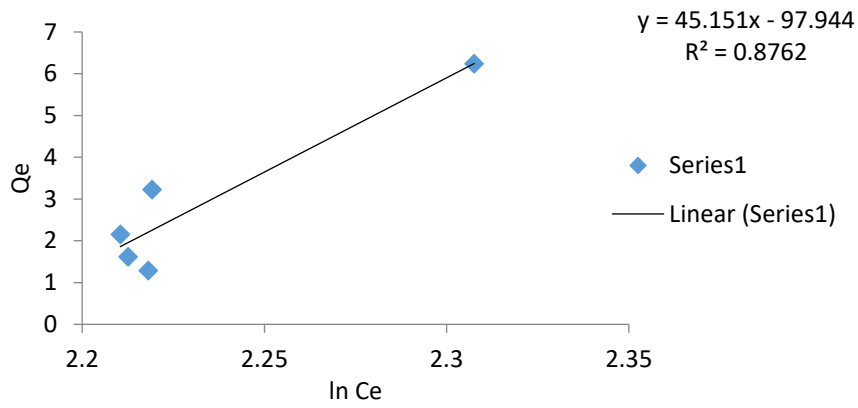

Figure 8Cb: Temkin plot for NH_4^+ removal at 50^0C

The graph for Thermodynamics studies is shown below;

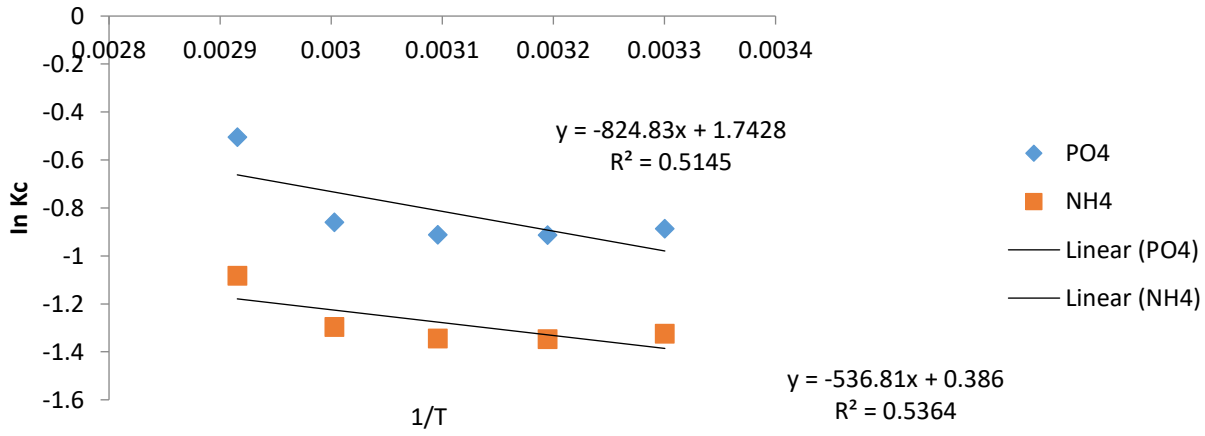

Figure 9: Thermodynamics plot for PO_4^{3-} and NH_4^+ removal